SYNTHESIS AND ANTIMICROBIAL EVALUATION OF SIDEROMYCINS

THE SYNTHESIS AND ANTIMICROBIAL EVALUATION OF NOVEL

SIDEROMYCINS

By ARNAV KAUL, B.Sc.

A Thesis Submitted to the School of Graduate Studies in Partial Fulfilment of the

Requirements for the Degree Master of Science

McMaster University MASTER OF SCIENCE (2022) Hamilton, Ontario (Biochemistry)

TITLE: The Synthesis and Antimicrobial Evaluation of Novel Sideromycins AUTHOR: Arnav Kaul, B.Sc. (McMaster University) SUPERVISOR: Professor J. Magolan NUMBER OF PAGES: xix, 110

Lay Abstract

This thesis is divided into two chapters. The first chapter is focused on the development of new sideromycin antibiotics. Sideromycins are "Trojan Horse"-like antibiotics that exploit the mechanisms of Gram-negative bacteria for obtaining iron, an essential nutrient, to enable antibiotic entry. This chapter details the synthesis of molecules that attach functionalities called "siderophores" to antibiotics, enabling them to be "smuggled" into Gram-negative microbes. This project uses a siderophore not previously utilized in sideromycin research. The second chapter is focused on the chemical synthesis of rare natural products that are phenols with prenyl substituents. Many such compounds are plant-derived and have potential for biomedical use. However, difficulty in isolating them makes them prohibitively expensive in the purity and quantity required for research. They are also challenging to make synthetically. This chapter details the application of a recently discovered process in the Magolan laboratory to synthesize coumarin-containing prenylated phenolic natural products.

Abstract

This thesis consists of two chapters, each of which is a unique research project. Chapter 1 is focused on the synthesis and biological evaluation of novel sideromycin antibiotics. Sideromycins are bifunctional "Trojan Horse" molecules that have an iron chelator "siderophore" moiety covalently bound to an antibiotic. Such molecules exploit existing bacterial mechanisms for obtaining iron from their environment. Antibiotics that would typically not pass Gram-negative membranes are allowed access via siderophore transporter proteins. This project utilized a siderophore that has not previously been used in this capacity. The synthesis and biological evaluation of multiple sideromycin conjugates is reported.

Chapter 2 describes the chemical synthesis of coumarin natural products using a synthetic process recently developed in the Magolan laboratory that enables the efficient prenylation of phenols. These natural products are molecules of biological interest in various capacities but are rare and difficult to isolate from their plant sources. They have also previously been cumbersome to make via chemical synthesis. The chemistry described herein constitutes an inexpensive and efficient process to produce these compounds that is superior to previously known methods.

Acknowledgements

My three years in the Magolan Lab have been an invaluable experience. First and foremost, I would like to thank my supervisor Dr. Jakob Magolan for his incredible kindness and mentorship. His willingness to take someone without any chemistry background under his wing and trust them to handle major projects speaks volumes about his ability as a teacher and motivator. Furthermore, his advice and guidance in and out of the lab has been extraordinarily meaningful to me.

I would also like to thank Dr. Jarrod Johnson and Meghan Fragis for providing me with the skillset to begin my journey in chemistry. Their continual support has meant a lot to me over the last three years. The same thanks extends to Dr. Nicholas Jentsch, Patrick Darveau, and Louie Borrillo as well. Over the last year, Dr. Marc MacKinnon, Dr. Mathew Piotrowski, and Dr. Lauren Irwin have also served as mentors to me, which I have appreciated immensely. They have always gone out of their way to ensure that I have the guidance and tools to continue to grow as a chemist. Before their arrival, Dr. Lakshmana Kinthada, Dr. Xiong Zhang, Parul Pal, Dr. My Cao, and Dr. Srinivas Dharavath were always willing to do the same.

My graduate advisory committee members, Dr. Eric Brown and Dr. Ryan Wylie have been hugely supportive over the course of my degree, and have facilitated my learning and critical thinking at every interaction, for which I owe them my gratitude. I am also very thankful to Dr. Brent Weber, my collaborator and the origin of the project that created the bulk of my work as a graduate student. He has been a wealth of

Table of Contents

List of Figures

List of Schemes

List of Abbreviations and Symbols

CDC – Centers for Disease Control and Prevention

WHO – World Health Organization

FDA – Food and Drug Administration

nm – nanometres

µM – micrometres

CE – common era

MRSA – Methicillin-Resistant *Staphylococcus aureus*

OM – outer membrane

ESBL – Extended-spectrum ß-lactamases

Tris/EDTA – tris(hydroxymethyl)aminomethane/ethylenediaminetetraacetic acid

LPS – lipopolysaccharide

Fe^{3+} – iron (III) ion

MIC – minimum inhibitory concentration

HQ – hydroxyquinoline

XDR – extensively drug-resistant

PDR – pan drug-resistant

DCM – dichloromethane

MeOH – methanol

pKa – Acid dissociation constant

PEG – polyethylene glycol

HBTU – hexafluorophosphate benzotriazole tetramethyl uronium

TBS – tert-butylsilyl protecting group

CAS – chrome azurol S assay

$NaHCO_3$ – sodium bicarbonate

NaH – sodium hydride

rt – room temperature

BuOH – butanol

HCl – hydrochloric acid

o/n – overnight

SAR – structure-activity relationship

LCMS – liquid chromatography/mass spectrometry

DCE – dichloroethane

THF – tetrahydrofuran

MAO – monoamine oxidase

CBG – cannabigerol

Al_2O_3 – alumina (aluminum oxide)

mCPBA – meta-chloroperoxybenzoic acid

THB – tri-n-butyltin hydride

AIBN – azobisisobutyronitrile

NMR – nuclear magnetic resonance

TNF – tumor necrosis factor

NaOMe – sodium methoxide

Declaration of Academic Achievement

1) Magolan, J., Jentsch, N., Zhang, X., Piotrowski, M. L., Darveau, P., Fragis, M., Johnson, J. W., Ritchie, N., & **Kaul, A.** Processes for the preparation of ortho-allylated hydroxyl aryl compounds (2021). WO 2021/237371, filed 5/28/2021, published 12/02/2021.

   Patent filed to protect alumina chemistry, on which I was named an inventor for my contribution of the synthesis of prenylated coumarin natural products.

2) **Kaul, A.**, D'Souza, R., Piotrowski, M. L., & Magolan, J.

   Manuscript regarding the synthesis of prenylated coumarin derivatives using alumina chemistry, comprising Chapter 2 of this thesis, is in preparation. Optimization of these reactions will be carried out by Dr. Mathew Piotrowski in the coming months. Expected to be published in 2022.

3) Weber, B. S., **Kaul, A.**, Johnson, J. W., Ritchie, N., Magolan, J., & Brown, E. D.

   Manuscript regarding the synthesis of novel sideromycins and their evaluation in human serum, comprising Chapter 1 of this thesis, is anticipated in the coming year. Any remaining syntheses will be carried out by Nikki Ritchie in the Magolan Lab.

Chapter 1: Synthetic Sideromycins

1.1: Introduction

1.1.1: Antimicrobial resistance is a growing concern

Antimicrobial resistance is a growing concern in the world today. According to the Centers for Disease Control and Prevention (CDC), 2.8 million people develop an antibiotic-resistant infection every year in the United States ("Antibiotic Resistance Threatens Everyone", 2021). The World Health Organization (WHO) estimates that by 2050, 10 million deaths per year are projected to occur due to antibiotic resistance ("New Report Calls for Action", 2019). These statistics contextualize the threat to the healthcare system imposed by this crisis. Given the importance of addressing this issue globally, the WHO has instituted a variety of initiatives to help mitigate antimicrobial resistance and is actively involved in aiding countries develop their own action plans ("Antibiotic Resistance", 2020). While a variety of factors are involved in the development of treatment-resistant strains of bacteria, three are prevalent:

(1) Excess use of antibiotics due to overprescription by physicians – a study conducted by the CDC in 2016 demonstrated that overprescription accounts for more than 30% of outpatient antibiotics prescribed in the US (Levy, 1998; Ventola, 2015; Harris et al., 2016; Ferrara, 2017).

(2) Unregulated access in developing countries – in Bangladesh, a study found that in a sample of children hospitalized with diarrhea, only 6% of those who took

antibiotics at home were provided prescriptions (Levy, 1998; Ventola, 2015; Lucas et al., 2019).

(3) Overuse use in agriculture – it is estimated that 80% of the world's antibiotics are utilized in animal husbandry (Levy, 1998; Ventola, 2015; Collignon, 2015).

Antibiotic stewardship consists of the judicious administration of an appropriate antibiotic treatment for an appropriate duration of time, which slows the spread of resistance (Doron and Davidson, 2011; Pollack and Srinivasan, 2014). However, antibiotic stewardship must be paired with continuous research and development of novel antibiotics to combat the ultimately inevitable emergence of resistance.

Despite the ever-increasing need for new antibiotics to help curb this growing pandemic, the approval of new candidates by the US Food and Drug Administration (FDA) decreased over time from 16 between 1983 and 1987 to only 2 between 2008 and 2012 (Spellberg, 2012; Durand et al., 2019). Moreover, the elucidation of novel classes of antibiotics has faced a considerable drought, with no significant discoveries since the 1980s (Durand et al., 2019).

Unfortunately, there is a lack of financial incentive for major pharmaceutical companies to invest in antibiotic development. This is due in part to the short-term nature of their use which contrasts with other, more profitable medications that are administered for longer durations (Collignon, 2015). In addition, concerns with the emergence of resistance result in limited use of novel antibiotics which further limits financial returns for a drug maker (Conly et al., 2005; Doron and Davidson, 2011).

1.1.2: The history of antibiotic resistance

Antibacterial microbes were used in the treatment of disease in ancient civilizations (Sengupta et al., 2013). Traces of the antibiotic tetracycline (Figure 1) were found on bone samples from a member of an ancient population that occupied modern-day Sudan, dated to 350-550 CE (Nelson et al., 2010). Antibiotic resistance genes have been found in mummies dated to the 11th century encoding antibiotic-degrading enzymes such as ß-lactamases and have even been observed in permafrost in Canada as old as 30,000 years (D'Costa et al., 2011; Santiago-Rodriguez et al., 2015; Perry et al., 2016).

penicillin

streptomycin

methicillin

tetracycline

vancomycin
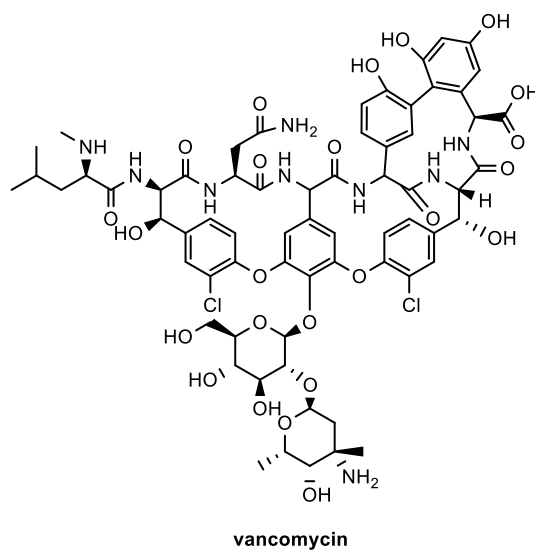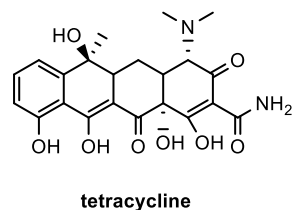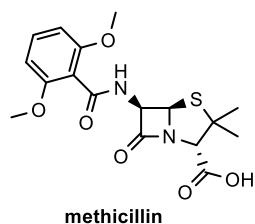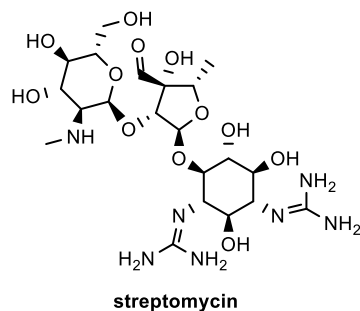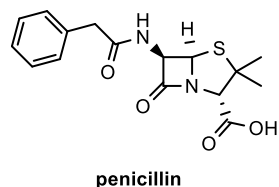
Figure 1: Structures of various antibiotics against which some bacterial strains have demonstrated resistance.

The modern history of antibiotics originates with the discovery of penicillin (Figure 1) by Alexander Fleming from a fungus of the genus *Penicillium* in 1928 (Sengupta et al., 2013; Ventola, 2015; Landecker, 2016). Penicillin became widely produced and used for the treatment of infections by the 1940s and was quickly incorporated as an important tool during the Second World War for treating soldiers (Ventola, 2015; Landecker, 2016). By the end of the decade, however, many instances of resistant strains to penicillin were recorded (Knowles, 1985). Alongside this commercialization of penicillin through the 1940s, Selman Waksman developed a screening platform that led to the discovery of streptomycin (Figure 1; Comroe Jr., 1978). This platform of elucidating antimicrobial candidates from soil-based organisms facilitated the discovery of hundreds of antibiotics and led Waksman to a Nobel prize in 1952 (Comroe Jr., 1978).

Methicillin (Figure 1), a common clinical antibiotic, was introduced in 1960, and only two years later, one of the most common resistant strains, Methicillin-resistant *Staphylococcus aureus* (MRSA) was identified (Ventola, 2015, Morehead and Scarbrough, 2018). Similar problems were observed with vancomycin (Figure 1), which is often used to target MRSA to overcome its methicillin resistance (Giuliano et al., 2010). It was isolated in 1972, and resistant strains of bacteria were observed in 1988 (Ventola, 2015; Morehead and Scarbrough, 2018).

With the gap in antibiotic discovery broadening over time due to the aforementioned lack of novel classes being developed since the 1980s (Durand et al., 2019), extensively drug-resistant (XDR) and pan drug-resistant (PDR) strains were observed as early as the 2000s (Ventola, 2015; Morehead and Scarbrough, 2018).

Given the continual evolution of resistance alongside antibiotic discovery, drug-discovery researchers must seek out new molecules that can kill resistant strains. This research project falls within that broad objective. The goal of this project is to synthesize novel antibiotic candidates that can kill treatment-resistant bacteria.

1.1.3: Challenges with killing Gram-negative bacteria

Bacteria are classified as Gram-positive and Gram-negative based on retention of Gram stain – Gram-positives retain it, while Gram-negatives do not (Popescu and Doyle, 1996). This staining process reflects structural features – the dye colors the peptidoglycan of the cell walls (Popescu and Doyle, 1996). Since Gram-positives have a large cell wall on the outside of their cell membrane (Silhavy et al., 2010), they hold the stain and demonstrate the associated color (Popescu and Doyle, 1996). However, Gram-negatives have an outer membrane (OM) surrounding a thinner cell wall and inner membrane, which does not allow for significant stain retention (Popescu and Doyle, 1996; Ventola, 2015).

Bacteria demonstrate various resistance mechanisms that prevent cell death upon exposure to toxins and antibiotics. These include:

(1) Production of enzymes that structurally modify or degrade antibiotics, including Extended-Spectrum ß-Lactamases (ESBLs) and Metallo-ß-Lactamases (Levy, 1998; Alanis, 2005; Hopwood, 2007).

(2) Efflux pumps that remove toxins entering the cell (Levy, 1998; Alanis, 2005; Hopwood, 2007; Lin et al., 2019).

(3) Modification of the receptor or target of the antibiotics within the cell to prevent binding and subsequent cell death (Alanis, 2005; Hopwood, 2007).

These resistance mechanisms are encoded in the bacterial genome. Resistance can be conferred from resistant to non-resistant bacterial cells through several gene transfer

mechanisms (Hopwood, 2007). Typically, three main methods of gene transfer are observed:

(1) Conjugation: Genes involving resistance mechanisms are encoded into small transposable elements called plasmids. The formation of a sex pilus between two bacterial cells allows for the transfer of plasmids from the resistant cell to the non-resistant. The plasmid can then be incorporated into the cell's own genome (Alanis, 2005; Hopwood, 2007).

(2) Transformation: Cellular components are released into the extracellular space. Adjacent bacterial cells can uptake free DNA, after which it can be added to their own genome (Bolla et al., 2011).

(3) Transduction: External vectors such as viral bacteriophages infect bacterial cells. Upon merging of their genome, some genes belonging to the host cell may be replicated along with the viral genes in the reproduced bacteriophages, and subsequently transmitted to other bacterial cells (Hemaiswarya and Doble, 2009).

Furthermore, the dual-membrane structure of Gram-negative bacteria makes them additionally difficult to target with traditional antibiotics. Interactions between sequestered cations and neighbouring negatively charged lipopolysaccharides (LPS) located along the outward face of the OM create a strong barrier (Hancock, 1997; Ruiz et al., 2006). Coupled with the aforementioned resistance mechanisms present in bacteria, killing Gram-negatives therefore presents a formidable challenge. As such, careful antibiotic design in addition to the development of novel antibacterial activity mechanisms is required to effectively kill such strains.

1.1.4: Existing strategies to target Gram-negative bacteria

There are various existing strategies to target Gram-negative bacteria, including but not limited to the following:

(1) Blocking efflux pumps to prevent removal of antibiotics entering the cell. This has been studied in a variety of species, including *P. aeruginosa*, in which the MexAB-OprM pump has been blocked using peptidomimetics to improve the retention of fluoroquinolone antibiotics such as ciprofloxacin (Bolla et al., 2011).

(2) Membrane permeators in conjunction with antibiotics. The former increases the permeability of the membrane to the latter. Eugenol is one such compound that has been used in conjunction with the ß-lactam antibiotic nitrocefin (Hemaiswarya and Doble, 2009; Bolla et al., 2011).

(3) Membrane disruptors to destabilize the OM structures. Tris/EDTA has been utilized to diffuse LPS from the OM, which the bacteria replace with phospholipids that are more permeable to antibiotics (Bolla et al., 2011).

(4) Polymyxins have been used to destabilize interactions between LPS and cations and have fatty tails that embed them into the membrane. Polymyxins are also opsonins and consequently recruit phagocytes to the site of the bacteria. However, both of these membrane disruptors have major downsides – Tris/EDTA is globally cytotoxic, and polymyxins are acutely nephrotoxic (Bolla et al., 2011).

Aside from these strategies, a well-known strategy that has recently gained much attention is that of the sideromycins.

1.1.5: Sideromycins as a strategy for Gram-negative permeation

Sideromycins consist of a drug covalently bound to a siderophore, a small organic molecule that chelates iron (Fe^{3+}) ions into stable complexes that can travel through the OM of Gram-negative bacteria (Figure 2; Braun et al., 2009; Lin et al., 2019). Often, the antibiotics in sideromycins are ineffective against Gram-negatives, and antibacterial activity is induced through achieving access past their membranes, upon which the covalent linkage may be cleaved, and the antibiotic binds to its target or receptor (Lin et al., 2019).
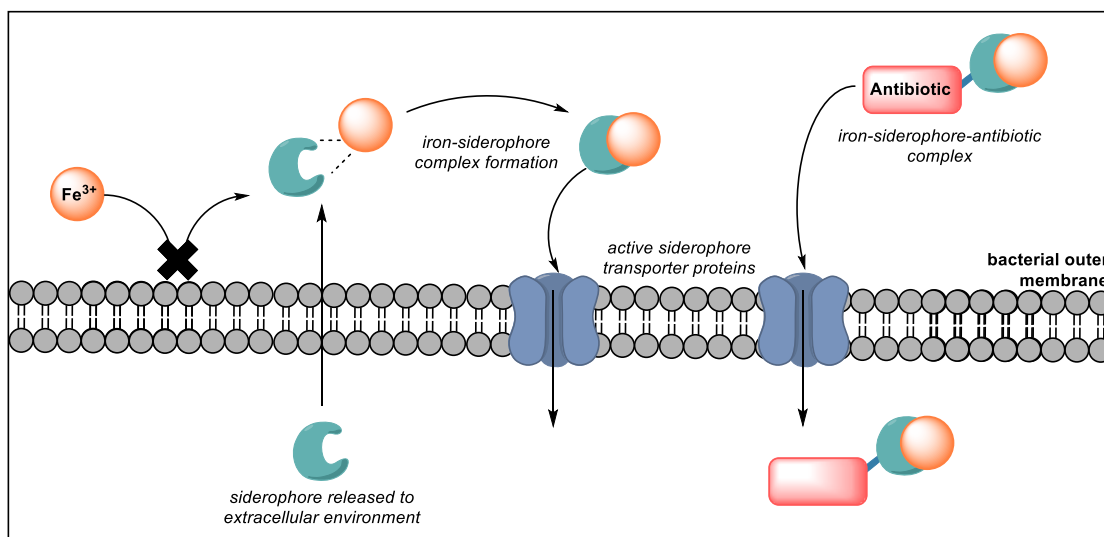
Figure 2: Siderophore being released from the cell, recruiting iron (III) and active siderophore transporters conducting reuptake of the complex. The same is demonstrated with a drug attached to the siderophore in a Trojan Horse strategy (right), and the conjugated "sideromycin" demonstrates uptake via the same active transport mechanism. Figure adapted with permission from Dr. Jarrod Johnson in the Magolan Lab.

Sideromycins can be naturally found. It is theorized that bacteria produce sideromycins such as the albomycins to compete with other species (Figure 3; Chater, 2006; Braun et al., 2009; Lin et al., 2019). Sideromycins compete with siderophores for active siderophore transport channels (Figure 2), which allow for entry through the Gram-negative dual membrane structure (Chater, 2006; Braun et al., 2009). In an experiment conducted by Lin et al. (2018), the albomycins were tested against a variety of Gram-positive and Gram-negative pathogens, with ciprofloxacin used as a control. It was found that both had comparable activities, and similar minimum inhibitory concentrations (MICs) were observed in *Neisseria gonorrhoeae* strain ATCC 49226 (Figure 3; Lin et al., 2018).
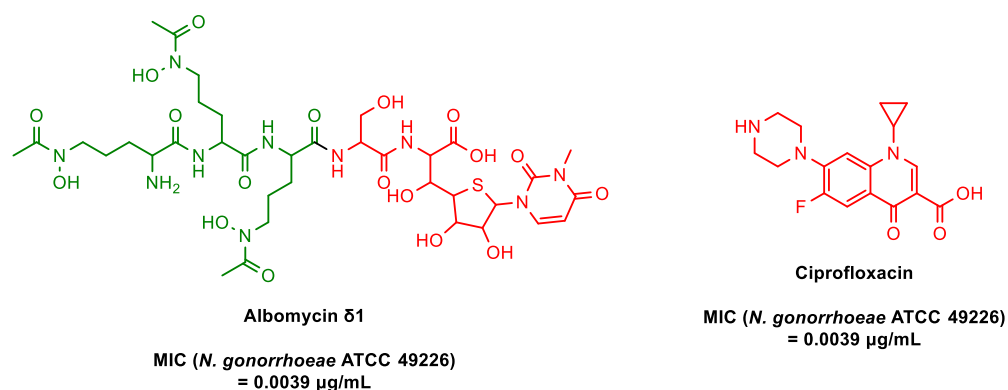
Figure 3: The structure of albomycin δ1, one of the earliest naturally discovered sideromycins, with the siderophore hydroxamate functionalities highlighted in green and antibiotic in red. After entry, albomycin's mechanism of activity involves tRNA synthetase inhibition (Saha et al., 2020). Similar MICs are observed to ciprofloxacin, observed on the right (Lin et al., 2018).

Research into the development of synthetic sideromycins has been prevalent for decades. In this section, such sideromycins are detailed with a comparison of MICs between the antibiotic and the conjugate, similarly to albomycin (above, Figure 3). In some cases, this data was not readily available, and in others, it was difficult to obtain data for the specific antibiotic used in conjugation. Consequently, data for a similar screened antibiotic is provided where possible. Finally, it was not possible to consistently highlight the same strain of bacteria tested for MIC data.

One of the earliest examples of a synthetic sideromycin is a trihydroxamate siderophore conjugated to a sulfonamide antibiotic made by Zahner in 1977 (Figure 4; Zahner et al., 1977; Möllmann et al., 2009). Due to its hexadentate coordination, iron (III) requires a trimer of siderophores to form a stable complex (Moulinet d'Hardemare et al., 2012), and the trihydroxamate structure of this antibiotic conjugate greatly improves siderophore molecular economy required to form a stable iron complex (observable in Figure 4). However, Zahner's conjugation of the siderophore to the antibiotic was found to worsen antibiotic activity. This was especially noted when the siderophore and antibiotic functionalities were bound without a linker creating distance between the two functionalities (Zahner et al., 1977; Möllmann et al., 2009).
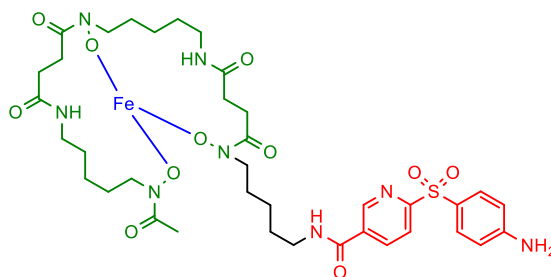
Figure 4: A sideromycin conjugate consisting of a sulfonamide antibiotic coupled to a trihydroxamate siderophore. Siderophore in green, antibiotic in red, chelated iron bound to the trihydroxamate siderophore in blue (Zahner et al., 1977).

Catechols have also been widely used in antibiotic research and have been a major siderophore conjugate in synthetic sideromycin design (Conly and Johnston, 2005; Möllmann et al., 2009). One of the early examples of the use of catechols in sideromycins was published in 1986, when Ohi et al. documented the syntheses and evaluation of ureidopenicillin-catechol conjugate sideromycins (Figure 5; Ohi et al., 1986). A structurally similar penicillin derivative was used as a control in the screening of the conjugate. It was discovered that the sideromycin demonstrated an MIC of 0.2 µg/mL in the tested bacteria, relative to 200 µg/mL for the control (Figure 5, Ohi et al., 1986).

This novel strategy was extended to other ß-lactams only a year later, when Watanabe et al. (1987) synthesized E-0702, a catechol and cephalosporin conjugate (Figure 5; Watanabe et al., 1987). Testing against cefoperazone, an antibiotic of relatively similar structure revealed high potency, with an MIC of 0.1 µg/mL relative to the antibiotic's 6.25 µg/mL in *P. aeruginosa* PAO1 (Watanabe et al., 1987).
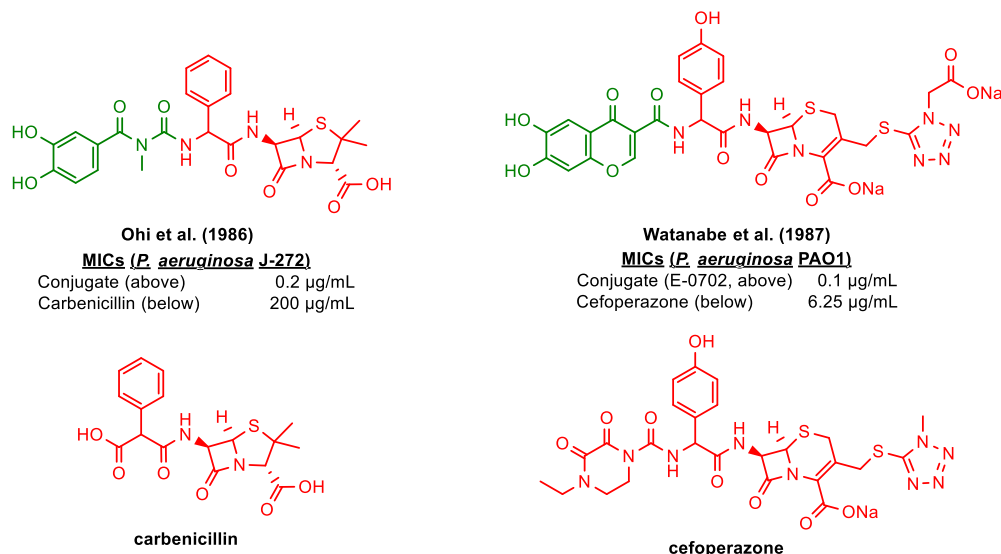
Figure 5: Early catechol and ß-lactam conjugates, with the siderophores indicated in green and the antibiotics in red (Ohi et al., 1986; Watanabe et al., 1987). MICs for control antibiotics as well as the sideromycins are indicated for comparison of the conjugation strategy.

Kinzel et al. (1998) utilized a siderophore produced by *Pseudomonas aeruginosa* called pyoverdine to make conjugates (Kinzel et al., 1998). One of these conjugates (Pv9446SebAmp) is highlighted below (Figure 6). This sideromycin contains a relatively simple ampicillin antibiotic attached to a pyoverdine derivative using a simple acid linker (Mislin and Schalk, 2014). Compared to the antibiotic alone (MIC = >100 µM), Pv9446SebAmp demonstrates considerably more potent activity (MIC = 0.39 µM, or 0.67 µg/mL), highlighting the efficacy of the conjugation of the pyoverdine.
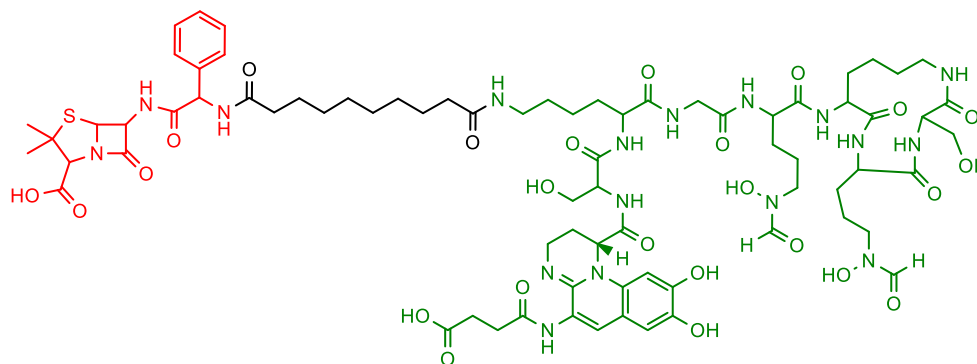
Pv9446SebAmp (Kinzel et al., 1998)

MICs (*P. aeruginosa* PAO1)
Ampicillin   >100 µM
Pv9446SebAmp   0.39 µM
(equivalent to 0.67 µg/mL)

Figure 6: Kinzel's pyoverdine conjugate, with the siderophore pyoverdine derivative indicated in green and the antibiotic in red (Kinzel et al., 1998; Ji et al., 2012). MICs are indicated below the figure to compare the antibiotic and sideromycin (Kinzel et al., 1998; Ji et al., 2012).

Siderophore trimers are also naturally observed. Species of Gram-negative bacteria such as *Salmonella typhimurium* and *Escherichia coli* secrete enterobactin, a catechol trimer to uptake extracellular iron (Figure 7; Raymond et al., 2003; Moulinet d'Hardemare et al., 2012). Enterobactin has been extensively studied to develop an understanding of the iron transport pathway using active siderophore transport channel proteins on bacterial cell membranes (Raymond et al., 2003). A siderophore trimer mimicking enterobactin was conjugated with ampicillin by Ji in 2012 (Figure 7; Ji et al., 2012), improving its MIC against *P. aeruginosa* greatly.
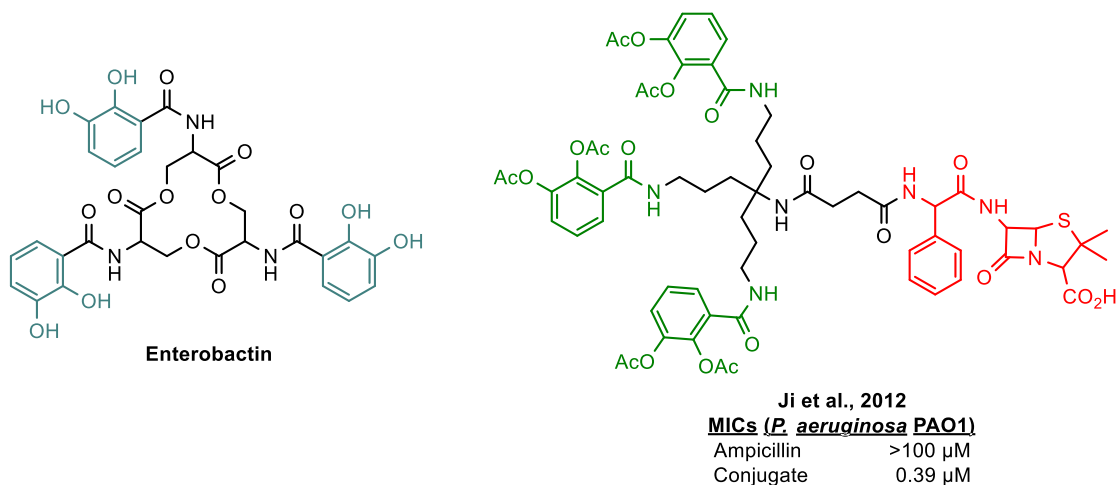
Figure 7: Enterobactin, a catechol trimer secreted naturally by E. coli (left; Moulinet

d'Hardemare et al., 2012) and an enterobactin mimic-ampicillin antibiotic conjugate

(right). In the enterobactin figure (left), iron chelating functionalities are indicated in blue.

In the sideromycin (right), siderophore functionalities are indicated in green and the

antibiotic in red (Ji et al., 2012).

Zheng and Nolan (2014) also developed enterobactin-ampicillin/amoxicillin

conjugates, with a PEG chain serving as the linker (Figure 8). It was found that, relative

to the antibiotic control, the conjugate decreased the minimum inhibitory concentration

(MIC) by 1000-fold in the tested strain of *E. coli* in the amoxicillin analog, highlighted in

the figure below (Zheng and Nolan, 2014).
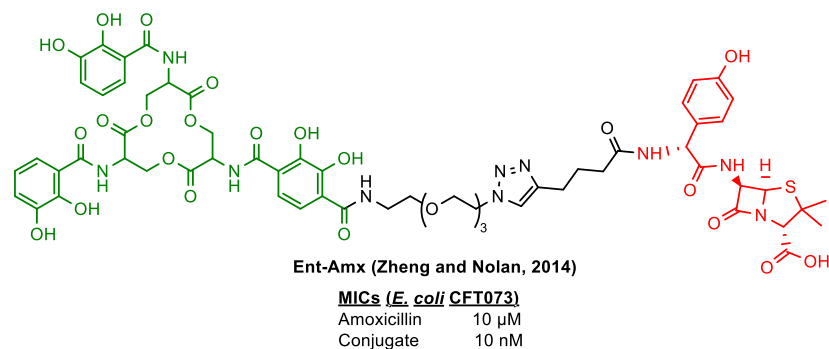
Figure 8: Zheng and Nolan's enterobactin conjugate, with the siderophore indicated in green and the antibiotic in red (Zheng and Nolan, 2014). MICs in a strain of *E. coli* are indicated below the figure.

Interestingly, heterogeneous (mixed ligand) siderophore trimers have also been developed in conjugation with antibiotics. Schobert et al. published the synthesis of a penicillin-biscatechol-hydroxamate mixed-ligand sideromycin in 2006 (Figure 9; Schobert et al., 2006).
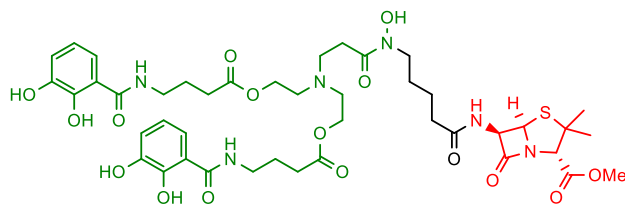
Figure 9: Schobert et al. (2006) made a mixed ligand sideromycin. Mixed siderophore ligand indicated in green, and the antibiotic in red.

Mixed siderophore conjugates have been researched extensively in the last decade. In 2013, Wencewicz and Miller published a synthesis of a similar bis-catechol/hydroxamate-cephalosporin sideromycin, as well as the synthesis of the same

siderophore conjugated to ciprofloxacin, a fluoroquinolone antibiotic (Figure 10; Wencewicz and Miller, 2013). Though the ß-lactam sideromycin demonstrated increased potency against the strain of *A. baumannii* tested, the fluoroquinolone analog was a much poorer antibiotic than its control (Wencewicz and Miller, 2013).
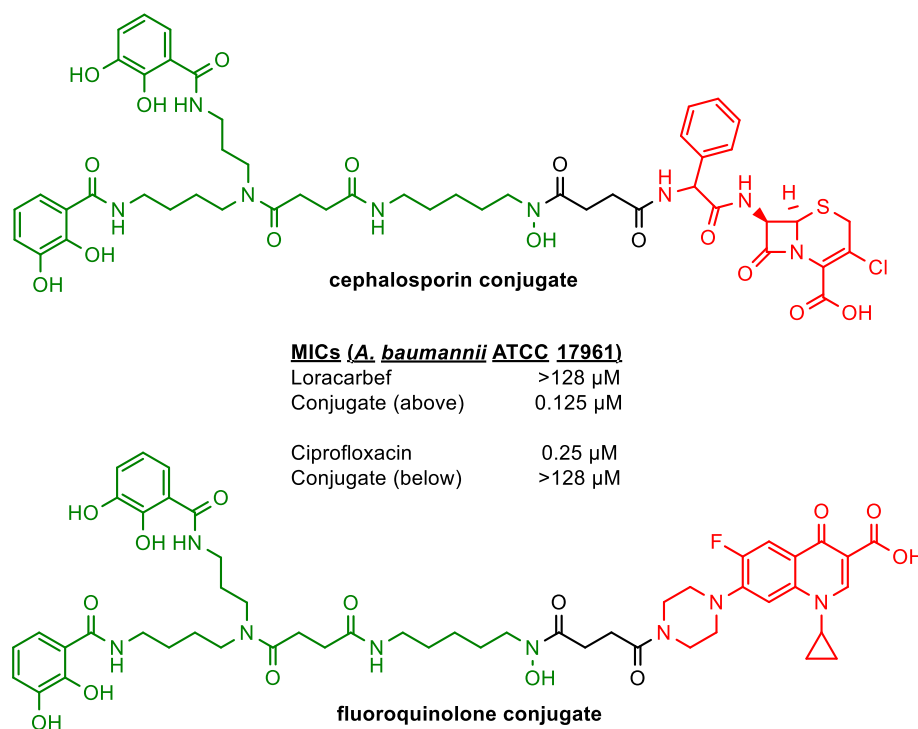
Figure 10: Wencewicz and Miller (2013) mixed ligand sideromycins with ß-lactams and fluoroquinolones. Mixed ligand siderophore trimer indicated in green, and both antibiotics indicated in red. MIC data against antibiotic controls is highlighted.

This was followed closely by the conjugation of the siderophore to daptomycin in 2017 (Figure 11), and teicoplanin in 2020 (Figure 12; Ghosh et al., 2017; Ghosh et al., 2020). Both of these are significantly larger molecules than any of the aforementioned antibiotics and have different mechanisms of action – daptomycin is a lipopeptide, and

teicoplanin is a glycopeptide. Both demonstrated strong efficacy against their respective strains of *A. baumannii* relative to their antibiotic controls (Ghosh et al., 2017; Ghosh et al., 2020).
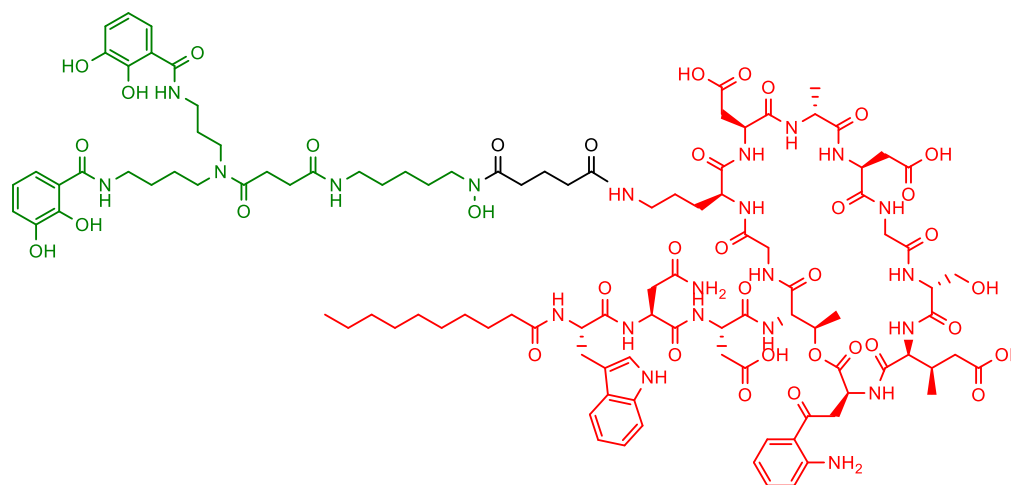
Daptomycin conjugate, Ghosh et al. (2017)

MICs (*A. baumannii* ATCC 17961)

Daptomycin	>100 µM
Conjugate	0.4 µM

Figure 11: Ghosh et al. daptomycin and mixed siderophore ligand conjugate (Ghosh et al., 2017). Siderophore ligand indicated in green and antibiotic in red. A comparison of MIC data for the conjugate is highlighted against a strain of *A. baumannii*.
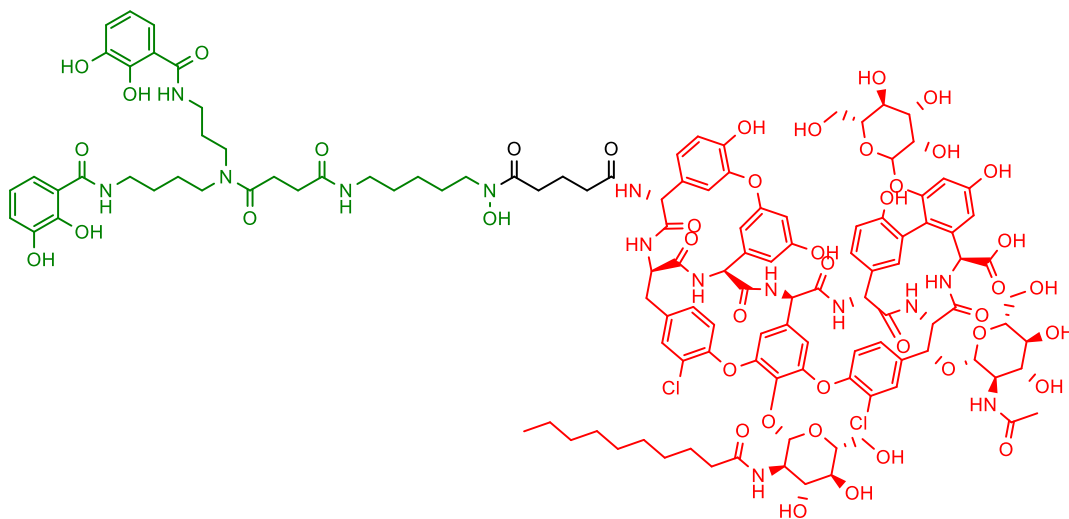
Teicoplanin subunit A$_2$-3 conjugate, Ghosh et al. (2020)

MICs (*A. baumannii* ATCC BAA1793)	
Teicoplanin	>50 µM
Conjugate	0.8-1.6 µM

Figure 12: Ghosh et al. teicoplanin and mixed ligand conjugate (Ghosh et al., 2020). Siderophore ligand indicated in green and antibiotic in red. A comparison of MIC data for the conjugate is highlighted against a strain of *A. baumannii*.

For more information about sideromycins and their development, a paper by Lin et al. (2019) entitled "Synthetic sideromycins (skepticism and optimism): selective generation of either broad or narrow spectrum Gram-negative antibiotics" is an excellent resource (Lin et al., 2019).

Sideromycins are currently a topic of interest in the scientific community due to the recent FDA approval of the synthetic sideromycin cefiderocol (Fetroja, Figure 13) in 2018 as an antibiotic (FDA, 2018). This is the first instance of the FDA approving a synthetic sideromycin for clinical use. Cefiderocol consists of a ß-lactam antibiotic

covalently bound to a catechol siderophore using a quaternary amine pyrrolidine linker, indicated in red, green, and black respectively in Figure 13 (below).
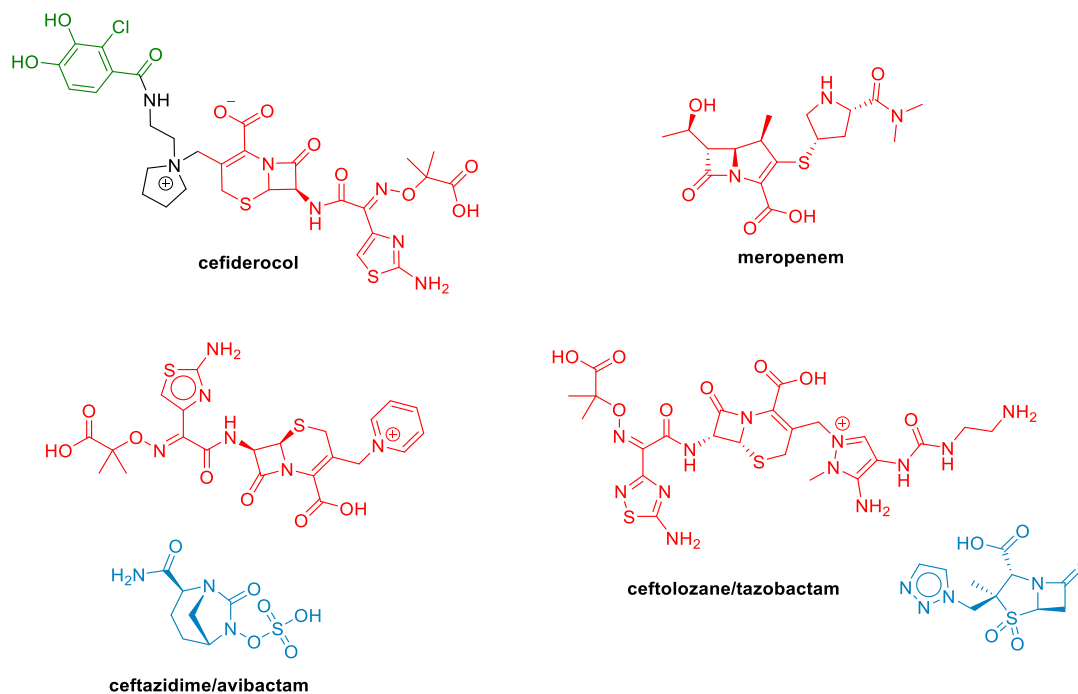
Figure 13: Cefiderocol (Fetroja, top left), a synthetic sideromycin that became approved by the FDA in 2018 (FDA, 2018). Meropenem (top right) is another potent antibiotic, and two antibiotic/ ß-lactamase inhibitor combinations have been highlighted in ceftazidime/avibactam (bottom left) and ceftolozane/tazobactam (bottom right). The siderophore is indicated in green, antibiotics in red, and ß-lactamase inhibitors in blue.

A recent study conducted by Wu et al. found that cefiderocol demonstrated an MIC range of ≤ 0.002–4 µg/mL when screened against more than 1500 North American strains of *K. pneumoniae*, compared to a range of ≤ 0.06 to > 64 µg/mL for meropenem (Figure 13), a particularly potent ß-lactam used in aggressive treatment of infection (Wu

et al., 2020). Cefiderocol was further compared to the β-lactam antibiotic/β-lactamase inhibitor combinations ceftazidime/avibactam and ceftolozane/tazobactam (Figure 13), both of which demonstrated considerably lower potencies against *K. pneumoniae* (≤ 0.06 to 8 µg/mL and ≤ 0.06 to > 64 µg/mL respectively; Wu et al., 2020). Similar results were found in over 1500 tested strains of *P. aeruginosa*, as cefiderocol demonstrated an MIC range of ≤ 0.002 to 4 µg/mL, improving on each of the aforementioned therapies by an order of magnitude (≤ 0.06 to > 64 µg/mL for meropenem, 0.12 to > 64 µg/mL for ceftazidime/avibactam, and ≤ 0.06 to > 64 µg/mL for ceftolozane/tazobactam; Wu et al., 2020). These findings demonstrate the considerable advantage of an optimized sideromycin against Gram-negative pathogens of interest.

Due to this reignited interest in the field, an opportunity exists to explore novel sideromycin candidates. With this goal in mind, Dr. Brent Weber of the Brown Lab at McMaster University screened a variety of compounds to uncover novel or relatively unused siderophores, the findings of which are highlighted in the next section.

1.1.6: Brown Lab screening data

Dr. Weber conducted a screen of 1600 FDA-approved compounds to determine which of these compounds act as bacterial growth promoters (Weber et al., 2020). As growth promoters typically demonstrate increased uptake, the purpose of the screen was to elucidate good candidates for attachment to antibiotics to act as Trojan Horse sideromycins.

This screening was conducted in human serum as opposed to standard *in vitro* broth conditions. Dr. Weber's prior research highlighted the viability of serum as a better predictor of *in vivo* conditions, which consequently produces contextually relevant screening results (Weber et al., 2020). Serum contains a variety of factors that are present in a biological infection model, such as proteases, the complement cascade, and nutrient-sequestering complexes such as transferrins which limit the concentration of extracellular iron available to bacteria (Weber et al., 2020).

Though initially the screen was utilized as a test to contextualize potential antibacterials in conditions that better mimic *in vivo* models, Dr. Weber hypothesized that some of the growth promoters mechanistically behaved as siderophores, and consequently could be utilized in sideromycin development. As such, the use of serum to test siderophores and sideromycins provides a more biologically relevant data pool than standard iron-deficient conditions.

A hydroxyquinoline ether (**5734687/1-23**, Figure 14) was found to be one of the growth promoting hits of the screen. Interestingly, its growth promoting activity is comparable to that of dopamine (Figure 14), a neurotransmitter and potent siderophore

due to its catechol functionality (Dichtl et al., 2019). While catechols are widely used siderophores in sideromycins (Lin et al., 2019), hydroxyquinolines have not been utilized to the same effect.
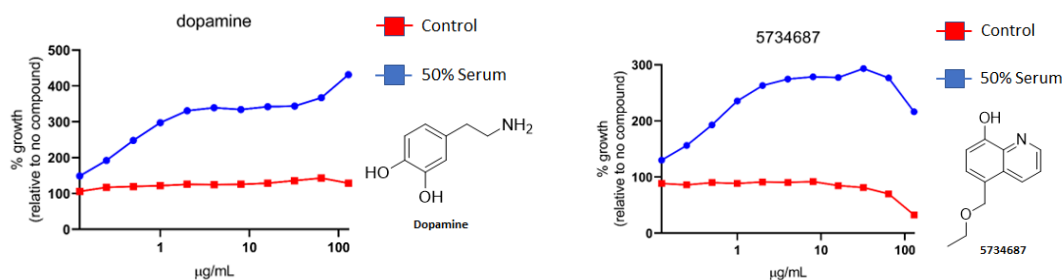
Figure 14: A comparison of *Klebsiella pneumonaie* growth in control broth against serum. Growth was modeled as a function of concentration of dopamine, a known siderophore, or a hydroxyquinoline ether (right). Both are hits on the screening conducted by Dr. Brent Weber. Graphs used with permission of Dr. Brent Weber from the Dr. Eric Brown Lab at McMaster University.

Hydroxyquinoline (HQ) is an iron-chelating molecule with a pyridine joined in an aromatic system with a phenol. The chelating ability of HQ has been used to develop iron-deficient bacterial culture media since the 1940s (Albert, 1950). The use of HQs in medicinal chemistry is well documented, but focuses on anti-fungal (Pippi et al., 2019), anthelmintic (Horta et al., 2015), anti-cancer (Kubanik et al., 2015), and anti-Alzheimer's Disease activity (Deraeve et al., 2008). Some studies exist outlining the use of hydroxy-quinolines in an antibacterial capacity, but the vast majority do not involve antibiotic conjugation and those that do have demonstrated limited efficacy (Shen et al., 1999; Al-Busafi et al., 2014). While there are several studies that attach hydroxyquinolines to an

antibiotic, no growth promotion studies are performed, and the scope is limited (Vu et al., 2019).

Due to the novelty of HQ as a sideromycin conjugate, we hypothesized that a novel class of hydroxyquinoline sideromycins could be synthesized and tested against a variety of Gram-negative strains.

1.2: Results and Discussion

A proof-of-concept sideromycin **1-5** was synthesized with 8-hydroxyquinoline and deacetylated linezolid (Scheme 1). Linezolid is a Gram-positive only antibiotic, and as such, its incorporation into a conjugate makes it a good candidate to test our sideromycin strategy in Gram-negative bacteria. The deacetylated form of linezolid (**1-4**), much like the parent antibiotic, shows no Gram-negative activity. This was attached to the siderophore 8-hydroxyquinoline-7-carboxylic acid (**1-1**) via peptide coupling using HBTU as the coupling reagent (Scheme 1). Purification of these conjugates required column chromatography in dichloromethane/methanol (DCM/MeOH) conditions. Impurities persisted, though recrystallization from dichloroethane (DCE) after column chromatography proved sufficient for purification.
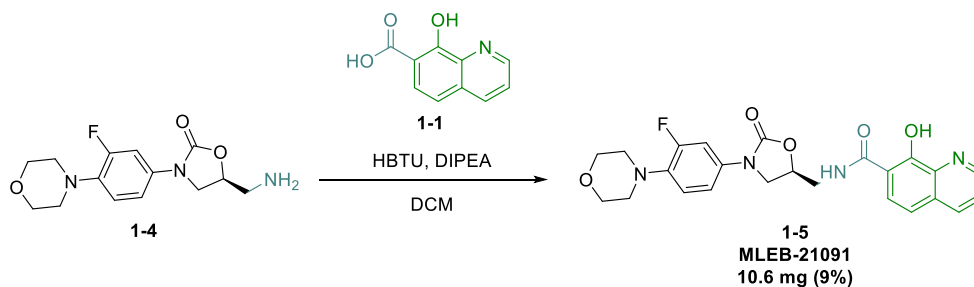
Scheme 1: Synthesis of HQ-linezolid conjugate **5** via peptide coupling. This was synthesized as a proof-of-concept sideromycin.

The siderophore **1-1** was later tested for iron chelation and growth promotion in three strains of *Klebsiella pneumoniae* and *Pseudomonas aeruginosa*, both Gram-negative pathogens. This analog of HQ was a poorer siderophore and growth promoter

than the original hit as well as the parent HQ scaffold. The results of this screen can be found in section 1.3.

However, the completed sideromycin conjugate **1-5** was screened for antibiotic activity by Dr. Weber in the aforementioned strains of bacteria and demonstrated a moderate MIC of 62.5 µM when tested in iron-deficient conditions (Figure 15). These conditions increase the need for siderophore uptake in bacteria (Rodriguez, 2006). Though **1-5** was not a potent antibiotic, this data validated this general approach because antimicrobial activity was clearly observed relative to the parent antibiotic **1-4**.
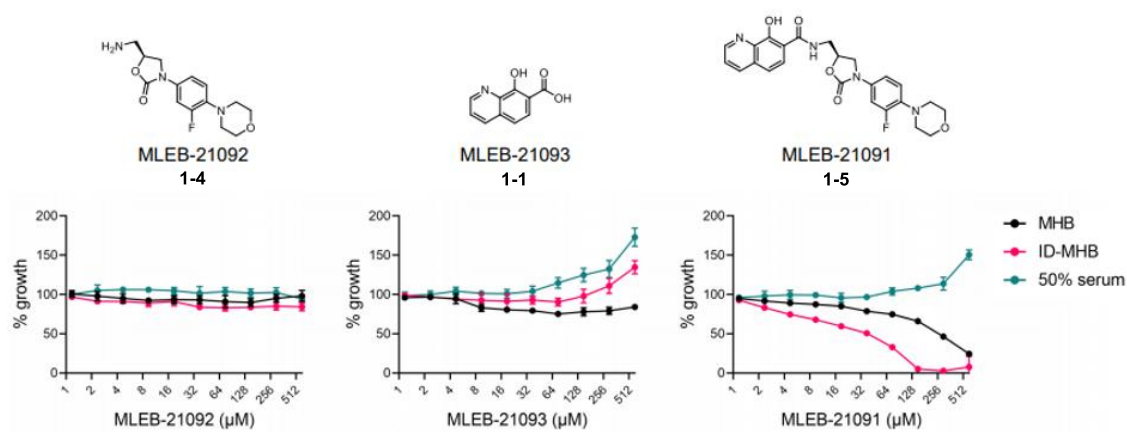
Figure 15: Proof-of-concept sideromycin assay data for the HQ-linezolid conjugate discussed in Scheme 1. Moderate MICs are observed in iron-deficient conditions but growth promotion similar to the HQ is observed in serum, potentially implying protease cleavage. Highlighted example of the assay was conducted in *K. pneumoniae*. Graphs used with permission of Dr. Brent Weber from the Dr. Eric Brown Lab at McMaster University.

Due to the success of the first sideromycin **1-5** in iron-deficient media, HQs were purchased with carboxylic acids at the 2- and 5- positions in an effort to optimize this hit and explore the effects of attachment at different positions on the HQ ring on antibiotic activity of the conjugate (Figure 16).
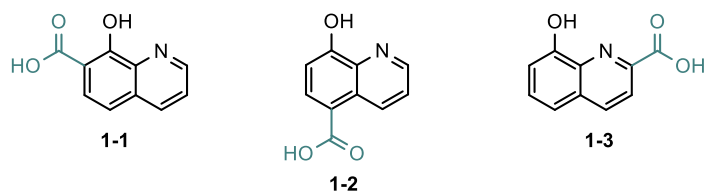
Figure 16: Hydroxyquinoline carboxylic acid starting materials for peptide couplings.

In a similar preparation to the prior analog, these conjugates were synthesized using HBTU-mediated peptide coupling. Purification once again required column chromatography in DCM/MeOH, but recrystallization proved difficult due to low yields. Reverse phase chromatography in water/methanol conditions was conducted to provide the products **1-6** and **1-7** (Scheme 2).
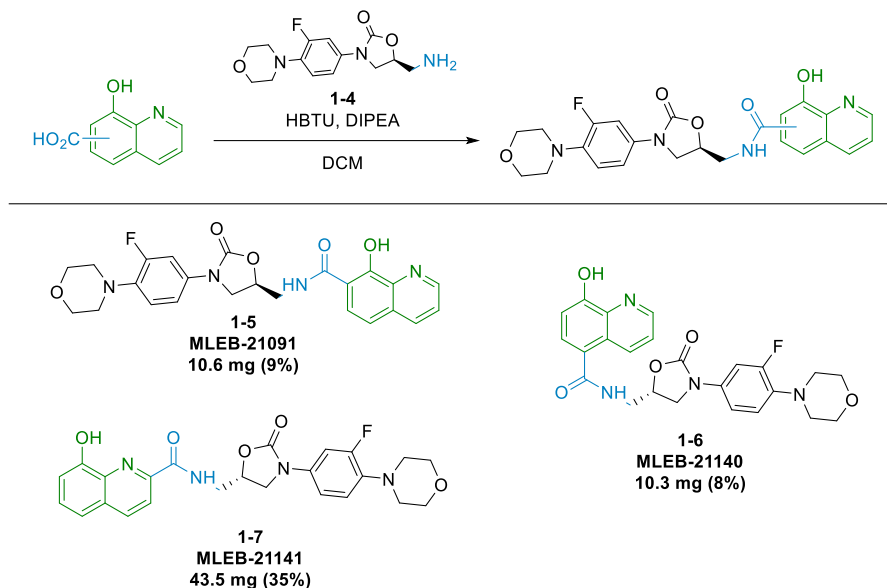
Scheme 2: Synthesis of sideromycins **1-5**, **1-6**, and **1-7** using HQ carboxylic acids, deacetylated linezolid, and HBTU as the coupling reagent.

Though the first analog demonstrated provided a good base to build on, analogs of HQ with the carboxylic acid at different positions on the ring structure yielded no significant activity when bound to deacetylated linezolid (**1-4**, Figure 17). Moreover, none of the linezolid analogs (**1-5** through **1-7**) demonstrated any killing activity in human serum in a subsequent screening by Dr. Weber. Instead, we found that growth promotion occurred in these conditions, and the bacteria began to proliferate at higher concentrations in a pattern resembling that of the unbound siderophore **1-1**, **1-2**, or **1-3** respectively. We hypothesized that the proteases in the serum were cleaving the peptide bond between the siderophores and the linezolids.
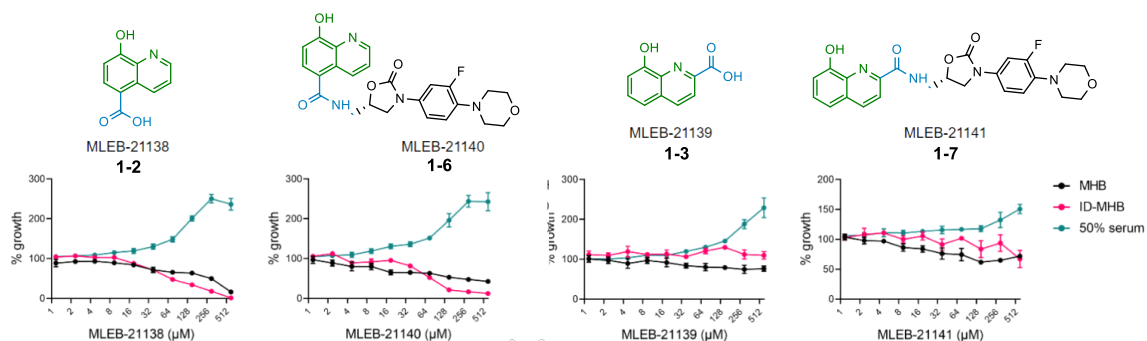
Figure 17: Assay data from two more HQ-linezolid conjugates, demonstrating poor MICs and even growth promotion similar to the control siderophores in human serum. Highlighted example of the assay was conducted in *K. pneumoniae*. Graphs used with permission of Dr. Brent Weber from the Dr. Eric Brown Lab at McMaster University.

The same siderophores were also combined with an alternative linezolid antibiotic conjugated via a piperazine ring functionality (compound **1-8**, Scheme 3). Steric bulk around the peptide linkages of these compounds may reduce the rate of degradation of these compounds via protease cleavage. These "aza-linezolids" were synthesized and purified similarly to the latter deacetylated linezolids. Peptide couplings were again conducted using HBTU, and after column chromatography, products required reverse phase chromatography in water/methanol (**1-9** through **1-11**, Scheme 3). Compound **1-9** was not pure after reverse phase, and recrystallization proved difficult. In the future, a preparatory LCMS purification should be conducted prior to submission.
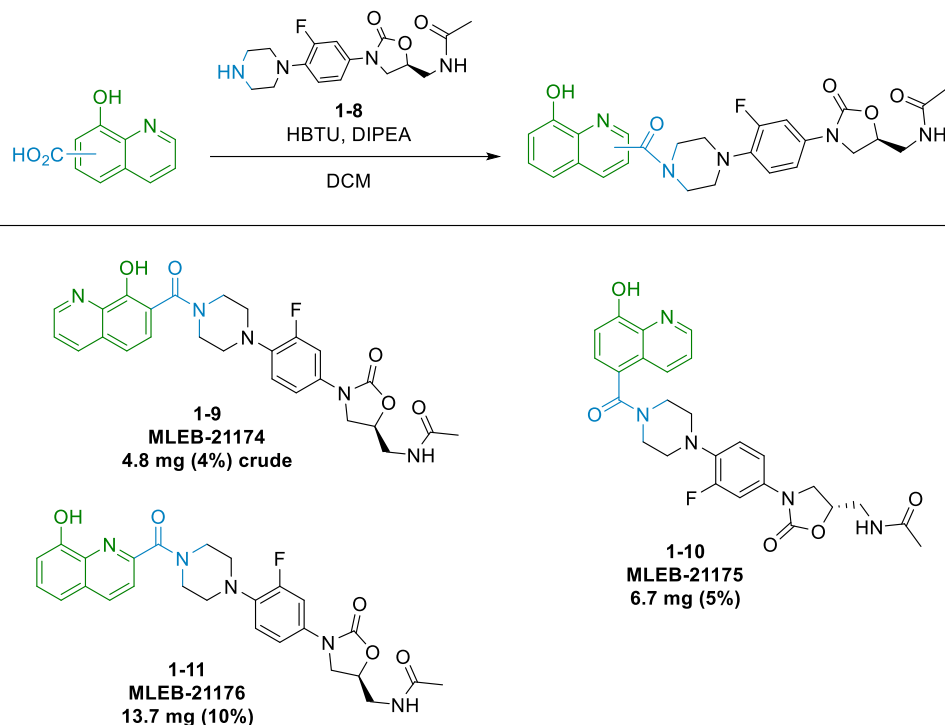
Scheme 3: Synthesis of aza-linezolid sideromycins using HQ carboxylic acids, aza-linezolid, and HBTU as the coupling reagent.

Despite increased steric bulk, **1-10** and **1-11** demonstrated growth promotion in serum similarly to the previous analogs **1-5** through **1-7** in a further screening by Dr. Weber (Figure 18).
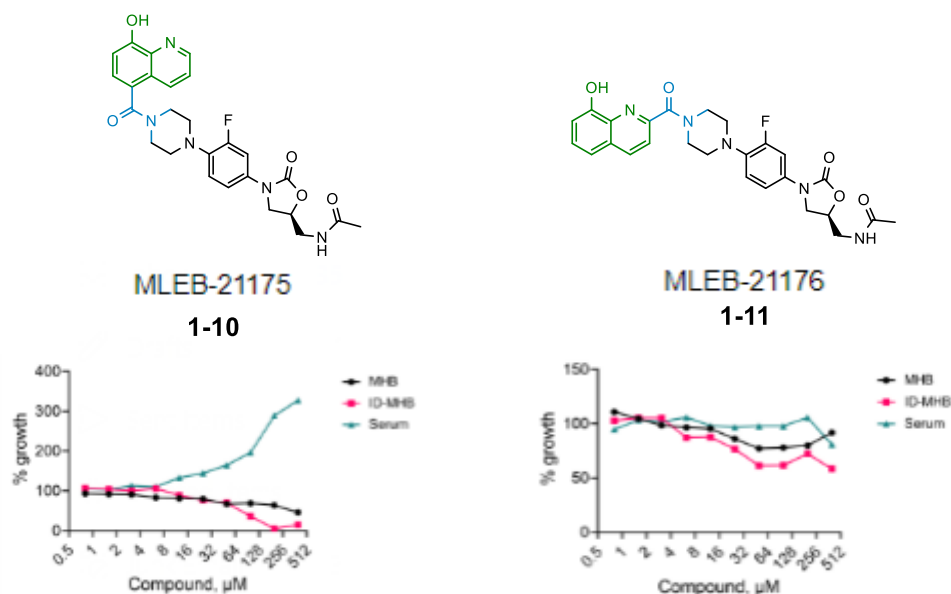
Figure 18: Antibiotic activity data for the aza-linezolid compounds. Similar to the prior compounds, poor MICs and growth promotion in serum are observed. Highlighted example of the assay was conducted in *K. pneumoniae*. Graphs used with permission of Dr. Brent Weber from the Dr. Eric Brown Lab at McMaster University.

The utilization of HQ as a siderophore scaffold proved to be very difficult. The most notable issues were found when performing peptide couplings with antibiotics containing acidic and basic functionalities, such as ß-lactams. Due to the acidic phenol and basic pyridine comprising the HQ backbone, the addition of further functionalities such as the carboxylic acids on ß-lactams (Figure 19) caused great difficulty in synthesis as well as isolation of the products via chromatography.
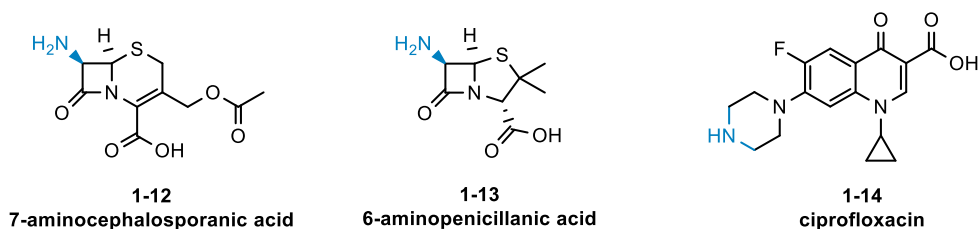
Figure 19: ß-lactams and fluoroquinolones attempted for peptide coupling of hydroxyquinoline acids.

Ciprofloxacin (**1-14**), a fluoroquinolone antibiotic (Figure 19), was also a target for attachment to HQ. However, due to the similar structural features to the ß-lactams in addition to several amines prone to protonation, similar issues were faced in synthesis and purification. Due to pKa ranges and their potential overlap for deprotonation of the acid and protonation of the HQ pyridine, purification at an acidic or basic pH typically does not provide the purifiable product. Peptide couplings with ß-lactams and **1-14** also often did not go to completion despite the usage of various coupling reagents, and NMRs after chromatography were difficult to read.

Consequently, it was deemed necessary to explore other methods of siderophore attachment. An avenue pursued to circumvent serum protease action was conjugation via a triazole ring synthesized using a "click reaction" between an azide and an alkyne (Scheme 4). The click reaction between HQ and ciprofloxacin was attempted. The syntheses of propargyl ciprofloxacin **1-17** and HQ azide **1-16** were conducted prior to this reaction (Scheme 4). The former was synthesized in one step by irradiating ciprofloxacin **1-14** and propargyl bromide in a microwave reactor. The siderophore **1-15** was made after

chloromethylation of stock HQ in one step with zinc chloride, formalin, and concentrated

hydrochloric acid, followed by substitution to institute the azide, forming **1-16**.
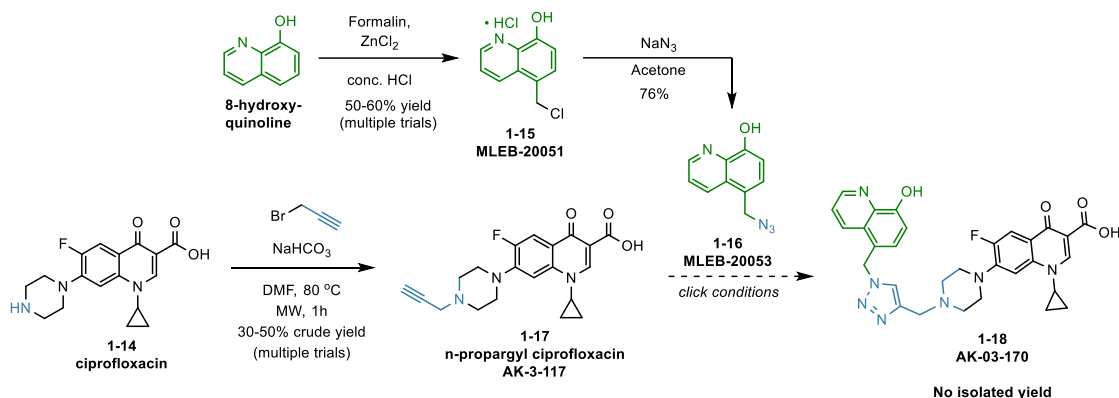
Scheme 4: The synthesis of HQ azide **1-16** and propargylated ciprofloxacin **1-17**,

followed by their click reaction. The synthesis of **1-18** was the target, but product could

not be isolated.

Ratios of reagents such as copper (II) sulfate and sodium ascorbate were varied,

and solvent systems including MeOH/H_2O, THF/MeOH/H_2O, and n-BuOH/H_2O were

attempted (Scheme 4). Reactions did not go to completion based on TLC, and product

was not isolated. To improve yield, a greater-than-stoichiometric ratio of copper catalyst

could be utilized, as the siderophore may be chelating the metal, thereby lowering yield of

the reaction considerably.

Sulfonamide bonds were also selected as an alternative to peptide linkages due to

their resistance to degradation. An 8-HQ-5-sulfonic acid siderophore **1-19** was selected

due to the synthetic feasibility of sulfonamides from sulfonic acids (Scheme 5). A

literature search was conducted to gain insight into HQ sulfonamides, and it was found

that these are somewhat tolerated *in vivo* in embryos of several species with some

evidence of dose-dependent toxicity (Pippi et al., 2020). As the original hit **5734687** was

immediately cytotoxic at high concentrations, the increased tolerability made this

siderophore an attractive target for conjugation to antibiotics. Findings from section 1.3

provide further insight into **1-19** as a strong iron binder and growth promoter.
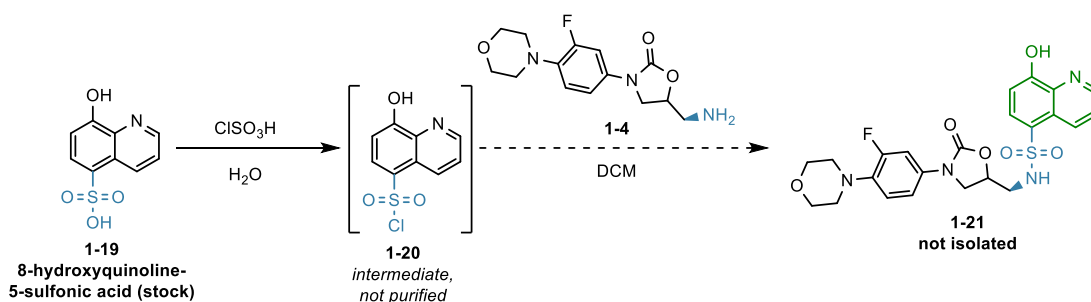
Scheme 5: Synthesis for the discussed sulfonamide conjugate, using a sulfonyl chloride

intermediate **1-20**. Product **1-21** was not able to be isolated.

A linezolid-HQ sulfonamide **1-21** was proposed (Scheme 5). Literature precedent

informed the design of these sulfonamides through a sulfonyl chloride intermediate by

stirring the starting material in chlorosulfonic acid (Aik et al., 2013; Pippi et al., 2020).

As such, **1-20** was synthesized, which was collected as a crude product and moved onto

the antibiotic amine attachment without further purification due to its reactive nature

(Scheme 5). However, it was difficult to purify **1-21**. As per an adapted procedure from

the literature (Pippi et al., 2020), column chromatography was conducted but did not yield

pure product. Despite further purification using preparatory LCMS in neutral water and

acetonitrile, significant impurities persisted as observed via NMR. This continued to be

the case even upon use of an ammonium acetate buffer system to control the aforementioned polarity and pKa-based issues.

To summarize, hydroxyquinoline-based sideromycins were synthesized. However, as HQ has an acidic phenol functionality in addition to a basic pyridine in the ring structure, it is associated with technical synthetic chemistry challenges that are related to high polarity, low solubility in organic solvents, and difficulties with purification using chromatography. As such, only linezolid-based sideromycins were able to be purified completely and screened due to their decreased complexity relative to the structural features of other antibiotic classes such as the fluoroquinolones.

1.3: Side Project – SAR of Hydroxyquinolines

1.3.1: Bioactivity of Hydroxyquinoline Siderophore Analogs
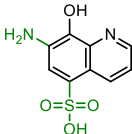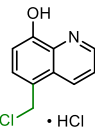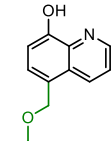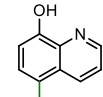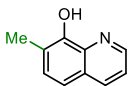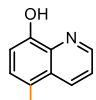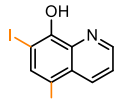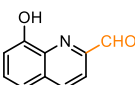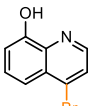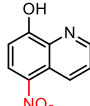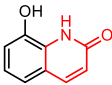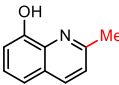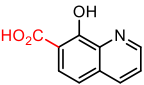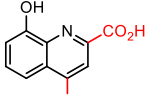
A further project was conducted analogous to the sideromycin study aimed at optimizing the original HQ ether hit **1-23** (alternatively labelled **5734687** or **MAC-0465126**). This study aimed to study the effects of modification at different positions on the HQ ring, as well as the role of different functionalities in iron binding and growth promotion. Though this study is not directly related to the sideromycin project, it is being documented in this thesis for posterity.

Iron chelation was studied by Dr. Weber using a chrome azurol S (CAS) assay, which measures iron binding as a function of color change in a solution, calculated with absorption values obtained by using a spectrophotometer (Patel et al., 2018). The growth promotion was tested by Dr. Weber in three strains of *Klebsiella* and *Pseudomonas*, both Gram-negative pathogens. Findings are observable below (Figure 20).

Two of these analogs were synthesized (**1-15** and **1-16**) and the vast majority were purchased. It was found that three were strong hits – **1-15**, **1-22**, and **1-23**, though the latter is the original ether hit. Each of these demonstrated concentrations equal to or lower than the parent scaffold to achieve the required color change cut-off on the CAS assay (absorbance of 0.3), indicating strong iron binding. The same was found regarding concentrations required to achieve growth promotion in the bacterial strains. Due to differences in growth rates for different strains, *K. pneumoniae* MKP103 data was

collected for concentration required to achieve 200% growth, whereas *K. pneumoniae*

ATCC and *P. aeruginosa* PAO1 were both recorded at 125% growth.

	Scaffold MLEB-20021	1-22 MAC-0461784	1-15 MLEB-20051	1-23 MAC-0465126	1-16 MLEB-20053
CAS assay (μM)	62.5	31.25	62.5	31.25	62.5
Kleb MKP103 (μM)	3.9	3.9	3.9	3.9	15.6
Kleb ATCC (μM)	7.8	1.95	1.95	1.95	7.8
Pseudo PAO1 (μM)	7.8	3.9	<1.95	15.6	62.5

	1-24 MLEB-20023	1-25 MLEB-20027	1-26 MLEB-20028	1-27 MLEB-20029	1-28 MLEB-20036
CAS assay (μM)	31.25	62.5	7.8	15.6	15.6
Kleb MKP103 (μM)	7.8	7.8	31.25	31.25	31.25
Kleb ATCC (μM)	31.25	15.6	62.5	62.5	62.5
Pseudo PAO1 (μM)	31.25	125	125	250	62.5

	1-29 MLEB-20052	1-30 MLEB-20031	1-31 MLEB-20030	1-32 MLEB-20026	1-33 MLEB-20032
CAS assay (μM)	None	31.25	15.6	None	1000
Kleb MKP103 (μM)	62.5	31.25	~250	31.25	62.5
Kleb ATCC (μM)	31.25	31.25	~62.5	62.5	15.6
Pseudo PAO1 (μM)	125	500	None	500	125

	1-34 MLEB-20022	1-1 MLEB-20024	1-35 MLEB-20025	1-36 MLEB-20033	1-37 MLEB-20034	1-38 MLEB-20035
CAS assay (μM)	500	500	None	2000	None	None
Kleb MKP103 (μM)	62.5	250	250	1000	None	None
Kleb ATCC (μM)	62.5	125	62.5	250	None	125
Pseudo PAO1 (μM)	125	125	250	None	None	None

Figure 20: SAR conducted on a variety of purchased and synthesized HQ analogs. CAS

assay indicates concentration required to achieve a pre-set cut-off for iron binding at an

absorbance of 0.3, and the next three rows indicate concentrations required to achieve a

pre-set cut-off for growth promotion in indicated strains of bacteria (200%, 125% and

125% respectively). Green functionalities indicate hits, orange indicates moderate

activity, and red indicates poor activity. Data used with permission of Dr. Brent Weber

from the Dr. Eric Brown Lab at McMaster University.

Due to two of the hits demonstrating modifications at the *para* benzyl position (**1-15** and **1-23**), it was decided that this was a strong preliminary site for modification. As **1-15** is modifiable at this position due to the chloromethyl functionality, it was decided that a family of ethers should be synthesized, mimicking the original ether hit **1-23** in an effort to optimize activity.

While this finding informed the further optimization of the HQs, an important finding in the context of the sideromycins was the data observed for **1-1**, the siderophore used in the first proof-of-concept sideromycin. This was discovered to be poor at iron binding as well as at promoting growth in the tested *Klebsiella* and *Pseudomonas* strains.

HQ ethers were synthesized, with their synthesis detailed in section 1.3.2. Unfortunately, these ethers did not demonstrate significant growth promotion except at higher concentrations, and iron-binding was equivalent to or worse than the parent HQ scaffold. At this time, focus was switched to the third hit from the initial screening (**1-22**, Figure 20). We hypothesized that the amine functionality located *ortho* to the hydroxyl was involved in the improved iron chelation relative to the parent scaffold (31.25 µM compared to 62.5 µM respectively) due to its position along the iron-binding portion of

the ring. The sulfonic acid was consequently hypothesized to be involved in the improved growth promotion.

To test this, an analog of the HQ scaffold was purchased with a sulfonic acid, but without the amine moiety (**1-19**). We expected to consequently find comparable iron binding to the HQ parent scaffold, but improved growth promotion. Findings are observable below (Figure 21).
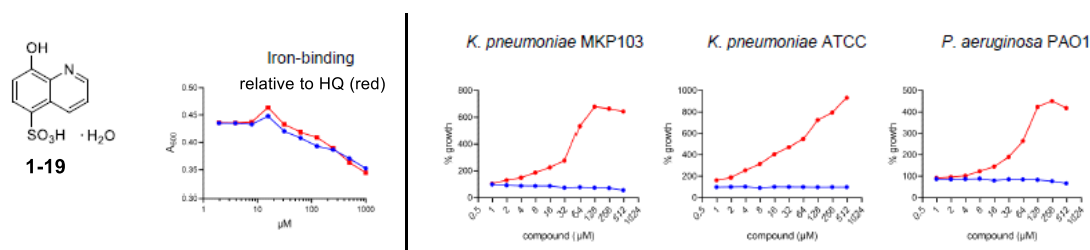
Figure 21: Screening results for **1-19** for iron-binding and growth promotion in *K. pneumoniae* and *P. aeruginosa*. The iron binding data (blue) is measured against an HQ control (red). Growth promotion is measured in serum (red) against an iron-rich broth (blue). Graphs used with permission of Dr. Brent Weber from the Dr. Eric Brown Lab at McMaster University.

Due to the aforementioned difficulties in working with the HQ functionalities in synthesis of complex sideromycins, the decision was made to avoid working with the amine-containing HQ-sulfonic acid **1-22**. As such, the HQ-sulfonic acid (**1-19**) was decided to be the optimized best hit. As discussed, literature precedent surrounding HQ-sulfonamides that can be synthesized from this functionality demonstrates some

tolerability *in vivo* in a variety of embryos (Pippi et al., 2020), which further strengthens

the suitability of **1-19** as the most optimized HQ siderophore.

1.3.2: Synthesis of Hydroxyquinoline Siderophore Analogs

Ether synthesis procedures were adapted from literature precedent surrounding related compounds (Xiao et al., 2015). **1-15** was used as the starting reagent, which was reacted with a variety of alcohols in tetrahydrofuran (THF). A variety of bases were utilized to deprotonate the alcohol, but due to the lower pKa of the HQ phenol than a primary alcohol, the HQ was more likely to deprotonate, and consequently, the unintended side reactions led to a variety of side products. This further led to difficult purification, made significantly more complex due to the acid-base functionalities of the HQ that have been discussed in prior sections.

Literature was found for a base-free reaction (Schulze et al., 2017), though only trace conversion to the product ethers was observed without its presence. As such, a weak base (sodium bicarbonate, $NaHCO_3$) was added, which lead to clean isolation of the products after column chromatography in hexane/ethyl acetate followed by reverse phase chromatography in water/methanol. However, as in the other cases, the ethers were minor products and were obtained in very low yields (Scheme 6).
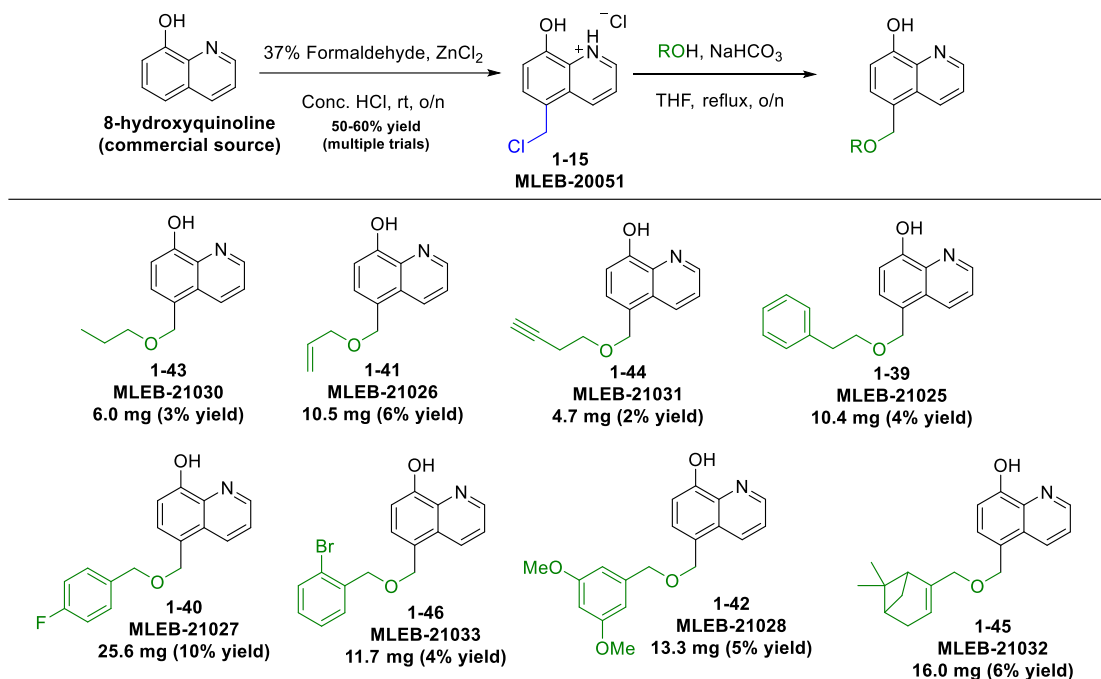
Scheme 6: Synthesis of HQ ethers.

To improve these yields, protection of the phenol on **1-15** was attempted using a tert-butyldimethylsilyl group (TBS) but was unsuccessful. This was not attempted on the parent scaffold HQ due to an expected (though unintended) removal of the TBS group during the chloromethylation under acidic conditions when attempting to synthesize **1-15**. If revisited in the future, we expect yields to improve with a different protecting group on the phenol (such as a benzyl group), and careful reaction planning. Alcohols should be deprotonated with a limiting amount of strong base such as sodium hydride (NaH) in solvent. After deprotonation is complete, this mixture should be slowly added to **1-15** being stirred in solvent. Following isolation of this product, deprotection of **1-15** can be attempted to produce the HQ ethers in improved yield.

As such, this project optimized the HQ siderophore for attachment to antibiotics and synthesized a family of ethers for SAR purposes. Though yields were low, a plan to improve yields has been provided. Findings have been documented in this thesis for posterity.

1.4: Summary and Future Work

The aim of this project has been to develop novel sideromycins for testing in human serum as a proxy for *in vivo* conditions. As such, peptide couplings were conducted between the siderophore HQ and linezolid derivatives. Due to synthetic difficulties and potential protease cleavage in serum, other types of bonds were explored, including click chemistry and sulfonamides, both of which proved difficult to work with in the context of HQs.

The click reaction (Scheme 4) did not seem to reliably form product **1-18** in the yields expected. The conducted reactions typically involved 0.15 to 0.2 equivalents of copper sulfate as the catalyst. However, as a metal, it is possible that the copper was sequestered by the present HQ siderophore reactant **1-16**, and consequently unavailable to catalyze the reaction. Increasing the amount of copper to 1.2 equivalents relative to each equivalent of the siderophore in this reaction may therefore improve yields significantly by ensuring the availability of the reagent for catalysis of the click reaction.

Optimization of the HQ sulfonamide reaction (Scheme 5) should further be attempted. The sulfonyl chloride intermediate **1-20** should immediately be converted to the sideromycin conjugate **1-21** due to the reactive nature of the functionality. It is possible that homodimerization may occur if allowed to sit. Using a large excess of the antibiotic will further prevent this unintended product forming.

At the time of writing, a wealth of viable unexplored conjugates exist for synthesis and screening. Despite our work in this capacity, HQ sideromycins lay largely unexplored

due to the difficulty experienced in their synthesis and purification. By utilizing LCMS

purification under buffer conditions, we may mitigate some of these concerns.

Attachment to ß-lactams via peptide coupling to better understand non-serum

antimicrobial activity has created isolation issues but can be revisited under these buffer

purification conditions.
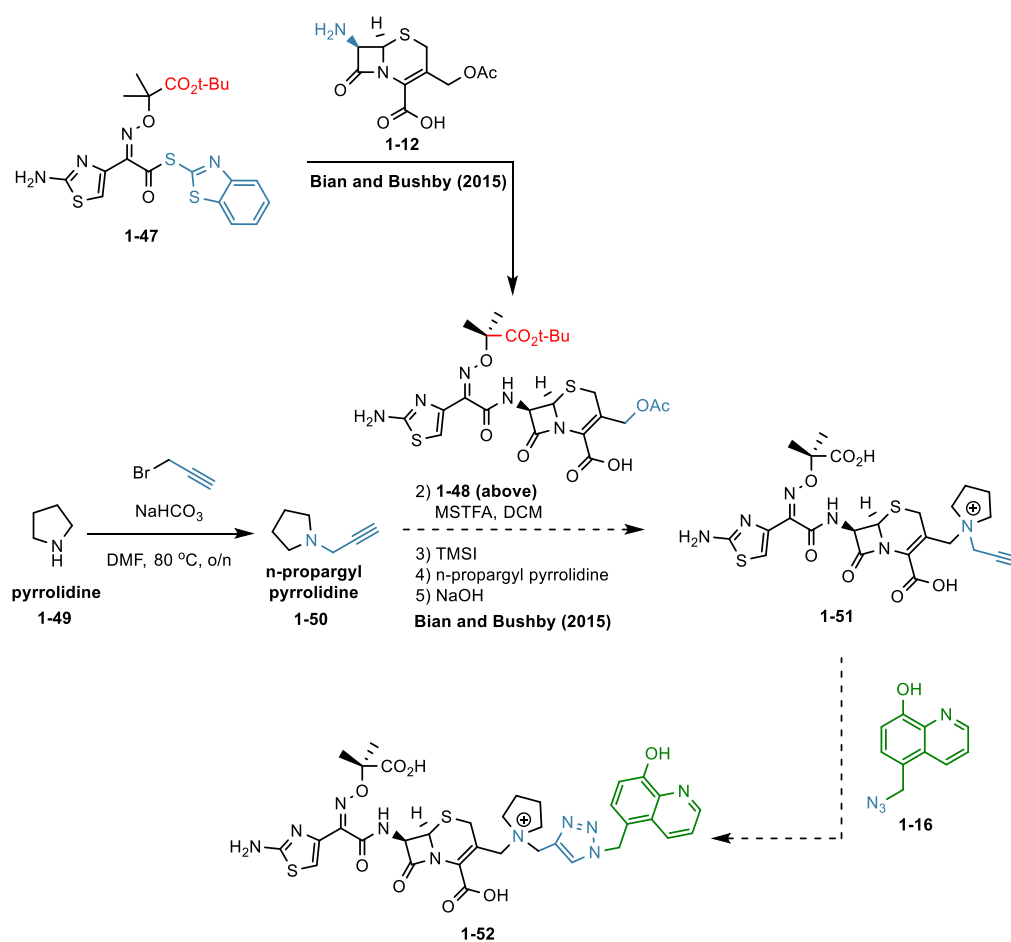
Scheme 7: Plan for the development of a cefiderocol mimic with a procedure adapted

from Bian and Bushby (2015).

The current gold standard in this space is cefiderocol (Figure 13) due to its FDA approval as a drug of last resort. As such, the most important short-term goal for this project is to develop a cefiderocol mimic (**1-52**), as outlined in Scheme 7. Though the early-stage reactions have been attempted based on literature precedent (Bian and Bushby, 2015), there have been issues with yields and purity, and as such, this preparation will require optimization.

While ß-lactams are a major class of clinical antibiotic, there has been limited representation of these compounds in this project to date. Moreover, limited exploration of other classes of antibiotics has been conducted. Antibiotics such as streptomycin (aminoglycoside), vancomycin (glycopeptide), and erythromycin (macrolide) are popular examples of antibiotics of vastly different classes that can be explored with some structural modifications (Figure 22).
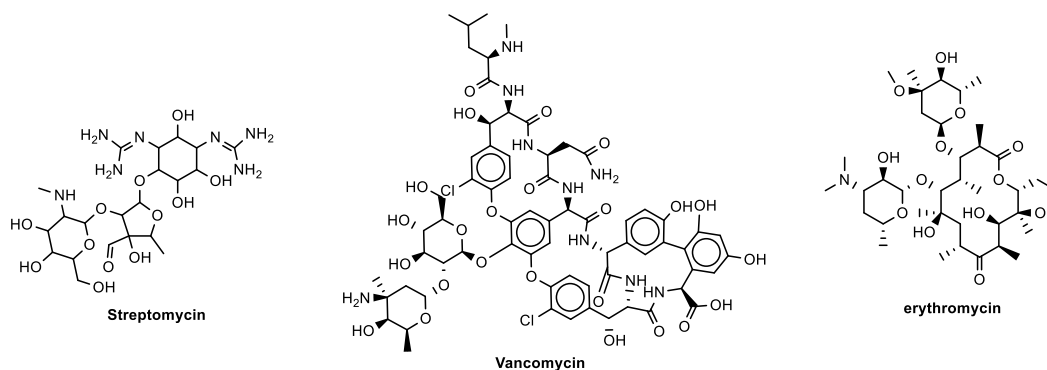
Figure 22: Potential antibiotics of different classes for attachment to siderophores.

Methods of linkage are another area of future study. There are several methods of conjugation in the literature that we have not attempted (Figure 23). One such example

utilizes succinate-based linkers between hydroxamates and antibiotics, resulting in a hydroxylated amide on the siderophore end, and an ester linking the antibiotic (Wencewicz et al., 2013). Another example, despite involving amides that may potentially be cleaved, explores the conjugate bond using a maleimide covalently linked to a free thiol (Juárez-Hernández et al., 2012). Finally, conducting a reductive amination at the peptide bond may be a viable way to prevent protease cleavage as observed in the linezolid sideromycins in this project through reduction of the amide carbonyl moiety.
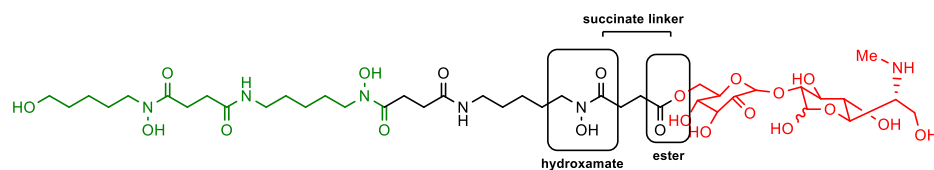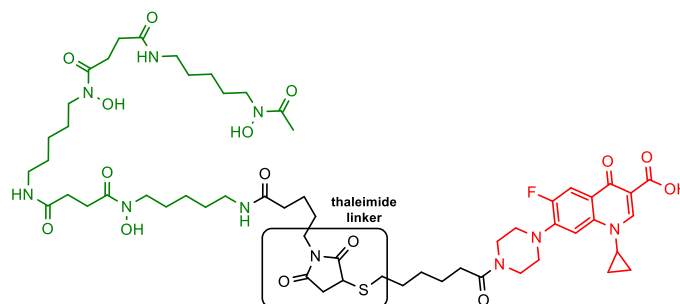
Figure 23: Structure of two antibiotics utilizing linkers that are unexplored in the context of this project (Juárez-Hernández et al., 2012; Wencewicz et al., 2013).

As briefly mentioned in section 1.1, siderophore trimers greatly improve molecular economy and consequently serve as powerful chelators for hexadentate iron ions. Given this concept, HQ trimers are an exciting prospect for the future of this project. Moreover, as highlighted in earlier sections, mixed-siderophore trimers have

demonstrated better antibiotic activity when conjugated in sideromycins than homogeneous trimers, potentially due to the increased coverage of a variety of structure-specific siderophore transporter proteins on Gram-negative membranes. As such, incorporating other classes of siderophores in a mixed-ligand trimer with HQ may yield an optimized siderophore for conjugation to antibiotics (Lin et al., 2019).

As with any other antibiotic synthesis project, the ultimate goal of this project would be to find strong conjugate hits that can be moved onto further trials. However, another aspect of this project that can be improved to pursue this goal can be computational prediction of siderophore and sideromycin activity through docking studies. Through binding-based simulations, better siderophore hits can be elucidated in the long-term, and it is possible that this can even be used to predict sideromycin uptake mechanisms. As such, in the future, this would be an exciting direction in which to take this project.

Chapter 2: Efficient Synthesis of Prenylated Coumarin Natural Products

2.1: Introduction

2.1.1: Prenylated coumarin natural products

Figure 24: Angelica gigas, a species of flowering plant belonging to the family Apiaceae. "Angelica gigas Dzięgiel 2020-08-07 01.jpg" by Agnieszka Kwiecień is licensed under CC BY-SA 4.0.

Prenylated coumarins proliferate in nature. Many such natural products are isolated from the family Apiaceae of flowering plants (Figure 24). Under this umbrella are several common species of herbs and vegetables, including coriander, dill, carrots, and celery (Plunkett et al., 2018). Some of the natural products from various species of this family belong to the coumarin family and are highlighted in the below figure (Figure 25) – umbelliferone (**2-1**), demethylsuberosin (**2-2**), osthenol (**2-3**), ostruthin (**2-4**), and 8-geranylumbelliferone (**2-5**).
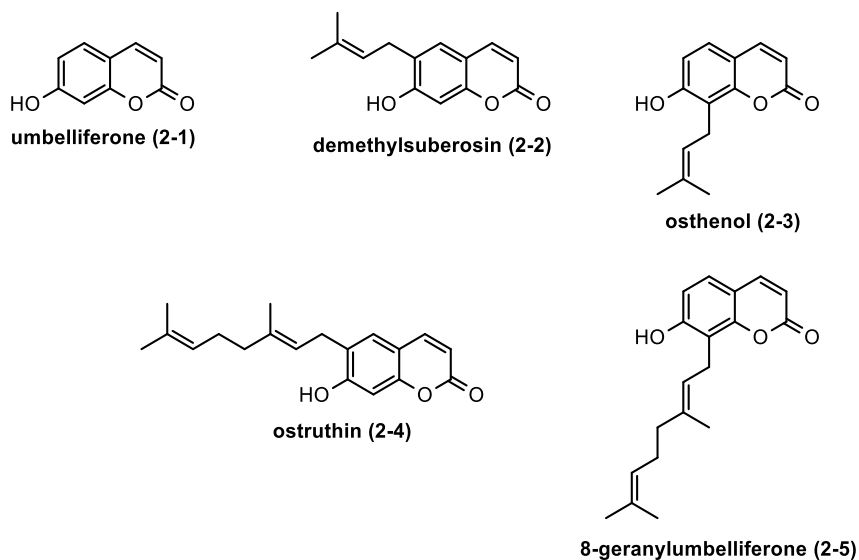
Figure 25: Umbelliferone and its prenylated natural product derivatives.

Each of these are prenylated derivatives of umbelliferone (**2-1**, Figure 25) and have a variety of biologically relevant effects including anticancer, antioxidant, antidepressant, and antibiotic activity (Schinkovitz et al., 2003; Tuan Anh et al., 2017; Baek et al., 2019; Cho et al., 2020; Paio et al., 2021). The purpose of this project is to propose a synthesis of each of these natural products using technology patented by the Magolan Lab at McMaster University.

2.1.2: Bioactivity and previous syntheses of the prenylated coumarins

2.1.2.1: Demethylsuberosin and osthenol syntheses
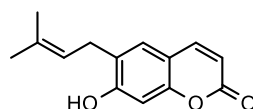
demethylsuberosin (2-2)

Figure 26: The structure of demethylsuberosin (**2-2**).

Demethylsuberosin (**2-2**, Figure 26) is typically isolated from *Angelica gigas*, a flowering plant from the Apiaceae family (Kim et al., 2014; Kim et al., 2015). It demonstrates proteasome inhibition and anti-inflammatory activity (Kim et al., 2015). It has also demonstrated neuroprotective activity and is a melanin inhibitor in melanoma cells (Kim et al, 2014).
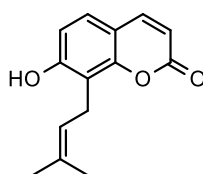
osthenol (2-3)

Figure 27: The structure of osthenol (**2-3**).

Osthenol (**2-3**, Figure 27) is isolated from *Angelica pubescens*, *Angelica koreana*, and *Angelica dahurica*, all Apiaceae-derived species (Baek et al., 2019; Cho et al., 2020). It has been linked with the inhibition of Monoamine Oxidase A, an enzyme linked with breakdown of dopamine and serotonin. Consequently, **2-3** is linked with anti-depressive activity (Baek et al., 2019). It has also been associated with some anti-tumor and anti-

fungal activity and is even somewhat active against several Gram-positive bacterial species (Cho et al., 2020).

There are numerous syntheses proposed for these compounds. Many of these procedures yield both prenylated regioisomers, and as such, the synthesis of both will be discussed in this section.

A synthesis of both natural products by Murray et al. was published in 1971 (Scheme 8) and is an early example of one of two major syntheses used to date (Murray et al., 1971). Umbelliferone (**2-1**) is alkylated with an alkyne halide at the phenolic oxygen, providing alkyne intermediate **2-6**. The use of a poisoned hydrogenation catalyst (Pd-BaSO$_4$, poisoned with quinoline-sulfur) serves the same purpose as Lindlar's catalyst, which is used in later preparations, reducing the alkyne to the desired terminal alkene intermediate **2-7**. This is followed by a Claisen rearrangement at high heat (130°C) to synthesize both *ortho* prenylated regioisomers, demethylsuberosin (**2-2**, 14%) and osthenol (**2-3**, 74%).
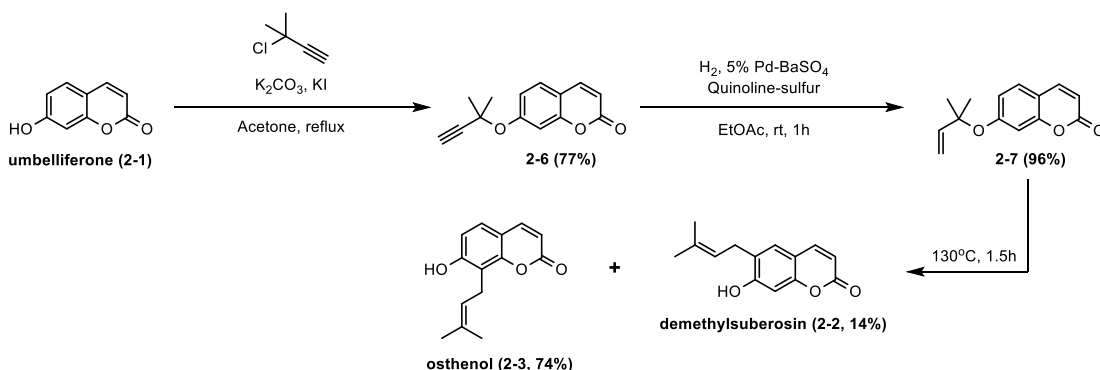
Scheme 8: The synthesis of demethylsuberosin and osthenol by Murray et al. (1971).

Though the *O*-allylation/Claisen rearrangement pathway is the most common preparation of the prenyl derivatives, a method to produce solely demethylsuberosin (**2-2**) was published only a few months later in 1971 by Warren Steck (Scheme 9). A prenyl-benzaldehyde starting material **2-8** undergoes a Perkin reaction in aniline to produce a coumarin cinnamic acid intermediate **2-9**. This is decarboxylated at high heat (215-220°C) in the presence of solid copper powder in quinoline to form demethylsuberosin (**2-2**) after HCl/water wash in 53% yield (Steck, 1971).
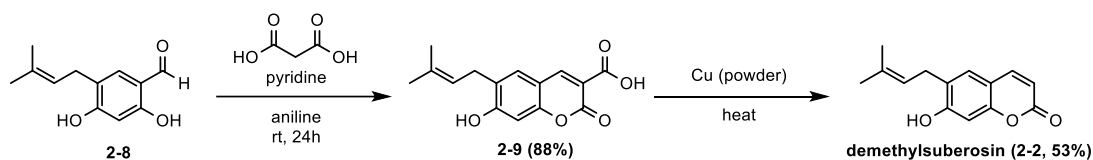
Scheme 9: Steck (1971) synthesis of demethylsuberosin in two steps.

Cairns et al. published one of the most cited syntheses of **2-2** in 1986 using a procedure that is completely different from the prior syntheses and involves the dismantling and eventual reconstruction of the coumarin scaffold (Scheme 10). The procedure begins with a -Bz protecting group instituted onto umbelliferone (**2-10**) and subsequently involves a ring opening at the ester using NaOMe in refluxing methanol to produce intermediate **2-11** in 92% yield. This is followed by *O*-prenylation using prenyl bromide to produce **2-12** (86%). Claisen rearrangement with the rearranged intermediates was conducted with *N, N*-diethylaniline and yielded the target intermediate **2-14** (78%), with side product **2-13**. Finally, a deprotection of the -Bz protecting group was carried out to produce **2-2** in 84% yield (Cairns et al., 1986).
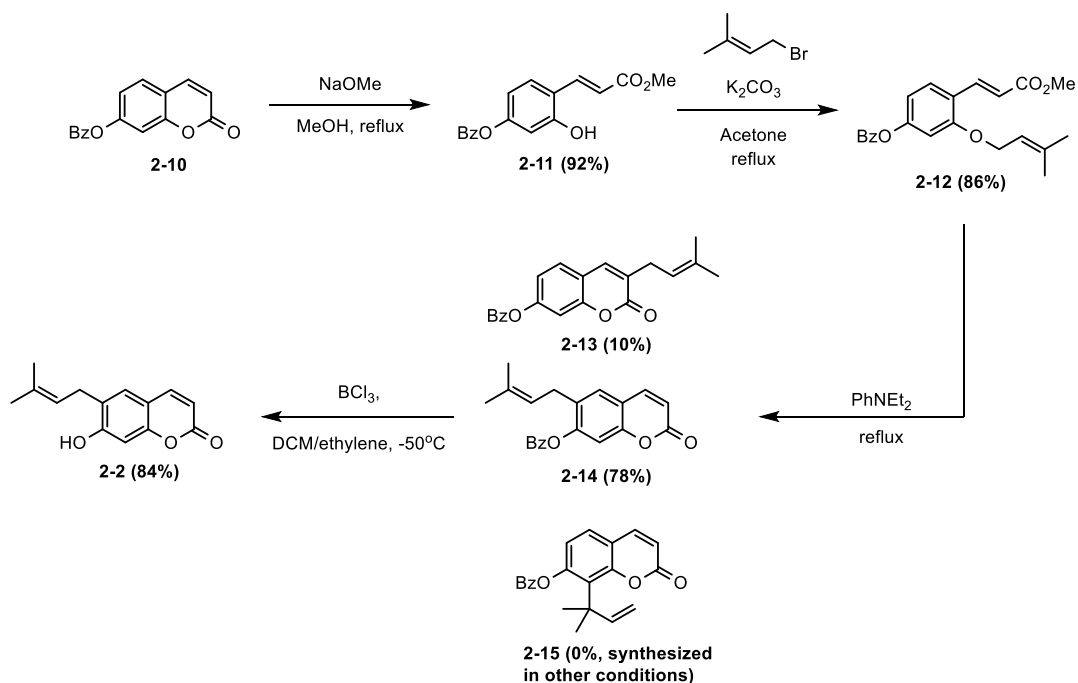
Scheme 10: Cairns et al. (1986) demethylsuberosin synthesis in 4 steps.

In 1986, Glüsenkamp and Büchi highlighted a particularly interesting finding in their research regarding prenylation of phenolic molecules (Scheme 11). Upon stirring **2-1** with prenyl bromide in hexane/ether for 5 days in the presence of basic/neutral alumina (aluminum oxide, Al_2O_3), contrary to observing entirely *O*-prenylation, it was observed that **2-3** formed in 29% yield (Glüsenkamp and Büchi, 1986).
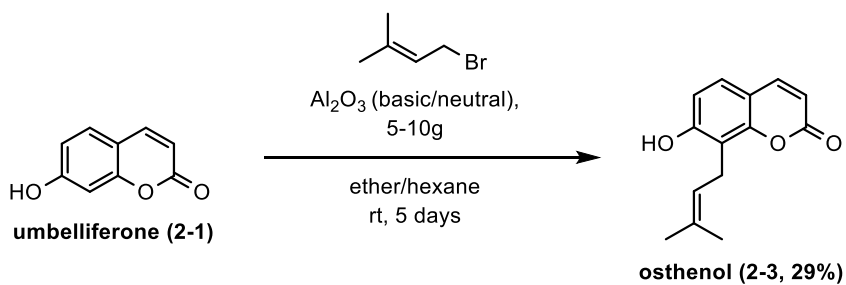
Scheme 11: Glusenkamp and Buchi (1986) synthesis of osthenol in one step.

This is the most concise synthesis yet, and uses relatively cheap reagents, with the only cons to this approach being yield and time required to conduct the reaction. However, this preparation was largely overlooked in future syntheses of **2-3** until recently, when the Magolan Lab used similar technology to optimize a procedure for one-step prenylation, discussed in Section 2.1.3 (Jentsch et al., 2020).

Daoubi et al. (2004) were concerned with potentially low yields observed through the numerous steps leading to Claisen rearrangements conducted after *O*-prenylation to produce demethylsuberosin (**2-2**) and osthenol (**2-3**). Consequently, they utilized 8-iodoumbelliferone (**2-16**) as a starting material which was reacted with tri-n-butyltin hydride (THB) and azobisisobutyronitrile (AIBN) in one pot, producing **2-2** and **2-3** in 38% and 18% yields respectively (Scheme 12; Daoubi et al., 2004). However, the umbelliferone derivative utilized is quite expensive and is made to order by only a select few vendors worldwide. Moreover, THB is toxic and AIBN is explosive, and as such, safer alternatives should be considered.
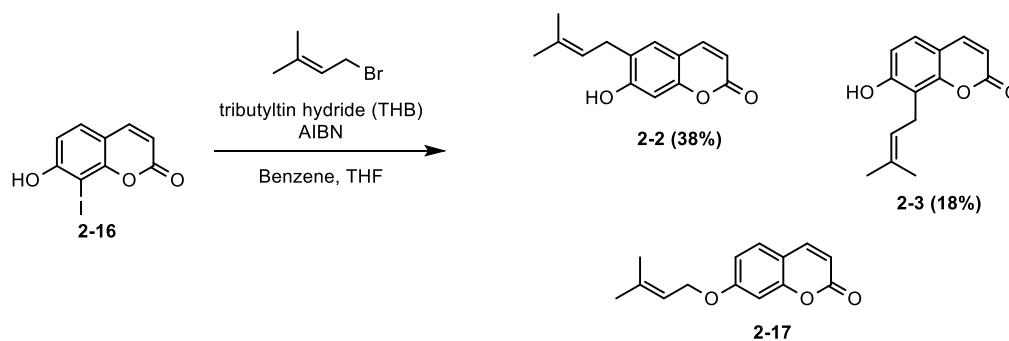
Scheme 12: Daoubi et al. (2004) synthesis of demethylsuberosin and osthenol.

A unique 2009 preparation of **2** by Xia et al. utilizes ß-resorcaldehyde (**2-18**) as a

starting material (Scheme 13). Following protection of the diol, the aldehyde of

intermediate **2-19** is reduced and undergoes a Grignard reaction to attach the prenyl

group. A second protection of the now-unprotected phenol **2-21** follows, and the 6-prenyl

product **2-23** is formylated at the *ortho* position to produce **2-24** (48%). Ring closure

occurs after addition of triphenyl-carbethoxymethylene-phosphorane to the reaction

mixture in diethylaniline at high heat. The formed intermediate **2-25** is then deprotected

to form **2-2** in 90% yield. Though this is an interesting departure from the Harwood

strategy and yield at most stages is high, it is significantly longer and utilizes various

protection and deprotection steps, including the institution of two different protecting

groups on the molecule simultaneously (Xia et al., 2009).
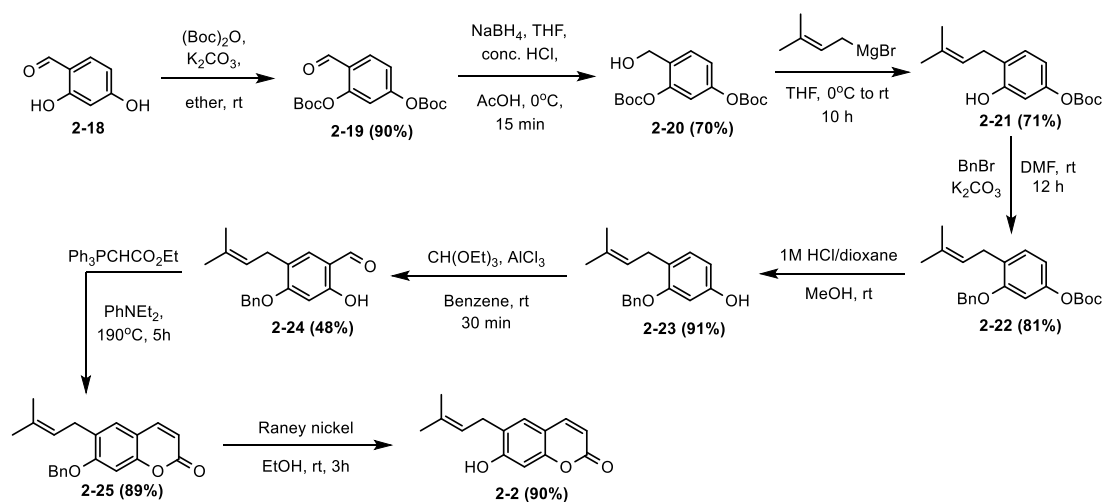
Scheme 13: Xia et al. (2009) synthesis of demethylsuberosin in 8 steps.

Magolan and Coster proposed a total synthesis of angelmarin, a coumarin natural

product, in 2009 (Scheme 14). During this process, they utilize allyl bromide to institute

an *O*-allyl group onto umbelliferone (**2-1**), which undergoes Claisen rearrangement followed by a Grubbs reaction using a Grubbs II catalyst and 2-methyl-2-butene to form the prenyl group on the resultant **2-3** in 72% overall yield (Magolan and Coster, 2009). Though this does not improve on the efficiency of the synthesis of **2-3**, it provides a novel mechanism for the last step of its synthesis and each step is high yielding.
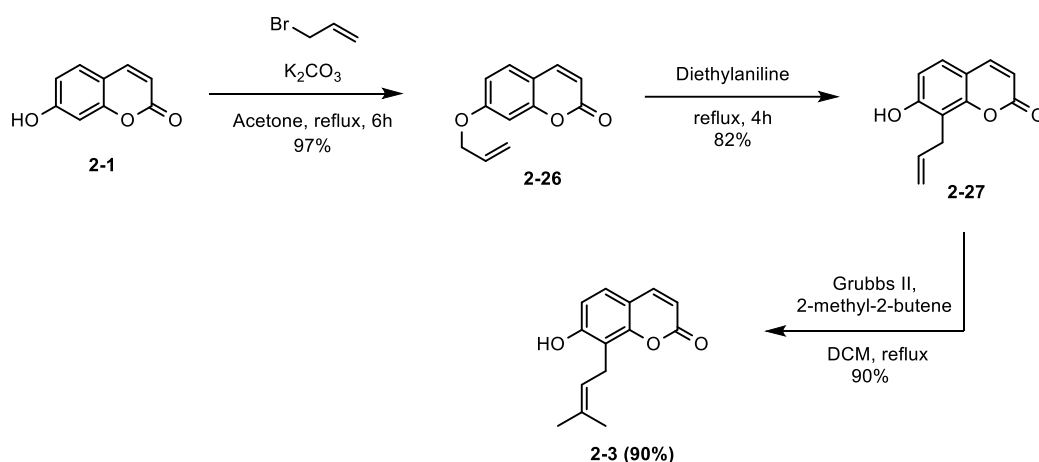
Scheme 14: Magolan and Coster (2009) preparation to make osthenol using a cross-metathesis.

Subsequent papers synthesizing **2-2** and **2-3** generally use one of the aforementioned strategies, with minor tweaks to reaction time or temperature. It is important to acknowledge the prevalence of two major strategies – Murray's *O*-alkylation followed by Claisen rearrangement, and Cairn's ring opening strategy (Murray et al., 1971; Cairns et al., 1986). Each of these requires multiple steps, and often some expensive reagents. Other strategies can be even less efficient or use potentially dangerous reagents.

2.1.2.2: Ostruthin and 8-geranylumbelliferone syntheses
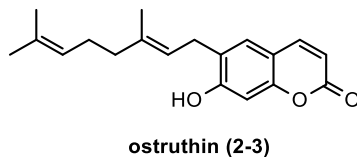
ostruthin (2-3)

Figure 28: The structure of ostruthin (**2-4**).

Ostruthin (**2-4**, Figure 28) is isolated from the roots of *Peucedanum ostruthium* and has demonstrated potent antimycobacterial activity against several species of mycobacteria (Schinkovitz et al., 2003). In addition, **2-4** exhibits inhibitory activity of smooth muscle cell growth, making it a molecule of interest in drug design for cardiac disease (Joa et al., 2011). It has also been posed as a potential anti-neuroinflammatory drug candidate (Tuan Anh et al., 2017). Finally, **2-4** acts as an antidepressant and an anxiolytic in mice (Joseph et al., 2018).

8-geranylumbelliferone (2-4)
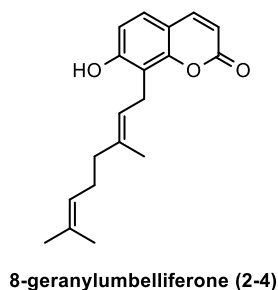
Figure 29: The structure of 8-geranylumbelliferone (**2-5**).

8-geranylumbelliferone (**2-5**, Figure 29) is isolated from *Paramignya timera*. It pursues an alternate pathway to TNF-mediated apoptosis to lead to anti-cancer activity (Paio et al., 2021). A synthesis of **2-5** has not been published to date. This creates a large

gap in the existing literature for prenylation at the *ortho* position to a phenol, as comparatively, both regioisomers for a prenyl addition have been explored extensively. Yet, there exists limited literature for the addition of a geranyl group at the 6-position, and no significant prior method to arrive at the 8-geranyl product.

The major synthesis of **2-4** proposed to date is predominantly credited to an experiment published by Cairns et al. in 1986 utilizing the same procedure outlined for demethylsuberosin (Scheme 15). This preparation involves the protection of the 7-hydroxyl group on umbelliferone (**2-1**), followed by an intramolecular ring opening at the cyclic ester. *O*-prenylation is the next step, which is conducted using geraniol instead of prenol as highlighted in section 2.1.2.1 followed by a Claisen rearrangement to obtain a variety of products, including **2-4** after a deprotection step. This preparation was also listed under a synthesis of **2-2** due to its flexibility in prenylation substrate (Cairns et al., 1986).
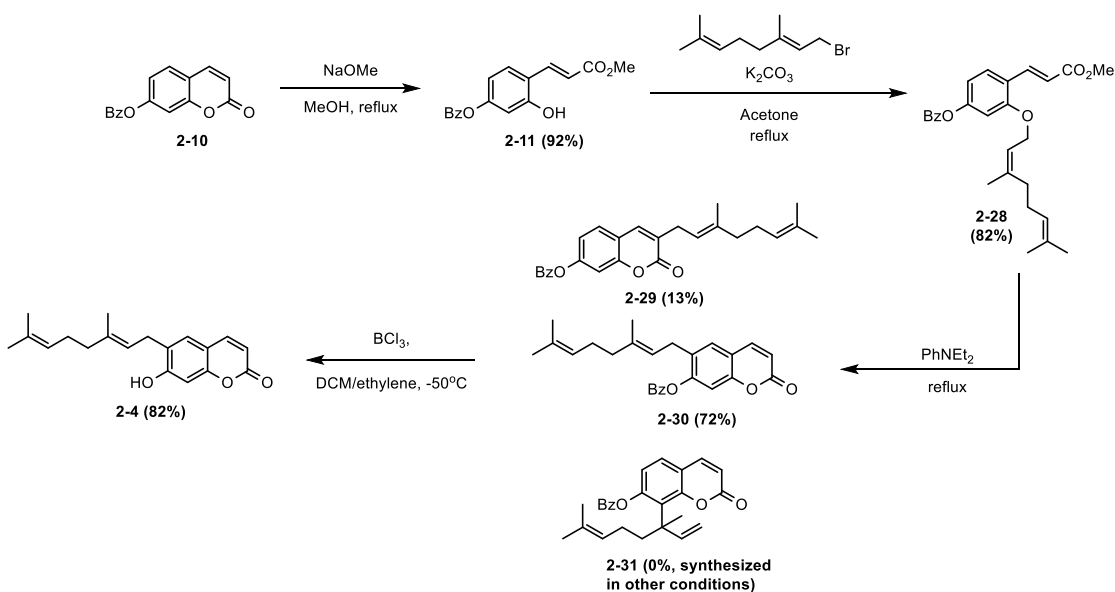
Scheme 15: Cairns et al. (1986) preparation to make ostruthin in 4 steps.

Given the numerous varied bioactivities reported regarding these compounds (Schinkovitz et al., 2003; Joa et al., 2011; Kim et al., 2014; Kim et al., 2015; Tuan Anh et al., 2017; Joseph et al., 2018; Baek et al., 2019; Cho et al., 2020; Paio et al., 2021), it is imperative to conduct further studies to understand their mechanisms of activity with the goal of developing novel medications. However, the reported syntheses are often many steps, or utilize expensive or potentially dangerous reagents. Many groups prefer to isolate these compounds from Apiaceae species via extraction but yields and purity tend to be lower than synthetic processes.

Moreover, purchasing these compounds for study is often prohibitively expensive. As such, there exists a need to develop a safe, cheap, and efficient route to synthesize these compounds in high purity, which this project seeks to provide.

2.1.3: Magolan Lab research

In a 2020 paper, the Magolan Lab at McMaster University published a paper
highlighting the utilization of acidic alumina to promote prenylation of the *ortho* position
to a phenol as a method of synthesizing cannabigerol (CBG) and other phenolic natural
products in high yield (Jentsch et al., 2020). Though there was prior precedent for a one-
step synthesis of CBG (**2-33**, Scheme 16), these preparations typically were low yielding
and reproduction of the procedures demonstrated lower yields than reported, which the
authors attributed to potential differences in the sourcing of the reagents (Baek et al.,
1996; Taura et al., 1996; Jentsch et al., 2020).
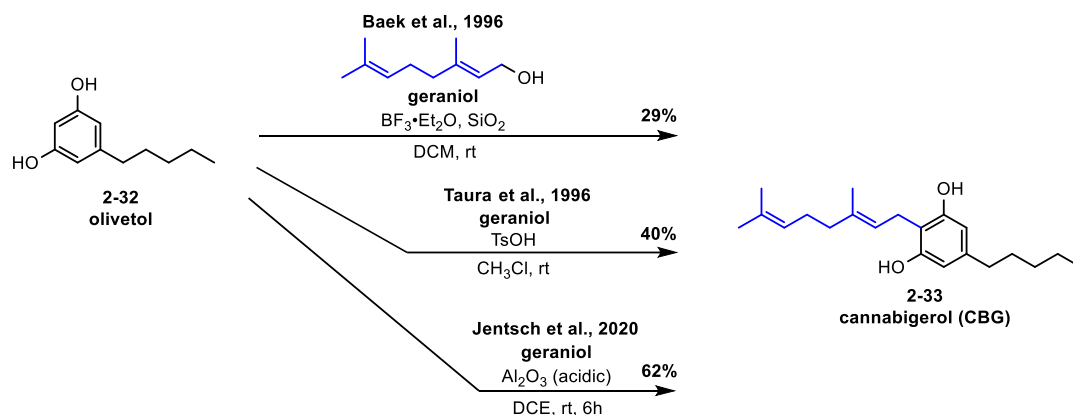
Scheme 16: Figure adapted from findings reported by Jentsch et al. (2020) highlighting
the synthesis of CBG (**2-33**) in relatively high yield in one step from olivetol (Baek et al.,
1996; Taura et al., 1996; Jentsch et al., 2020).

This process of utilizing acidic alumina to promote allylation at the *ortho* position
of phenols was patented the following year. This technology was applied to a variety of
phenolic natural products as well as structurally novel prenylated scaffolds as part of the

patent. I was listed as one of the inventors, focusing specifically on the synthesis of a variety of prenylated coumarins. As such, this chapter focuses on the design of these compounds using the powerful technology developed by the Magolan Lab.

2.2: Results and Discussion

We were able to synthesize each of the aforementioned prenylated coumarin natural products (**2-2** through **2-5**) in one step, using cost-efficient reagents. Each of these reactions was conducted using umbelliferone (**2-1**) and the required prenyl alcohol (prenol or geraniol) in the presence of acidic alumina.

Umbelliferone (**2-1**) was converted to a mixture of demethylsuberosin (**2-2**) and osthenol (**2-3**) in 5% and 4% yields respectively when stirred overnight in dry dichloroethane (DCE) in the presence of acidic alumina and prenol (Scheme 17). Considerable optimization is required for this reaction to improve yields.
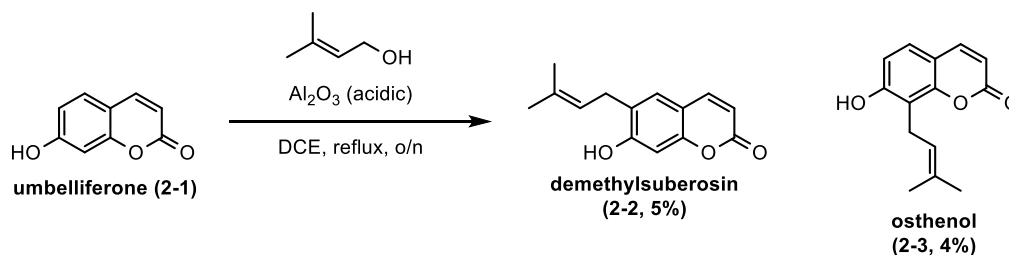
Scheme 17: The synthesis of **2-2** and **2-3** in one step from umbelliferone (**2-1**) using acidic alumina in DCE.

Similarly, **2-1** was converted to a mixture of the geranylated products ostruthin (**2-4**) and 8-geranylumbelliferone (**2-5**) in 36% and 11% yields respectively in the presence of acidic alumina and geraniol. However, instead of DCE like the previous reaction, **2-4** and **2-5** were synthesized in xylene in a sealed pressure tube heated to 160°C in a monowave reactor for two hours (Scheme 18).
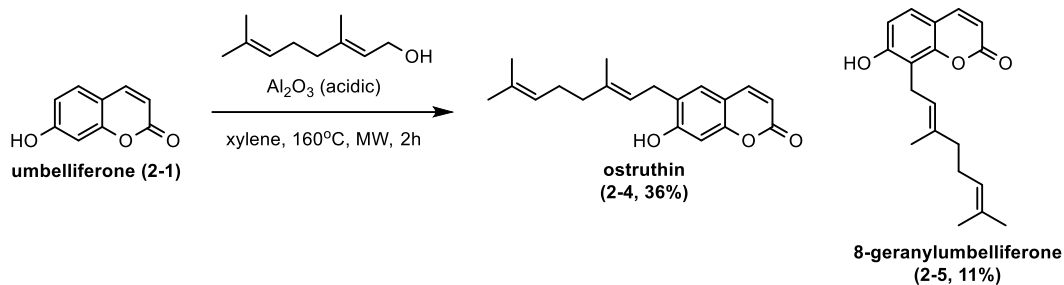
Scheme 18: The synthesis of **2-4** and **2-5** in one step from umbelliferone (**2-1**) using acidic alumina in xylene.

Interestingly, it was noted that in the above conditions, the reaction of **2-1** with prenol did not yield the expected products **2-2** and **2-3**. The cyclized natural products dihydroxanthyletin and dihydroseselin were instead observed. These were synthesized in one total step in the same monowave conditions in 23% and 19% yields respectively (Scheme 19).
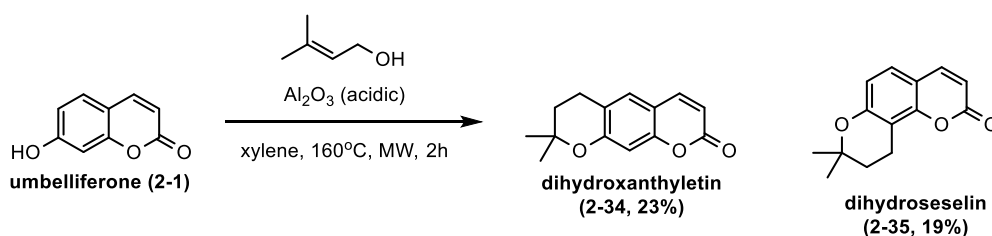
Scheme 19: The synthesis of **2-34** and **2-35** in one step from umbelliferone (**2-1**) using acidic alumina.

Optimization of these reactions is required, as the products were not able to be synthesized in acceptable yields and will be conducted by a member of the Magolan Lab

in the coming months to complete this project and publish the relevant data. As outlined above, this is most evident in the case of **2-2** and **2-3**.

2.3: Summary and Future Work

The aim of this work is to contribute an efficient, cost-effective synthesis of prenylated coumarin natural products. These compounds are broadly bioactive in a variety of capacities and more thorough testing should be done to elucidate both their efficacy and mechanism of action. However, they are typically very expensive, which may be a deterrent to researchers hoping to utilize such molecules. With this in mind, this project will hopefully provide a simple method of producing large quantities of these natural products for purchase at significantly lower prices and will ensure their availability for future research.

Natural products **2-2** through **2-5** as well as **2-34** and **2-35** were synthesized through this project in one step. However, yields were much lower than anticipated, notably for demethylsuberosin (**2-2**) and osthenol (**2-3**). As such, the aforementioned optimization needs to be conducted to improve yields for these reactions prior to publication.

This project will be published in the near future as a concise, cost-effective, one step synthesis of prenylated natural products. There are a variety of difficult to synthesize natural products that are accessible with one further step using molecules synthesized using this research (Figure 30). For example, Marmesin (**2-37**) can be synthesized using demethylsuberosin (**2-2**) and conducting an oxidation with mCPBA in ethyl acetate at 0°C (Trumble and Millar, 1996). Columbianetin (**2-38**) has been similarly synthesized with the same procedure and osthenol (**2-3**) as the substrate (Magolan and Coster, 2009).

Osthol (**2-36**) can likely be synthesized from osthenol by conducting an O-methylation in one step. These compounds can also be synthesized as part of this initial paper.
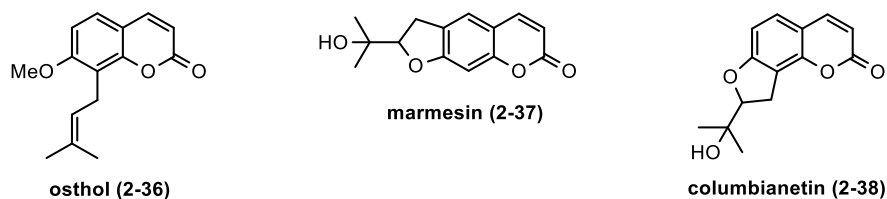
Figure 30: Structure of several derivatives that are one step away from the synthesized prenylated natural products.

Though the aforementioned compounds of interest will comprise the majority of the first paper, a follow up project could explore further syntheses of more complex natural products using this robust methodology developed in the Magolan Lab. For example, Magolan and Coster synthesized angelmarin (**2-39**) in 2009 in 8 steps (Figure 31). This procedure could be reduced to 4 steps through synthesis of the columbianetin intermediate in 2 steps as discussed above (Magolan and Coster, 2009). Many more such syntheses could be shortened significantly in follow-up research, and as such, are a longer-term goal to be pursued.
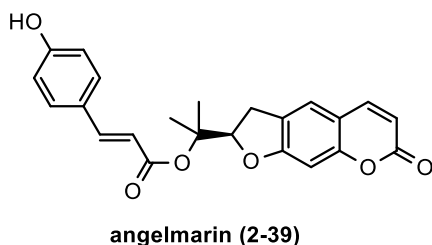
angelmarin (2-39)

Figure 31*:* Structure of angelmarin (**2-39**), a natural product derived from demethylsuberosin (**2-2**).

Finally, as briefly mentioned at the start of this section, there exists a need to further evaluate these compounds in a variety of medicinal capacities. The syntheses of larger quantities of the coumarin derivatives will allow for largescale screening at a broad level. This should be a high priority long-term follow-up to this synthesis project.

Bibliography

1. Aik, W., Demetriades, M., Hamdan, M. K., Bagg, E. A., Yeoh, K. K., Lejeune, C., … Schofield, C. J. (2013). Structural basis for inhibition of the fat mass and obesity associated protein (FTO). *Journal of medicinal chemistry*, *56*(9), 3680-3688.

2. Alanis, A. J. (2005). Resistance to antibiotics: are we in the post-antibiotic era?. *Archives of medical research*, *36*(6), 697-705.

3. Albert, A. (1950). Selective toxicity. *Nature*, 165(4184), 12-16.

4. Al-Busafi, S. N., Suliman, F. E. O., & Al-Alawi, Z. R. (2014). 8-hydroxyquinoline and its derivatives: Synthesis and applications. *ChemInform*, 45(49), no-no.

5. Ando, T., Nagumo, M., Ninomiya, M., Tanaka, K., Linhardt, R. J., & Koketsu, M. (2018). Synthesis of coumarin derivatives and their cytoprotective effects on t-BHP-induced oxidative damage in HepG2 cells. *Bioorganic & Medicinal Chemistry Letters*, *28*(14), 2422-2425.

6. *"*Angelica gigas Dzięgiel 2020-08-07 01.jpg*"* by Agnieszka Kwiecień is licensed under CC BY-SA 4.0.

7. Antibiotic Resistance Threatens Everyone. (2021). Retrieved 16 February 2021, from https://www.cdc.gov/drugresistance/index.html

8. Antibiotic Resistance – World Health Organization. (2020). Retrieved 25 March 2022, from https://www.who.int/news-room/fact-sheets/detail/antibiotic-resistance

9. Baek, S. H., Du Han, S., Yook, C. N., Kim, Y. C., & Kwak, J. S. (1996). Synthesis and antitumor activity of cannabigerol. *Archives of Pharmacal Research*, *19*(3), 228-230.

10. Baek, S. C., Kang, M. G., Park, J. E., Lee, J. P., Lee, H., Ryu, H. W., … Kim, H. (2019). Osthenol, a prenylated coumarin, as a monoamine oxidase A inhibitor with high selectivity. *Bioorganic & medicinal chemistry letters*, *29*(6), 839-843.

11. Beare, K. D., & McErlean, C. S. (2013). Accessing columbianetin-containing natural products via a domino on-water, in-water process. *Tetrahedron Letters*, *54*(9), 1056-1058.

12. Bian, L., & Bushby, N. (2015). Synthesis of [2H6] ceftazidime as a stable isotopically labeled internal standard. *Journal of Labelled Compounds and Radiopharmaceuticals*, *58*(7), 313-316.

13. Bolla, J. M., Alibert-Franco, S., Handzlik, J., Chevalier, J., Mahamoud, A., Boyer, G., … Pagès, J. M. (2011). Strategies for bypassing the membrane barrier in multidrug resistant Gram-negative bacteria. *FEBS letters*, *585*(11), 1682-1690.

14. Boucher, H. W., Talbot, G. H., Bradley, J. S., Edwards, J. E., Gilbert, D., Rice, L. B., … Bartlett, J. (2009). Bad bugs, no drugs: no ESKAPE! An update from the Infectious Diseases Society of America. *Clinical infectious diseases*, *48*(1), 1-12.

15. Bougharraf, H., Benallal, R., Sahdane, T., Mondieig, D., Negrier, P., Massip, S., … Kabouchi, B. (2017). Study of 5-azidomethyl-8-hydroxyquinoline structure by X-ray diffraction and HF–DFT computational methods. *Russian Journal of Physical Chemistry A, 91*(2), 358-365.

16. Braun, V., Pramanik, A., Gwinner, T., Köberle, M., & Bohn, E. (2009). Sideromycins: tools and antibiotics. *Biometals*, *22*(1), 3.

17. Cairns, N., Harwood, L. M., & Astles, D. P. (1986). Synthesis of linear coumarins via para-Claisen rearrangement of coumarate ester derivatives: total synthesis of suberosin, demethylsuberosin, and ostruthin. *Journal of the Chemical Society, Chemical Communications*, (16), 1264-1266.

18. Chater, K. F. (2006). Streptomyces inside-out: a new perspective on the bacteria that provide us with antibiotics. *Philosophical Transactions of the Royal Society B: Biological Sciences, 361*(1469), 761-768.

19. Cho, P., Choi, S. M., Kim, Y., Lee, D. H., Noh, Y., Kim, S., … Lee, S. (2020). Characterization of osthenol metabolism in vivo and its pharmacokinetics. *Xenobiotica*, *50*(7), 839-846.

20. Collignon, P. (2015). Antibiotic resistance: are we all doomed?. *Internal medicine journal*, *45*(11), 1109-1115.

21. Comroe Jr, J. H. (1978). Pay dirt: the story of streptomycin: Part I. From Waksman to Waksman. *American Review of Respiratory Disease*, *117*(4), 773-781.

22. Conly, J. M., & Johnston, B. L. (2005). Where are all the new antibiotics? The new antibiotic paradox. *Canadian Journal of Infectious Diseases and Medical Microbiology*, *16*(3), 159-160.

23. D'Costa, V. M., King, C. E., Kalan, L., Morar, M., Sung, W. W., Schwarz, C., … Wright, G. D. (2011). Antibiotic resistance is ancient. *Nature*, *477*(7365), 457-461.

24. Daoubi, M., Durán-Patrón, R., Hmamouchi, M., Hernández-Galán, R., Benharref, A., & Collado, I. G. (2004). Screening study for potential lead compounds for natural product-based fungicides: I. Synthesis and in vitro evaluation of coumarins against Botrytis cinerea. *Pest management science*, *60*(9), 927-932.

25. Deraeve, C., Boldron, C., Maraval, A., Mazarguil, H., Gornitzka, H., Vendier, L., … Meunier, B. (2008). Preparation and study of new poly-8-hydroxyquinoline chelators for an anti-Alzheimer strategy. *Chemistry–A European Journal, 14*(2), 682-696.

26. Dichtl, S., Demetz, E., Haschka, D., Tymoszuk, P., Petzer, V., Nairz, M., … Weiss, G. (2019). Dopamine is a siderophore-like iron chelator that promotes Salmonella enterica serovar typhimurium virulence in mice. *MBio*, *10*(1).

27. Doron, S., & Davidson, L. E. (2011, November). Antimicrobial stewardship. In Mayo Clinic Proceedings (Vol. 86, No. 11, pp. 1113-1123). *Elsevier.*

28. Drug Approval: FETROJA (cefiderocol). (2020). Retrieved 6 April 2020, from https://www.accessdata.fda.gov/drugsatfda_docs/nda/2019/209445Orig1s000TOC.cfm

29. Durand, G. A., Raoult, D., & Dubourg, G. (2019). Antibiotic discovery: history, methods and perspectives. *International journal of antimicrobial agents*, *53*(4), 371-382.

30. Ferrara, M. (2017). Antibiotic overprescribing: still a major concern. *The Journal of family practice*, *66*(12).

31. Ghosh, M., Miller, P. A., Möllmann, U., Claypool, W. D., Schroeder, V. A., Wolter, W. R., … Miller, M. J. (2017). Targeted antibiotic delivery: selective siderophore conjugation with daptomycin confers potent activity against multidrug resistant Acinetobacter baumannii both in vitro and in vivo. *Journal of medicinal chemistry*, *60*(11), 4577-4583.

32. Ghosh, M., Miller, P. A., & Miller, M. J. (2020). Antibiotic repurposing: bis-catechol- and mixed ligand (bis-catechol-mono-hydroxamate)-teicoplanin conjugates are active against multidrug resistant Acinetobacter baumannii. *The Journal of Antibiotics*, *73*(3), 152-157.

33. Giuliano, C., Haase, K. K., & Hall, R. (2010). Use of vancomycin pharmacokinetic–pharmacodynamic properties in the treatment of MRSA infections. *Expert review of anti-infective therapy*, *8*(1), 95-106.

34. Glüsenkamp, K. H., & Büchi, G. (1986). C-prenylation of phenols promoted by aluminum oxide surfaces. *The Journal of Organic Chemistry*, *51*(23), 4481-4483.

35. Hancock, R. E. (1997). The bacterial outer membrane as a drug barrier. *Trends in microbiology*, *5*(1), 37-42.

36. Harris, A. M., Hicks, L. A., Qaseem, A., & High Value Care Task Force of the American College of Physicians and for the Centers for Disease Control and Prevention. (2016). Appropriate antibiotic use for acute respiratory tract infection in adults: advice for high-value care from the American College of Physicians and the Centers for Disease Control and Prevention. *Annals of internal medicine*, *164*(6), 425-434.

37. Hemaiswarya, S., & Doble, M. (2009). Synergistic interaction of eugenol with antibiotics against Gram negative bacteria. *Phytomedicine*, *16*(11), 997-1005.

38. Hopwood, D. A. (2007). How do antibiotic-producing bacteria ensure their self-resistance before antibiotic biosynthesis incapacitates them?. *Molecular microbiology*, *63*(4), 937-940.

39. Horta, P., Kuş, N., Henriques, M. S. C., Paixao, J. A., Coelho, L., Nogueira, F., … Cristiano, M. L. S. (2015). Quinolone–hydroxyquinoline tautomerism in quinolone 3-esters. Preserving the 4-oxoquinoline structure to retain antimalarial activity. *The Journal of organic chemistry*, *80*(24), 12244-12257.

40. Jentsch, N. G., Zhang, X., & Magolan, J. (2020). Efficient Synthesis of Cannabigerol, Grifolin, and Piperogalin via Alumina-Promoted Allylation. *Journal of Natural Products, 83*(9), 2587-2591.

41. Ji, C., Miller, P. A., & Miller, M. J. (2012). Iron transport-mediated drug delivery: practical syntheses and in vitro antibacterial studies of tris-catecholate siderophore–aminopenicillin conjugates reveals selectively potent antipseudomonal activity. *Journal of the American Chemical Society*, *134*(24), 9898-9901.

42. Jiang, X., Li, J., Zhang, R., Guo, H., Huang, S., & Shen, J. (2009). Improved preparation of 3-(1, 1-dimethylallyl) decursinol. *Journal of Heterocyclic Chemistry*, *46*(3), 560-562.

43. Joa, H., Vogl, S., Atanasov, A. G., Zehl, M., Nakel, T., Fakhrudin, N., … Dirsch, V. M. (2011). Identification of ostruthin from Peucedanum ostruthium rhizomes as

an inhibitor of vascular smooth muscle cell proliferation. *Journal of natural products*, *74*(6), 1513-1516.

44. Joseph, A., Thuy, T. T. T., Thanh, L. T., & Okada, M. (2018). Antidepressive and anxiolytic effects of ostruthin, a TREK-1 channel activator. *PloS one*, *13*(8), e0201092.

45. Juárez-Hernández, R. E., Miller, P. A., & Miller, M. J. (2012). Syntheses of siderophore–drug conjugates using a convergent thiol–maleimide system. *ACS medicinal chemistry letters*, *3*(10), 799-803.

46. Kim, S., Ko, H., Son, S., Shin, K. J., & Kim, D. J. (2001). Enantioselective syntheses of (+)-decursinol and (+)-trans-decursidinol. *Tetrahedron Letters*, *42*(43), 7641-7643.

47. Kim, B. H., Kwon, J., Lee, D., & Mar, W. (2015). Neuroprotective Effect of Demethylsuberosin, a Proteasome Activator, against MPP+-induced Cell Death in Human Neuroblastoma SH-SY5Y Cells. Planta Medica Letters, 2(01), e15-e18.

48. Kim, Y. A., Park, S. H., Kim, B. Y., Kim, A. H., Park, B. J., & Kim, J. J. (2014). Inhibitory effects on melanin production of demethylsuberosin isolated from Angelica gigas Nakai. *Korean Journal of Pharmacognosy*, *45*(3), 209-213.

49. Kinzel, O., Tappe, R., Gerus, I., & Budzikiewicz, H. (1998). The synthesis and antibacterial activity of two pyoverdin-ampicillin conjugates, entering Pseudomonas aeruginosa via the pyoverdin-mediated iron uptake pathway. *The Journal of antibiotics*, *51*(5), 499-507.

50. Knowles, J. R. (1985). Penicillin resistance: the chemistry of. beta.-lactamase inhibition. *Accounts of Chemical Research*, *18*(4), 97-104.

51. Kommera, R., & Bhimapaka, C. R. (2020). A simple and efficient approach for the preparation of dihydroxanthyletin, xanthyletin, decursinol and marmesin. *Synthetic Communications*, *50*(21), 3204-3211.

52. Kubanik, M., Holtkamp, H., Söhnel, T., Jamieson, S. M., & Hartinger, C. G. (2015). Impact of the halogen substitution pattern on the biological activity of organoruthenium 8-hydroxyquinoline anticancer agents. *Organometallics*, *34*(23), 5658-5668.

53. Landecker, H. (2016). Antibiotic resistance and the biology of history. *Body & Society*, *22*(4), 19-52.

54. Lucas, P. J., Uddin, M. R., Khisa, N., Akter, S. S., Unicomb, L., Nahar, P., … Rousham, E. K. (2019). Pathways to antibiotics in Bangladesh: A qualitative study investigating how and when households access medicine including antibiotics for humans or animals when they are ill. *PLoS One*, *14*(11), e0225270.

55. Levy, S. B. (1998). The challenge of antibiotic resistance. *Scientific American*, *278*(3), 46-53.

56. Li, Y., Xia, L., Chen, J., Lian, Y., Dandekar, A. A., Xu, F., & Wang, M. (2021). Resistance elicited by sub-lethal concentrations of ampicillin is partially mediated by quorum sensing in Pseudomonas aeruginosa. *Environment International*, *156*, 106619.

57. Lin, Y. M., Ghosh, M., Miller, P. A., Möllmann, U., & Miller, M. J. (2019). Synthetic sideromycins (skepticism and optimism): Selective generation of either broad or narrow spectrum Gram-negative antibiotics. *Biometals, 32*(3), 425-451.

58. Lin, Z., Xu, X., Zhao, S., Yang, X., Guo, J., Zhang, Q., … He, Y. (2018). Total synthesis and antimicrobial evaluation of natural albomycins against clinical pathogens. *Nature communications*, *9*(1), 1-8.

59. Magolan, J., & Coster, M. J. (2009). Total synthesis of (+)-angelmarin. *The Journal of Organic Chemistry*, *74*(14), 5083-5086.

60. Mislin, G. L., & Schalk, I. J. (2014). Siderophore-dependent iron uptake systems as gates for antibiotic Trojan horse strategies against Pseudomonas aeruginosa. *Metallomics*, *6*(3), 408-420.

61. Möllmann, U., Heinisch, L., Bauernfeind, A., Köhler, T., & Ankel-Fuchs, D. (2009). Siderophores as drug delivery agents: application of the "Trojan Horse" strategy. *Biometals*, *22*(4), 615-624.

62. Morehead, M. S., & Scarbrough, C. (2018). Emergence of global antibiotic resistance. *Primary care: clinics in office practice*, *45*(3), 467-484.

63. Moulinet d'Hardemare, A. D., Gellon, G., Philouze, C., & Serratrice, G. (2012). Oxinobactin and sulfoxinobactin, abiotic siderophore analogues to enterobactin involving 8-hydroxyquinoline subunits: thermodynamic and structural studies. *Inorganic chemistry*, *51*(22), 12142-12151.

64. Murray, R. D. H., Ballantyne, M. M., & Mathai, K. P. (1971). Claisen rearrangements—III: Convenient syntheses of the coumarins, osthenol, demethylsuberosin and coumurrayin. *Tetrahedron*, *27*(6), 1247-1251.

65. Nelson, M. L., Dinardo, A., Hochberg, J., & Armelagos, G. J. (2010). Brief communication: mass spectroscopic characterization of tetracycline in the skeletal remains of an ancient population from Sudanese Nubia 350–550 CE. *American journal of physical anthropology*, *143*(1), 151-154.

66. New report calls for urgent action to avert antimicrobial resistance crisis. (2021). Retrieved 16 February 2021, from https://www.who.int/news/item/29-04-2019-new-report-calls-for-urgent-action-to-avert-antimicrobial-resistance-crisis#:~:text=By%202030%2C%20antimicrobial%20resistance%20could,die%20from%20multidrug%2Dresistant%20tuberculosis

67. Ohi, N., Aoki, B., Shinozaki, T., Moro, K., Noto, T., Nehashi, T., … Matsunaga, I. (1986). Semisynthetic β-lactam antibiotics I. Synthesis and antibacterial activity of new ureidopenicillin derivatives having catechol moieties. *The Journal of Antibiotics*, *39*(2), 230-241.

68. Patre, R. E., Shet, J. B., Parameswaran, P. S., & Tilve, S. G. (2009). Cascade Wittig reaction-double Claisen and Cope rearrangements: one-pot synthesis of diprenylated coumarins gravelliferone, balsamiferone, and 6, 8-diprenylumbelliferone. *Tetrahedron Letters*, *50*(47), 6488-6490.

69. Perry, J., Waglechner, N., & Wright, G. (2016). The prehistory of antibiotic resistance. *Cold Spring Harbor perspectives in medicine*, *6*(6), a025197.

70. Phutdhawong, W., Chuenchid, A., Taechowisan, T., Sirirak, J., & Phutdhawong, W. S. (2021). Synthesis and biological activity evaluation of coumarin-3-carboxamide derivatives. *Molecules*, *26*(6), 1653.

71. Piao, X., Byun, H. S., Lee, S. R., Ju, E., Park, K. A., Sohn, K. C., … Hur, G. M. (2021). 8-Geranylumbelliferone isolated from Paramignya trimera triggers RIPK1/RIPK3-dependent programmed cell death upon TNFR1 ligation. *Biochemical Pharmacology*, *192*, 114733.

72. Pippi, B., Joaquim, A. R., Merkel, S., Zanette, R. A., Nunes, M. E. M., da Costa Silva, D. G., … Fuentefria, A. M. (2020). Antifungal activity and toxicological parameters of 8-hydroxyquinoline-5-sulfonamides using alternative animal models. *Journal of Applied Microbiology*.

73. Pippi, B., Lopes, W., Reginatto, P., Silva, F. É. K., Joaquim, A. R., Alves, R. J., … Fuentefria, A. M. (2019). New insights into the mechanism of antifungal action of 8-hydroxyquinolines. *Saudi pharmaceutical journal*, 27(1), 41-48.

74. Plunkett, G. M., Pimenov, M. G., Reduron, J. P., Kljuykov, E. V., Wyk, B. E. V., Ostroumova, T. A., … Muckensturm, B. (2018). Apiaceae. In *Flowering Plants. Eudicots* (pp. 9-206). Springer, Cham.

75. Pollack, L. A., & Srinivasan, A. (2014). Core elements of hospital antibiotic stewardship programs from the Centers for Disease Control and Prevention. *Clinical Infectious Diseases*, *59*(suppl_3), S97-S100.

76. Popescu, A., & Doyle, R. J. (1996). The Gram stain after more than a century. *Biotechnic & histochemistry*, *71*(3), 145-151.

77. Raymond, K. N., Dertz, E. A., & Kim, S. S. (2003). Enterobactin: an archetype for microbial iron transport. *Proceedings of the National Academy of Sciences*, *100*(7), 3584-3588.

78. Rodriguez, G. M. (2006). Control of iron metabolism in Mycobacterium tuberculosis. *Trends in microbiology*, *14*(7), 320-327.

79. Ruiz, N., Kahne, D., & Silhavy, T. J. (2006). Advances in understanding bacterial outer-membrane biogenesis. *Nature Reviews Microbiology, 4*(1), 57-66.

80. Saha, A., Dutta, S., & Nandi, N. (2020). Inhibition of seryl tRNA synthetase by seryl nucleoside moiety (SB-217452) of albomycin antibiotic. *Journal of Biomolecular Structure and Dynamics*, *38*(8), 2440-2454.

81. Santiago-Rodriguez, T. M., Fornaciari, G., Luciani, S., Dowd, S. E., Toranzos, G. A., Marota, I., & Cano, R. J. (2015). Gut microbiome of an 11th century AD pre-Columbian Andean mummy. *PloS one*, *10*(9), e0138135.

82. Schinkovitz, A., Gibbons, S., Stavri, M., Cocksedge, M. J., & Bucar, F. (2003). Ostruthin: an antimycobacterial coumarin from the roots of Peucedanum ostruthium. *Planta medica*, *69*(04), 369-371.

83. Schobert, R., Stangl, A., & Hannemann, K. (2006). Conjugates of methyl 6-aminopenicillanate with biscatechol-hydroxamate chelators: Synthesis and siderophoric activity. *Tetrahedron*, *62*(33), 7799-7808.

84. Schulze, M. M., Boehme, U., Schwarzer, A., & Weber, E. (2017). Intermolecular interactions in the solid state structures of neutral and N-protonated 5-

alkoxymethyl-8-hydroxyquinolines. *Journal of Molecular Structure*, *1133*, 307-319.

85. Sengupta, S., Chattopadhyay, M. K., & Grossart, H. P. (2013). The multifaceted roles of antibiotics and antibiotic resistance in nature. *Frontiers in microbiology*, *4*, 47.

86. Serratrice, G., Boukhalfa, H., Béguin, C., Baret, P., Caris, C., & Pierre, J. L. (1997). O-TRENSOX, a new tripodal iron chelator based on 8-hydroxyquinoline subunits: Thermodynamic and kinetic studies. *Inorganic Chemistry*, *36*(18), 3898-3910.

87. Shen, A. Y., Chen, C. P., & Roffler, S. (1999). A chelating agent possessing cytotoxicity and antimicrobial activity: 7-morpholinomethyl-8-hydroxyquinoline. *Life sciences, 64*(9), 813-825.

88. Silhavy, T. J., Kahne, D., & Walker, S. (2010). The bacterial cell envelope. *Cold Spring Harbor perspectives in biology*, *2*(5), a000414.

89. Spellberg, B. (2012). New antibiotic development: barriers and opportunities in 2012. *APUA Clin Newsl*, *30*, 8-10.

90. Steck, W. (1971). New synthesis of columbianetin and related coumarins. *Canadian Journal of Chemistry, 49*(8), 1197-1201.

91. Taura, F.; Morimoto, S.; Shoyama, Y. *J. Biol. Chem.* 1996, *271*, 17411– 17416

92. Trumble, J. T., & Millar, J. G. (1996). Biological activity of marmesin and demethylsuberosin against a generalist herbivore, Spodoptera exigua (Lepidoptera: Noctuidae). *Journal of Agricultural and Food Chemistry*, *44*(9), 2859-2864.

93. Tuan Anh, H. L., Kim, D. C., Ko, W., Ha, T. M., Nhiem, N. X., Yen, P. H., … Kiem, P. V. (2017). Anti-inflammatory coumarins from Paramignya trimera. *Pharmaceutical biology*, *55*(1), 1195-1201.

94. Vanammoole, L., Kommera, R., Hariprasad Kurma, S., Rao Vaidya, J., & Raju Bhimapaka, C. (2020). Regioselective Halogenation of 2H-Chromenones Promoted by Oxone and NaX: A Facile Approach for the Preparation of Halochromenones and 2H-Chromenone Natural Products. *ChemistrySelect*, *5*(28), 8875-8880.

95. Ventola, C. L. (2015). The antibiotic resistance crisis: part 1: causes and threats. *Pharmacy and therapeutics*, *40*(4), 277.

96. Vu, T. H., Ha-Duong, N. T., Aubry, A., Capton, E., Fechter, P., Plesiat, P., … Serradji, N. (2019). In vitro activities of a new fluoroquinolone derivative highly active against Chlamydia trachomatis. *Bioorganic Chemistry*, *83*, 180-185.

97. Watanabe, N. A., Nagasu, T., Katsu, K., & Kitoh, K. (1987). E-0702, a new cephalosporin, is incorporated into Escherichia coli cells via the tonB-dependent iron transport system. *Antimicrobial agents and chemotherapy*, *31*(4), 497-504.

98. Weber, B. S., De Jong, A. M., Guo, A. B., Dharavath, S., French, S., Fiebig-Comyn, A. A., … Brown, E. D. (2020). Genetic and chemical screening in human blood serum reveals unique antibacterial targets and compounds against Klebsiella pneumoniae. *Cell Reports*, *32*(3), 107927.

99. Wencewicz, T. A., Long, T. E., Möllmann, U., & Miller, M. J. (2013). Trihydroxamate siderophore–fluoroquinolone conjugates are selective

sideromycin antibiotics that target Staphylococcus aureus. *Bioconjugate chemistry*, *24*(3), 473-486.

100. Wencewicz, T. A., & Miller, M. J. (2013). Biscatecholate–monohydroxamate mixed ligand siderophore–carbacephalosporin conjugates are selective sideromycin antibiotics that target Acinetobacter baumannii. *Journal of medicinal chemistry*, *56*(10), 4044-4052.

101. Wu, J. Y., Srinivas, P., & Pogue, J. M. (2020). Cefiderocol: a novel agent for the management of multidrug-resistant Gram-negative organisms. *Infectious diseases and therapy*, *9*(1), 17-40.

102. Xia, Y., Min, K. H., & Lee, K. (2009). Synthesis and biological evaluation of decursin, prantschimgin and their derivatives. *Bulletin of the Korean Chemical Society*, *30*(1), 43-48.

103. Xiao, M., Wang, J., Lin, Z., Lu, Y., Li, Z., White, S. W., … Li, W. (2015). Design, synthesis and structure-activity relationship studies of novel survivin inhibitors with potent anti-proliferative properties. *PLoS One*, *10*(6), e0129807.

104. Yang, Y., Gao, G., Zhang, X., & Li, F. (2014). Facile fabrication of composition-tuned Ru–Ni bimetallics in ordered mesoporous carbon for levulinic acid hydrogenation. *ACS Catalysis, 4*(5), 1419-1425.

105. Zähner, H., Diddens, H. E. Y. K. E., Keller-Schierlein, W., & Nägeli, H. U. (1977). Some experiments with semisynthetic sideromycins. *The Japanese journal of antibiotics*, *30*, 201-206.

106. Zheng, T., & Nolan, E. M. (2014). Enterobactin-mediated delivery of β-lactam antibiotics enhances antibacterial activity against pathogenic Escherichia coli. *Journal of the American Chemical Society*, *136*(27), 9677-9691.

Appendix: Experimental Section

A.1: Experimental Procedures for Chapters 1 and 2

Reagents, substrates, and solvents were purchased from commercial suppliers and used without purification unless otherwise specified. Reaction progress was monitored by analytical thin-layer chromatography using aluminum-backed plates (silica gel F254 Silicycle Inc.), visualized under ultraviolet light. Compounds purified by flash chromatography used Teledyne CombiFlash Rf+ and NextGen 300+ purification systems with pre-packed silica columns (with a particle size of either 40–63 µM or 20–40 µM). NMR spectra were recorded at 25 °C using either a Bruker AVIII 700 (^{1}H at 700 MHz) or Bruker NEO 400 (^{1}H at 400 MHz). Chemical shifts in ^{1}H NMR spectra are reported in parts per million (ppm) with reference to residual solvents as follows: Chloroform-*d* (referenced to 7.26 ppm for ^{1}H NMR), DMSO-*d*6 (referenced to 2.50 ppm for ^{1}H NMR). Coupling constants (J) are reported in hertz.

All molecules and reaction schemes in this document were drawn using ChemDraw.

A.1.1: Procedures for Chapter 1

Synthesis of 5-chloromethyl-8-hydroxyquinoline hydrochloride (1-15)
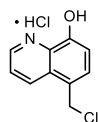
1-15 was synthesized according to a literature procedure (Yang et al., 2014). 4.672 g (32.2 mmol) of 8-hydroxyquinoline, 5.12 mL of formalin, and 0.48 g of zinc chloride

were added to 40 mL of concentrated (12 M) hydrochloric acid and stirred at room temperature overnight. The mixture was filtered, and the collected precipitate was washed with cold acetone to obtain 5-chloromethyl-8-hydroxyquinoline hydrochloride (**1-15**) as a yellow powder in 50-60% yield over multiple trials. ^{1}H NMR (700 MHz, DMSO-*d*6) δ 9.25 (d, *J* = 8.6 Hz, 1H), 9.12 – 9.05 (m, 1H), 8.09 – 8.03 (m, 1H), 7.72 (d, *J* = 7.8 Hz, 1H), 7.47 (d, *J* = 7.9 Hz, 1H), 4.92 (s, 2H).

Synthesis of 5-azidomethyl-8-hydroxyquinoline (1-16)
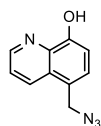
1-16 was synthesized according to a literature procedure (Bougharraf et al., 2017). 1 g (4.33 mmol, 1 equiv.) of **1-15** was stirred into 40 mL of acetone and the mixture was added to a suspension of 1.3 g (17 mmol, 3 equiv.) of sodium azide in 10 mL of acetone. The mixture was refluxed overnight, and the solvent was evaporated under reduced pressure. The product was extracted from water with chloroform, and the organic phase was dried with sodium sulfate. The solution was concentrated, and the product **1-16** was recrystallized in the form of white crystals from ethanol (0.65 g, 76% yield). ^{1}H NMR (700 MHz, Chloroform-*d*) δ 8.84 (dd, *J* = 4.2, 1.5 Hz, 1H), 8.38 (dd, *J* = 8.5, 1.5 Hz, 1H), 7.55 (dd, *J* = 8.5, 4.2 Hz, 1H), 7.45 (d, *J* = 7.7 Hz, 1H), 7.14 (d, *J* = 7.7 Hz, 1H), 4.66 (s, 2H).

General procedure for synthesis of deacetyl linezolid conjugates:

50 mg of the desired HQ carboxylic acid (**1-1** through **1-3**) and 120.3 mg of HBTU were added to 3 mL of DCM in a 50 mL round-bottom flask. 102.5 mg of DIPEA was added

and the mixture was stirred until no more particulate was visible at the bottom of the flask. 94 mg of deacetyl linezolid (**1-4**) was added to the reaction mixture which was stirred overnight at room temperature. Solvent was evaporated under reduced pressure and the residue was collected and adhered to silica. Regular phase column chromatography was conducted on a CombiFlash with a DCM/MeOH gradient from 100% DCM to 9:1 DCM/MeOH. **1-5** was purified by recrystallizing from dichloroethane (DCE) after collecting relevant fractions from chromatography. Relevant fractions of the other analogs were collected and run through reverse phase chromatography in water/MeOH gradient from 10-100% to isolate **1-6** and **1-7**.

(*S*)-*N*-((3-(3-fluoro-4-morpholinophenyl)-2-oxooxazolidin-5-yl)methyl)-8-hydroxyquinoline-7-carboxamide (1-5):
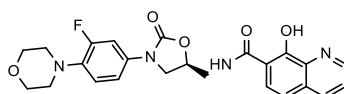
Yield was 10.6 mg (9%). ^{1}H NMR (400 MHz, DMSO-*d*6) δ 9.13 (t, *J* = 5.9 Hz, 1H), 8.92 (dd, *J* = 4.2, 1.7 Hz, 1H), 8.37 (dd, *J* = 8.3, 1.7 Hz, 1H), 7.99 (d, *J* = 8.8 Hz, 1H), 7.67 (dd, *J* = 8.3, 4.2 Hz, 1H), 7.49 (dd, *J* = 15.0, 2.6 Hz, 1H), 7.43 (d, *J* = 8.8 Hz, 1H), 7.23 – 7.16 (m, 1H), 7.05 (dd, *J* = 9.9, 8.9 Hz, 1H), 4.92 (dq, *J* = 8.8, 5.8 Hz, 1H), 4.17 (t, *J* = 9.0 Hz, 1H), 3.86 (dd, *J* = 9.2, 6.1 Hz, 1H), 3.82 – 3.69 (m, 6H), 2.98 – 2.91 (m, 4H).

**(*S*)-*N*-((3-(3-fluoro-4-morpholinophenyl)-2-oxooxazolidin-5-yl)methyl)-8-hydroxyquinoline-5-carboxamide (1-6):**
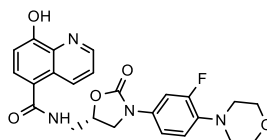
Yield was 10.3 mg (8%). ^{1}H NMR (400 MHz, DMSO-$d6$) δ 8.95 – 8.83 (m, 3H), 7.72 (d, J = 8.0 Hz, 1H), 7.64 (dd, J = 8.7, 4.3 Hz, 1H), 7.49 (dd, J = 15.0, 2.6 Hz, 1H), 7.24 – 7.17 (m, 1H), 7.13 (d, J = 8.0 Hz, 1H), 7.06 (t, J = 9.4 Hz, 1H), 4.91 (dq, J = 10.3, 5.3 Hz, 1H), 4.19 (t, J = 9.0 Hz, 1H), 3.93 (dd, J = 9.2, 5.7 Hz, 1H), 3.75 – 3.71 (m, 5H), 3.70 – 3.59 (m, 1H), 2.99 – 2.92 (m, 4H).

(*S*)-*N*-((3-(3-fluoro-4-morpholinophenyl)-2-oxooxazolidin-5-yl)methyl)-8-hydroxyquinoline-2-carboxamide (1-7):
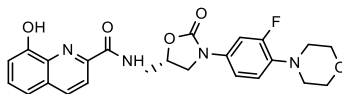
Yield was 43.5 mg (35%). ^{1}H NMR (400 MHz, DMSO-$d6$) δ 10.21 (s, 1H), 9.96 (t, J = 6.2 Hz, 1H), 8.49 (d, J = 8.6 Hz, 1H), 8.14 (d, J = 8.5 Hz, 1H), 7.56 (dd, J = 8.2, 7.6 Hz, 1H), 7.51 – 7.43 (m, 2H), 7.21 – 7.13 (m, 2H), 7.01 (dd, J = 9.9, 8.8 Hz, 1H), 4.93 (dq, J = 8.7, 5.7 Hz, 1H), 4.20 (t, J = 9.0 Hz, 1H), 3.88 (dd, J = 9.2, 6.2 Hz, 1H), 3.77 (t, J = 5.8 Hz, 2H), 3.74 – 3.68 (m, 4H), 2.96 – 2.89 (m, 4H).

General procedure for synthesis of aza-linezolid conjugates:

50 mg of the desired HQ carboxylic acid (**1-2** and **1-3**) and 120.3 mg of HBTU were added to 3 mL of DCM in a 50 mL round-bottom flask. 102.5 mg of DIPEA was added and the mixture was stirred until no more particulate was visible at the bottom of the flask. 107 mg of aza-linezolid (**1-9**) was added to the reaction mixture which was then stirred overnight at room temperature. Solvent was evaporated under reduced pressure and the residue was collected and adhered to silica. Regular phase column

chromatography was conducted on a CombiFlash with a DCM/MeOH gradient from 100% DCM to 9:1 DCM/MeOH. Relevant fractions were collected and run through reverse phase chromatography in a water/MeOH gradient from 10-100% MeOH to isolate **1-10** and **1-11**.

(*S*)-*N*-((3-(3-fluoro-4-(4-(8-hydroxyquinoline-5-carbonyl)piperazin-1-yl)phenyl)-2-oxooxazolidin-5-yl)methyl)acetamide (1-10):
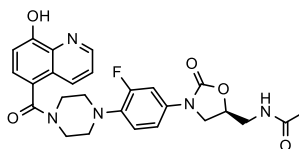

Yield was 6.7 mg (5%). ^{1}H NMR (400 MHz, DMSO-*d*6) δ 10.24 (s, 1H), 8.91 (dd, *J* = 4.1, 1.6 Hz, 1H), 8.32 – 8.18 (m, 2H), 7.63 (dd, *J* = 8.6, 4.1 Hz, 1H), 7.51 – 7.42 (m, 2H), 7.17 (dd, *J* = 8.8, 2.6 Hz, 1H), 7.12 (d, *J* = 7.9 Hz, 1H), 7.08 (t, *J* = 9.3 Hz, 1H), 4.84 – 4.57 (m, 1H), 4.07 (t, *J* = 9.0 Hz, 1H), 3.70 (dd, *J* = 9.2, 6.4 Hz, 1H), 3.60 (dtt, *J* = 13.4, 6.8, 3.4 Hz, 1H), 3.39 (t, *J* = 5.5 Hz, 2H), 3.13 (qd, *J* = 6.8, 6.2, 3.7 Hz, 2H), 2.86 (s, 2H), 1.82 (s, 3H).

(*S*)-*N*-((3-(3-fluoro-4-(4-(8-hydroxyquinoline-2-carbonyl)piperazin-1-yl)phenyl)-2-oxooxazolidin-5-yl)methyl)acetamide (1-11):
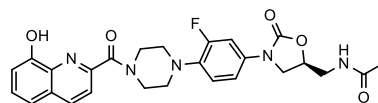
Yield was 13.7 mg (10%). ^{1}H NMR (400 MHz, DMSO-*d*6) δ 9.79 (s, 1H), 8.44 (d, *J* = 8.5 Hz, 1H), 8.23 (t, *J* = 5.9 Hz, 1H), 7.69 (d, *J* = 8.5 Hz, 1H), 7.55 – 7.42 (m, 3H), 7.23 –

7.06 (m, 3H), 4.76 – 4.65 (m, 1H), 4.13 – 4.04 (m, 1H), 3.91 – 3.84 (m, 2H), 3.70 (dd, $J =$ 9.1, 6.4 Hz, 1H), 3.62 (t, $J = 4.9$ Hz, 2H), 3.40 (t, $J = 5.5$ Hz, 2H), 3.12 (t, $J = 5.1$ Hz, 2H), 3.00 (t, $J = 5.0$ Hz, 2H), 1.83 (s, 3H).

Synthesis of 8-hydroxyquinoline 5-methyl ethers (1-39 to 1-46):

Hydroxyquinoline ethers were synthesized according to a preparation modified from a literature procedure (Xiao et al., 2015). 0.2 g (0.8692 mmol, 1 equiv.) of **1-15** was added to a mixture of 0.146 g (0.8692 mmol, 2 equiv.) of sodium bicarbonate and 4.346 mmol (5 equiv.) of the alcohol stirring in approximately 3 mL of tetrahydrofuran (THF). This mixture was refluxed overnight. The excess solvent was evaporated under reduced pressure, and the organic phase was extracted in ethyl acetate from water. The organic phase was concentrated, and the crude product was obtained from column chromatography (hexane/ethyl acetate). Reverse phase chromatography was conducted in water/methanol to give the products **1-39** to **1-46** in 2-10% yield.

5-(phenethoxymethyl)quinolin-8-ol (1-39):
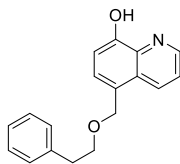
10.4 mg yield, 4%. 1H NMR (700 MHz, Chloroform-*d*) δ 8.77 (dd, $J = 4.2$, 1.5 Hz, 1H), 8.31 (dd, $J = 8.5$, 1.6 Hz, 1H), 7.40 – 7.36 (m, 2H), 7.24 (d, $J = 0.7$ Hz, 1H), 7.23 – 7.19 (m, 1H), 7.18 – 7.16 (m, 2H), 7.08 (d, $J = 7.6$ Hz, 1H), 4.82 (d, $J = 0.7$ Hz, 2H), 3.73 (t, $J = 7.0$ Hz, 2H), 2.90 (t, $J = 6.9$ Hz, 2H).

5-((((4-fluorobenzyl)oxy)methyl)quinolin-8-ol (1-40):
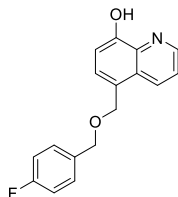
25.6 mg yield, 10%. 1H NMR (700 MHz, Chloroform-*d*) δ 8.81 (dd, *J* = 4.2, 1.6 Hz, 1H), 8.48 (dd, *J* = 8.5, 1.6 Hz, 1H), 7.49 (dd, *J* = 8.5, 4.2 Hz, 1H), 7.42 (d, *J* = 7.7 Hz, 1H), 7.32 – 7.26 (m, 2H), 7.11 (d, *J* = 7.7 Hz, 1H), 7.06 – 7.00 (m, 2H), 5.30 (s, 0H), 4.87 (d, *J* = 0.6 Hz, 2H), 4.50 (s, 2H).
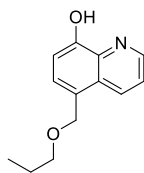
5-((allyloxy)methyl)quinolin-8-ol (1-41):
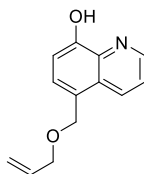
10.5 mg yield, 6%. 1H NMR (700 MHz, Chloroform-*d*) δ 8.86 (d, *J* = 4.6 Hz, 1H), 8.71 (s, 1H), 7.65 – 7.56 (m, 0H), 7.54 – 7.48 (m, 1H), 7.31 – 7.26 (m, 1H), 5.95 (ddt, *J* = 17.2, 10.3, 5.7 Hz, 1H), 5.35 – 5.19 (m, 2H), 4.91 – 4.84 (m, 2H), 4.04 (dt, *J* = 5.7, 1.4 Hz, 2H).

**5-((((3,5-dimethoxybenzyl)oxy)methyl)quinolin-8-ol (1-42):**
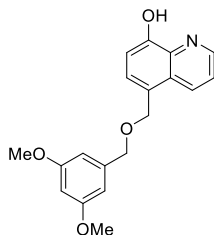
13.3 mg yield, 5%. 1H NMR (700 MHz, Chloroform-*d*) δ 8.81 (dd, *J* = 4.2, 1.5 Hz, 1H), 8.55 (dd, *J* = 8.5, 1.5 Hz, 1H), 8.15 (s, 1H), 7.52 (dd, *J* = 8.5, 4.2 Hz, 1H), 6.96 (d, *J* = 7.9 Hz, 1H), 6.71 (dt, *J* = 8.4, 1.5 Hz, 2H), 6.53 (d, *J* = 2.5 Hz, 1H), 4.54 (d, *J* = 5.3 Hz, 2H), 4.36 – 4.33 (m, 2H), 3.87 (s, 3H), 3.74 (s, 3H).

5-(propoxymethyl)quinolin-8-ol (1-43):

6.0 mg yield, 3%. 1H NMR (700 MHz, Chloroform-*d*) δ 8.86 (s, 1H), 8.74 (s, 1H), 7.61 (s, 1H), 7.51 (d, *J* = 7.8 Hz, 1H), 4.85 (s, 2H), 3.46 (t, *J* = 6.6 Hz, 2H), 1.66 – 1.58 (m, 2H), 0.90 (t, *J* = 7.4 Hz, 3H).

5-((but-3-yn-1-yloxy)methyl)quinolin-8-ol (1-44):
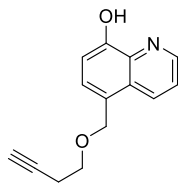
4.7 mg yield, 2%. 1H NMR (700 MHz, Chloroform-*d*) δ 8.80 (dd, *J* = 4.2, 1.6 Hz, 1H), 8.55 (dd, *J* = 8.5, 1.5 Hz, 1H), 8.33 (s, 1H), 7.49 (dd, *J* = 8.5, 4.1 Hz, 1H), 7.42 (d, *J* = 7.6 Hz, 1H), 7.09 (d, *J* = 7.7 Hz, 1H), 4.89 (d, *J* = 0.7 Hz, 2H), 3.61 (t, *J* = 6.8 Hz, 2H), 2.47 (td, *J* = 6.8, 2.7 Hz, 2H), 1.97 (t, *J* = 2.7 Hz, 1H).

5-((((6,6-dimethylbicyclo[3.1.1]hept-2-en-2-yl)methoxy)methyl)quinolin-8-ol (1-45):
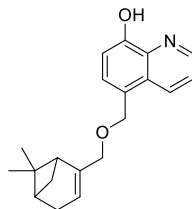
16.0 mg yield, 6%. 1H NMR (700 MHz, Chloroform-*d*) δ 8.80 (dd, *J* = 4.2, 1.6 Hz, 1H), 8.56 – 8.50 (m, 1H), 7.50 (dd, *J* = 8.5, 4.2 Hz, 1H), 7.41 (d, *J* = 7.7 Hz, 1H), 7.12 (d, *J* = 7.7 Hz, 1H), 5.53 (tp, *J* = 2.8, 1.4 Hz, 1H), 4.81 (dd, *J* = 11.7, 0.7 Hz, 1H), 4.77 (dd, *J* = 11.7, 0.7 Hz, 1H), 3.89 (p, *J* = 1.6 Hz, 2H), 2.41 (dt, *J* = 8.7, 5.6 Hz, 1H), 2.36 – 2.22 (m, 2H), 2.17 (td, *J* = 5.7, 1.5 Hz, 1H), 2.12 (ttd, *J* = 5.7, 2.7, 1.3 Hz, 1H), 1.28 (s, 3H), 1.20 (d, *J* = 8.7 Hz, 1H), 0.85 (s, 3H).

5-((((2-bromobenzyl)oxy)methyl)quinolin-8-ol (1-46):
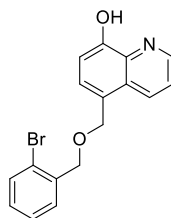
11.7 mg yield, 4%. 1H NMR (700 MHz, Chloroform-*d*) δ 8.80 (dd, *J* = 4.2, 1.5 Hz, 1H), 8.54 (dd, *J* = 8.5, 1.5 Hz, 1H), 8.34 (s, 1H), 7.54 (dd, *J* = 8.0, 1.2 Hz, 1H), 7.49 (dd, *J* = 8.5, 4.2 Hz, 1H), 7.47 (d, *J* = 7.7 Hz, 1H), 7.46 – 7.43 (m, 1H), 7.29 (td, *J* = 7.5, 1.2 Hz, 1H), 7.17 – 7.13 (m, 1H), 7.12 (d, *J* = 7.7 Hz, 1H), 4.96 (d, *J* = 0.7 Hz, 2H), 4.64 (s, 2H).

A.1.2: Procedures for Chapter 2

General procedure for synthesis of prenylated coumarins:

The synthesis of demethylsuberosin (**2-2**) and osthenol (**2-3**) was adapted from a literature procedure (Jentsch et al., 2020). 150 mg (3 equiv.) of umbelliferone (7-hydroxycoumarin) and 26.6 mg (1 equiv.) of prenol (3-methyl-2-buten-1-ol) were suspended in dry dichloroethane (DCE). 1.5 g/mmol of dry acidic alumina (Al_2O_3) relative to the scaffold was added to the reaction mixture, which was subsequently heated overnight at reflux. The mixture was then poured over diatomaceous earth and washed with ethyl acetate. The collected solution was concentrated under reduced pressure. **2-2** and **2-3** were eluted through column chromatography using hexanes/ethyl acetate.

Demethylsuberosin (2-2):
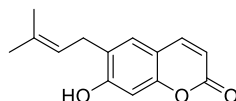
3.5 mg, 5% yield. ^{1}H NMR (400 MHz, Chloroform-d) δ 7.61 (d, J = 8.9 Hz, 1H), 7.19 (s, 1H), 6.81 (s, 1H), 6.23 (d, J = 9.5 Hz, 1H), 6.08 (s, 1H), 5.34 – 5.27 (m, 1H), 3.38 (d, J = 7.2 Hz, 2H), 1.87 – 1.70 (m, 6H).

Osthenol (2-3):
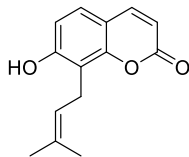
2.7 mg, 4% yield. ^{1}H NMR (400 MHz, Chloroform-d) δ 7.63 (d, J = 9.5 Hz, 1H), 7.36 (d, J = 8.5 Hz, 1H), 6.82 (d, J = 2.4 Hz, 1H), 6.24 (d, J = 9.5 Hz, 1H), 5.47 (ddq, J = 8.1, 5.6, 1.4 Hz, 1H), 4.58 (dt, J = 6.7, 0.9 Hz, 2H), 1.79 (dt, J = 16.0, 1.0 Hz, 6H).

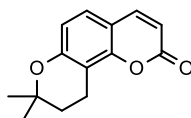**General procedure for synthesis of cyclized prenyl-coumarins:**

The synthesis of **2-34** and **2-35** was adapted from a literature procedure (Jentsch et al., 2020). 3 equivalents of umbelliferone (7-hydroxycoumarin) and 1 equivalent of prenol were suspended in xylene. 1.5 g/mmol of dry acidic alumina (Al_2O_3) relative to the scaffold were added to the reaction mixture, which was heated in a monowave reactor to 160ºC for 2 hours. The mixture was then poured over diatomaceous earth and washed with ethyl acetate. The collected solution was concentrated under reduced pressure. **2-34** and **2-35** were eluted through column chromatography using hexanes/ethyl acetate.

Dihydroxanthyletin (2-34):
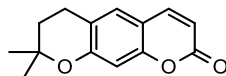
16.6 mg, 23% yield. ^{1}H NMR (400 MHz, DMSO-d_6) δ 7.92 (dd, J = 9.5, 0.7 Hz, 1H),

7.45 (s, 1H), 6.70 (s, 1H), 6.23 (d, J = 9.5 Hz, 1H), 2.80 (td, J = 6.8, 1.1 Hz, 2H), 1.81 (t,

J = 6.8 Hz, 2H), 1.32 (s, 6H).

Dihydroseselin (2-35):

13.4 mg, 19% yield. ^{1}H NMR (400 MHz, DMSO-d_6) δ 7.95 (d, J = 9.5 Hz, 1H), 7.43 (d, J

= 8.5 Hz, 1H), 6.75 (d, J = 8.6 Hz, 1H), 6.24 (d, J = 9.5 Hz, 1H), 2.78 (t, J = 6.8 Hz, 2H),

1.83 (t, J = 6.8 Hz, 2H), 1.31 (s, 6H).

General procedure for synthesis of geranylated coumarins:

The synthesis of ostruthin (**2-4**) and 8-geranylumbelliferone (**2-5**) was adapted from a

literature procedure (Jentsch et al., 2020). 100 mg (2.1 equiv.) of umbelliferone (7-

hydroxycoumarin) and 45 mg (1 equiv.) of geraniol (3,7-dimethylocta-trans-2,6-dien-1-

ol) were suspended in xylenes. 1.5 g/mmol of dry acidic alumina (Al$_2$O$_3$) relative to the

scaffold was added to the reaction mixture, which was subsequently heated at 160ºC for 2

hours in a monowave reactor. The mixture was then poured over diatomaceous earth and

washed with ethyl acetate, acetone, and hexane. The collected solvents were combined

and concentrated under reduced pressure. **2-4** and **2-5** were eluted through column chromatography using hexanes/ethyl acetate.

Ostruthin (2-4):
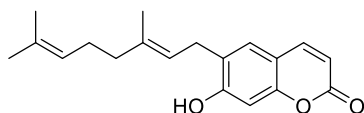
31.2 mg, 36% yield. ^{1}H NMR (400 MHz, Chloroform-*d*) δ 7.61 (d, *J* = 9.5 Hz, 1H), 7.19 (s, 1H), 6.84 (s, 1H), 6.24 (d, *J* = 9.4 Hz, 1H), 5.97 (s, 1H), 5.35 – 5.27 (m, 1H), 5.08 (dddd, *J* = 6.9, 5.5, 3.5, 1.7 Hz, 1H), 3.40 (d, *J* = 7.2 Hz, 2H), 2.13 (q, *J* = 5.3, 4.8 Hz, 4H), 1.77 (d, *J* = 1.4 Hz, 3H), 1.69 (d, *J* = 1.3 Hz, 3H), 1.61 (d, *J* = 1.3 Hz, 3H).

8-geranylumbelliferone (2-5):
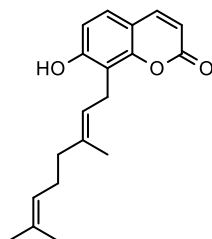
9.7 mg, 11% yield. ^{1}H NMR (400 MHz, Chloroform-*d*) δ 7.63 (d, *J* = 9.5 Hz, 1H), 7.24 (d, *J* = 8.4 Hz, 1H), 6.80 (d, *J* = 8.5 Hz, 1H), 6.24 (d, *J* = 9.4 Hz, 1H), 6.20 (s, 1H), 5.27 (tq, *J* = 7.2, 1.3 Hz, 1H), 5.03 (dddt, *J* = 6.8, 5.4, 2.8, 1.4 Hz, 1H), 3.64 (d, *J* = 7.3 Hz, 2H), 2.14 – 2.02 (m, 4H), 1.85 (q, *J* = 1.0 Hz, 3H), 1.66 (d, *J* = 1.3 Hz, 3H), 1.58 (d, *J* = 1.3 Hz, 3H).

A.2: Spectra for Chapters 1 and 2

A.2.1: Spectra for Chapter 1

5-(chloromethyl)-8-hydroxyquinoline (**1-15**)

5-(azidomethyl)-8-hydroxyquinoline (**1-16**)
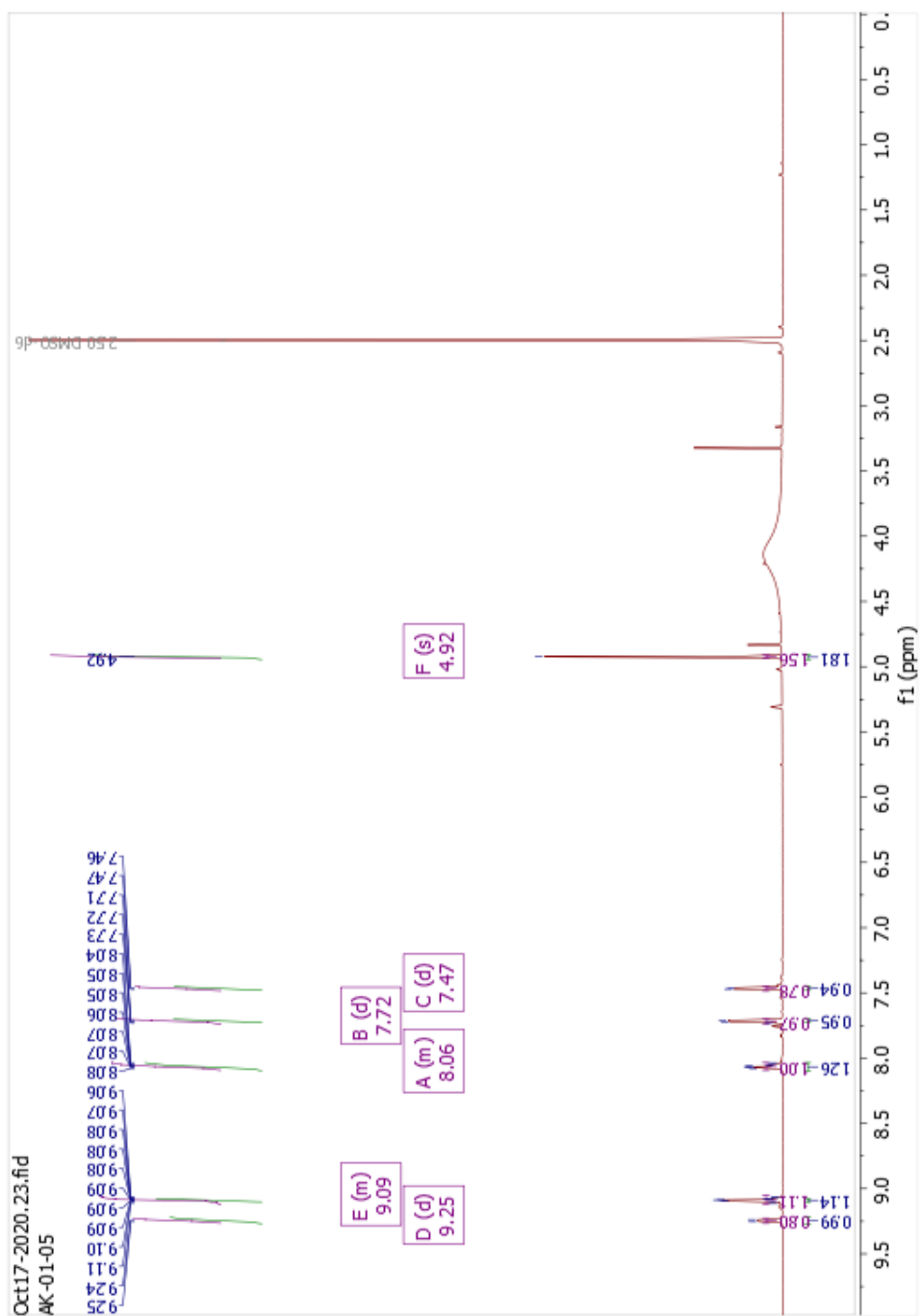
HQ-2-COOH/deacetylated linezolid analog (**1-7**):
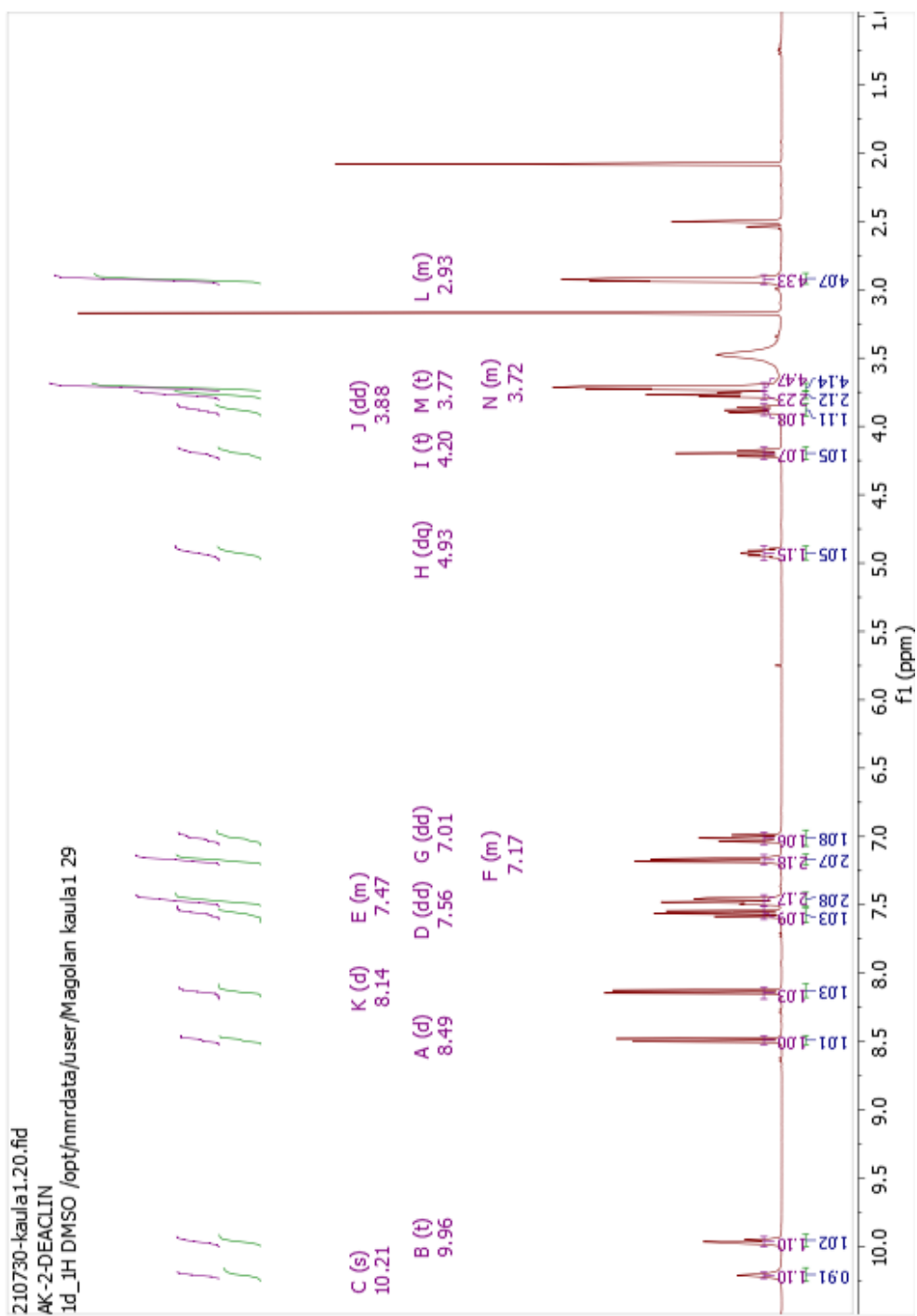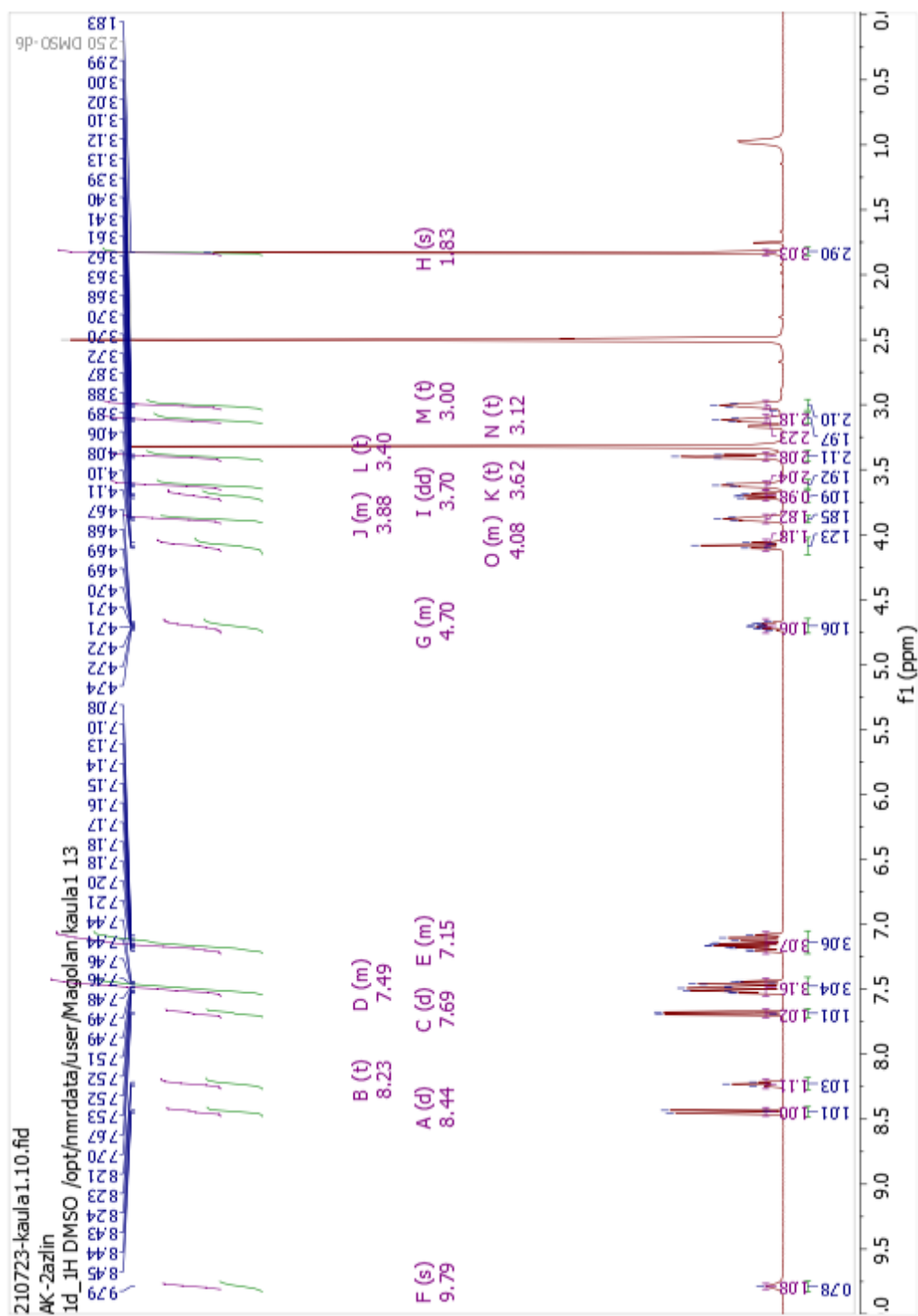
HQ-5-COOH/deacetylated linezolid analog (**1-6**):
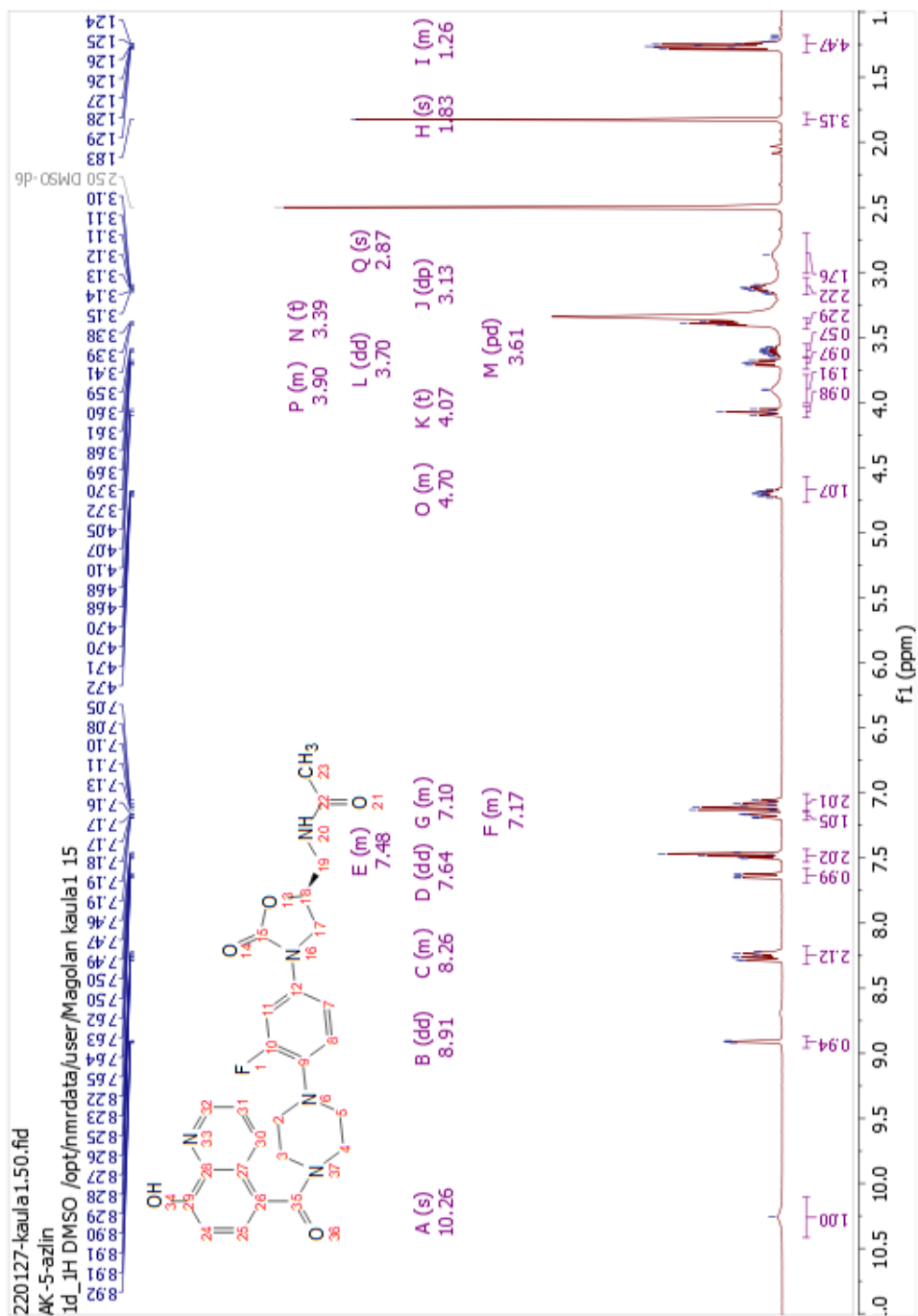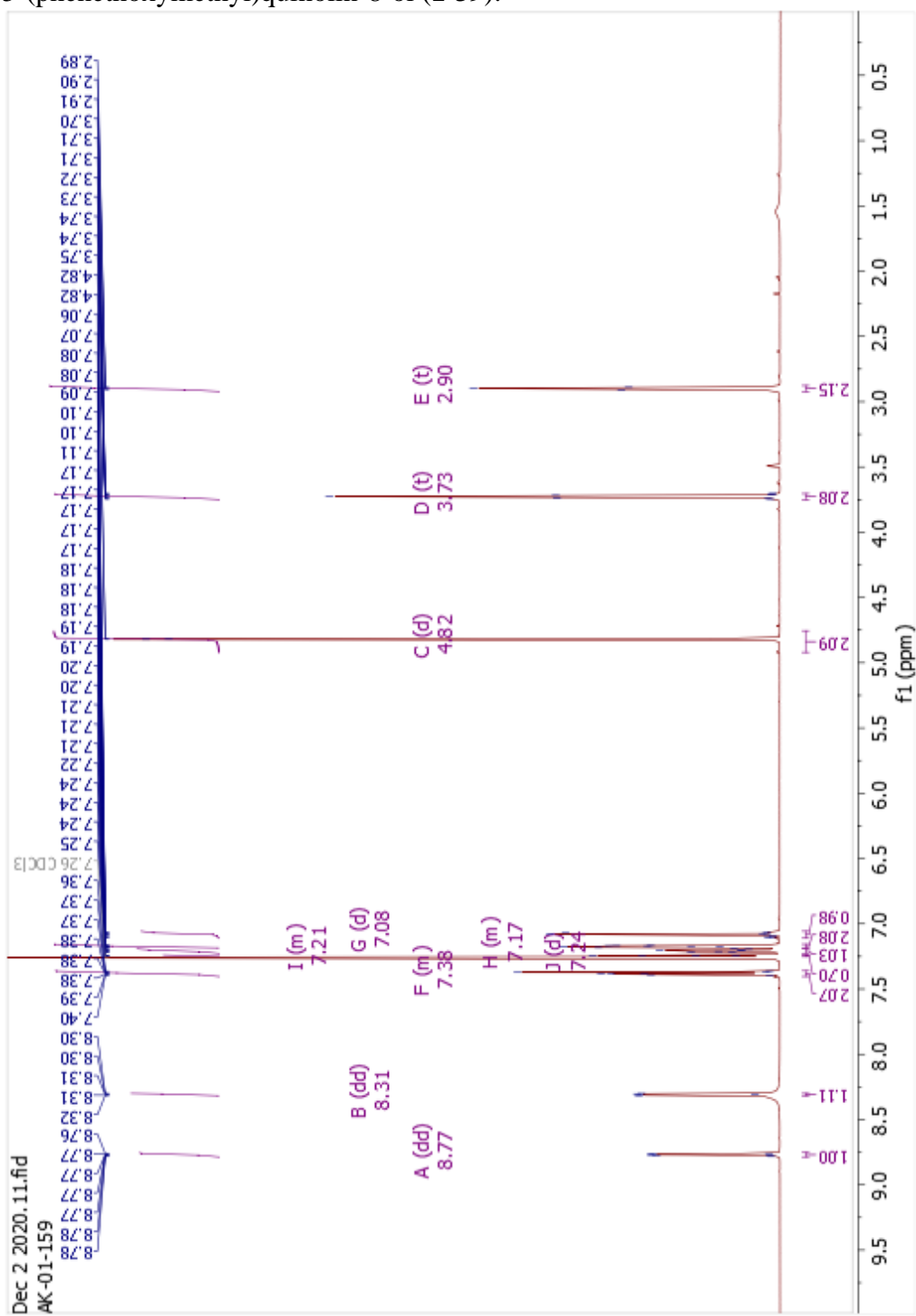
HQ-7-COOH/deacetylated linezolid analog (**1-5**):
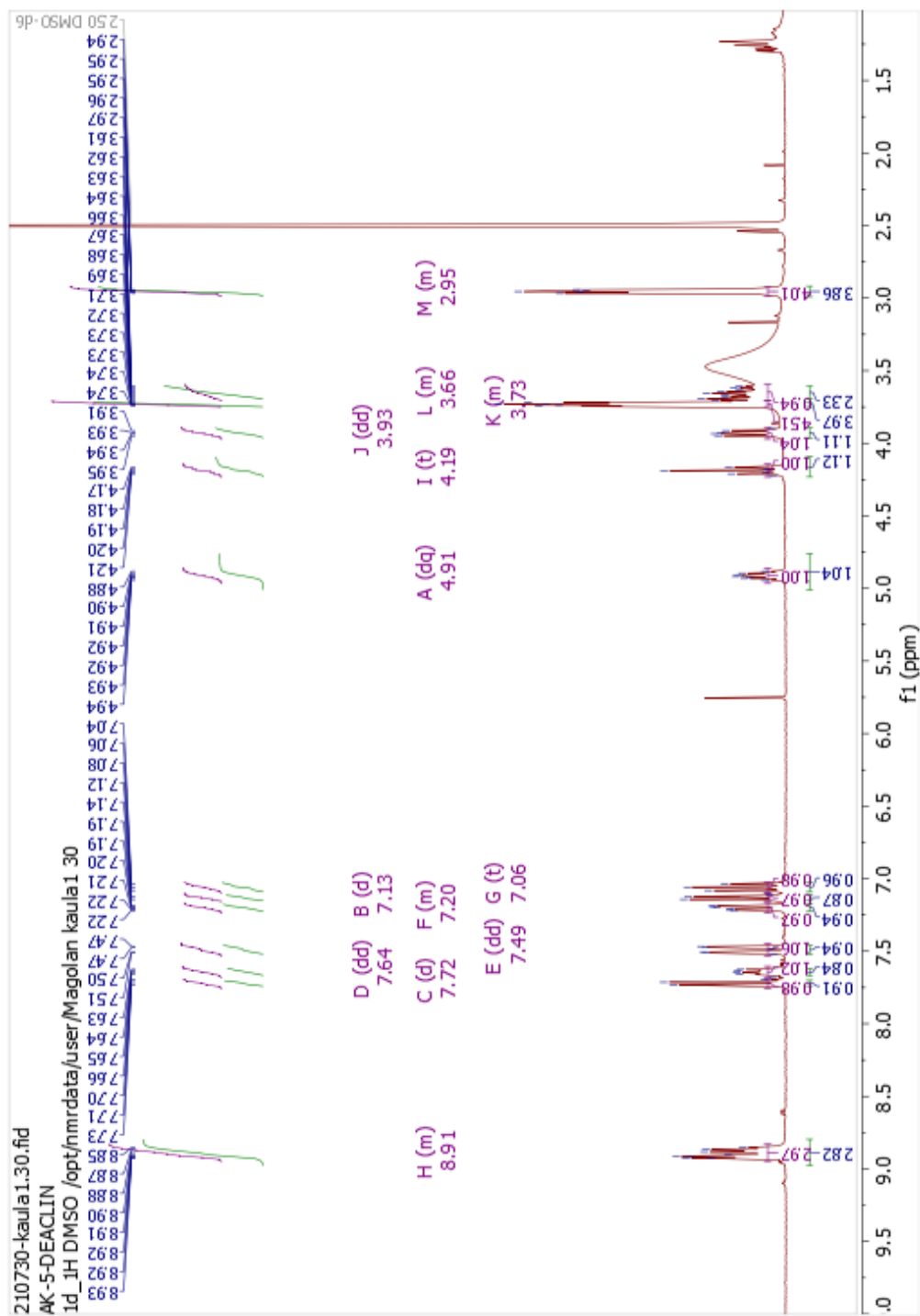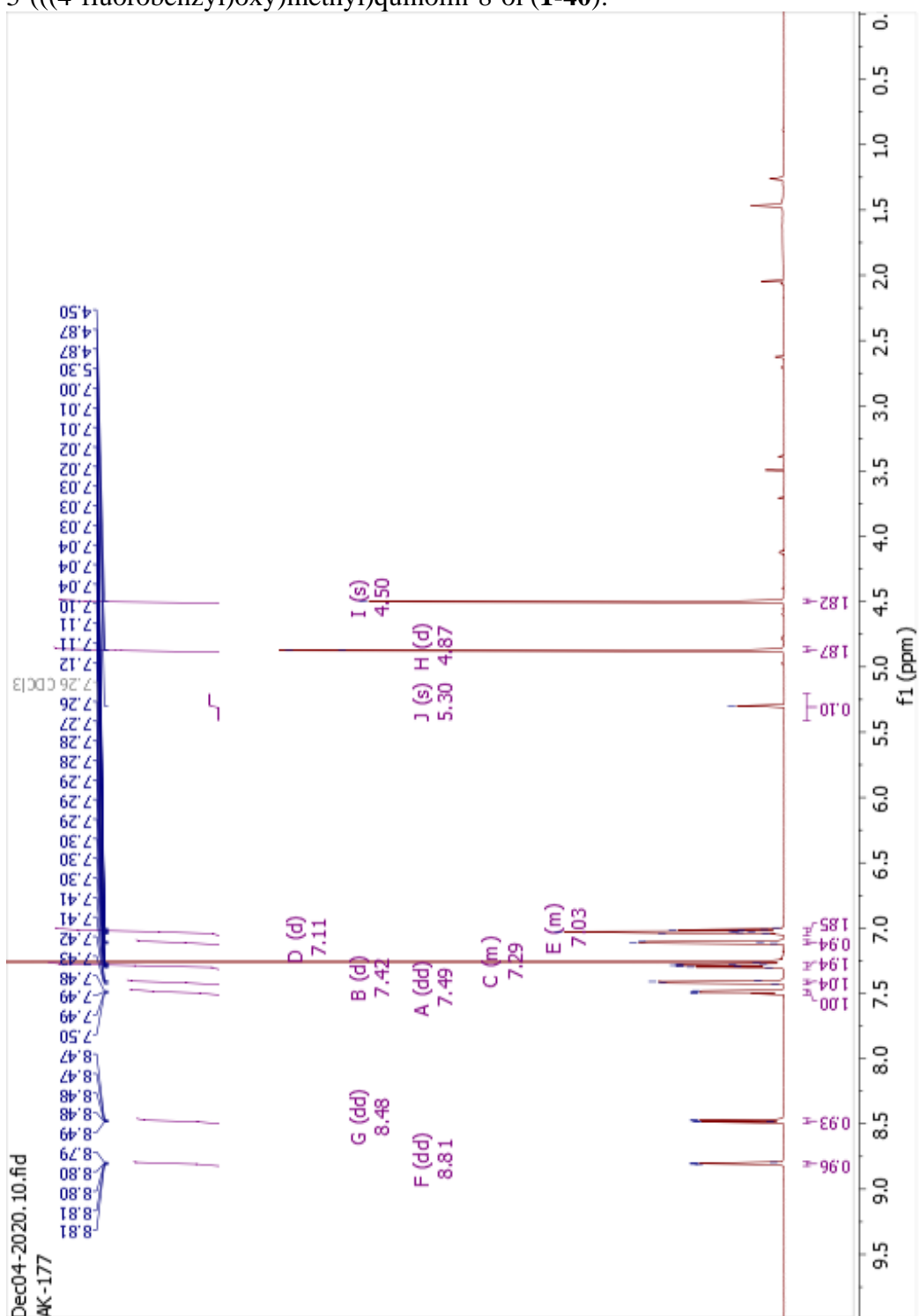
HQ-2-COOH/aza-linezolid analog (**1-11**):

HQ-5-COOH/aza-linezolid analog (**1-10**):
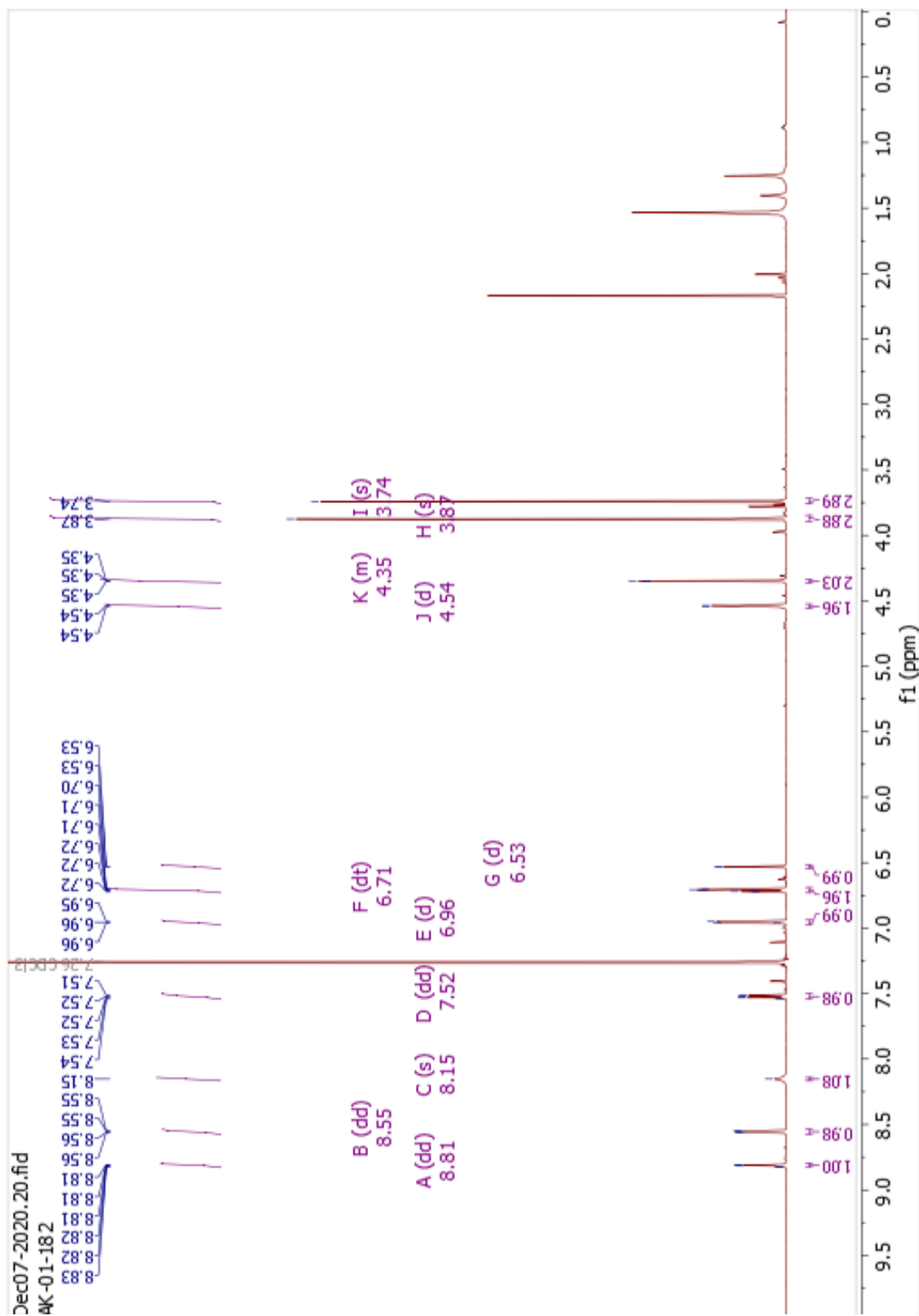
5-(phenethoxymethyl)quinolin-8-ol (**1-39**):

5-(((4-fluorobenzyl)oxy)methyl)quinolin-8-ol (**1-40**):

5-((allyloxy)methyl)quinolin-8-ol (**1-41**):

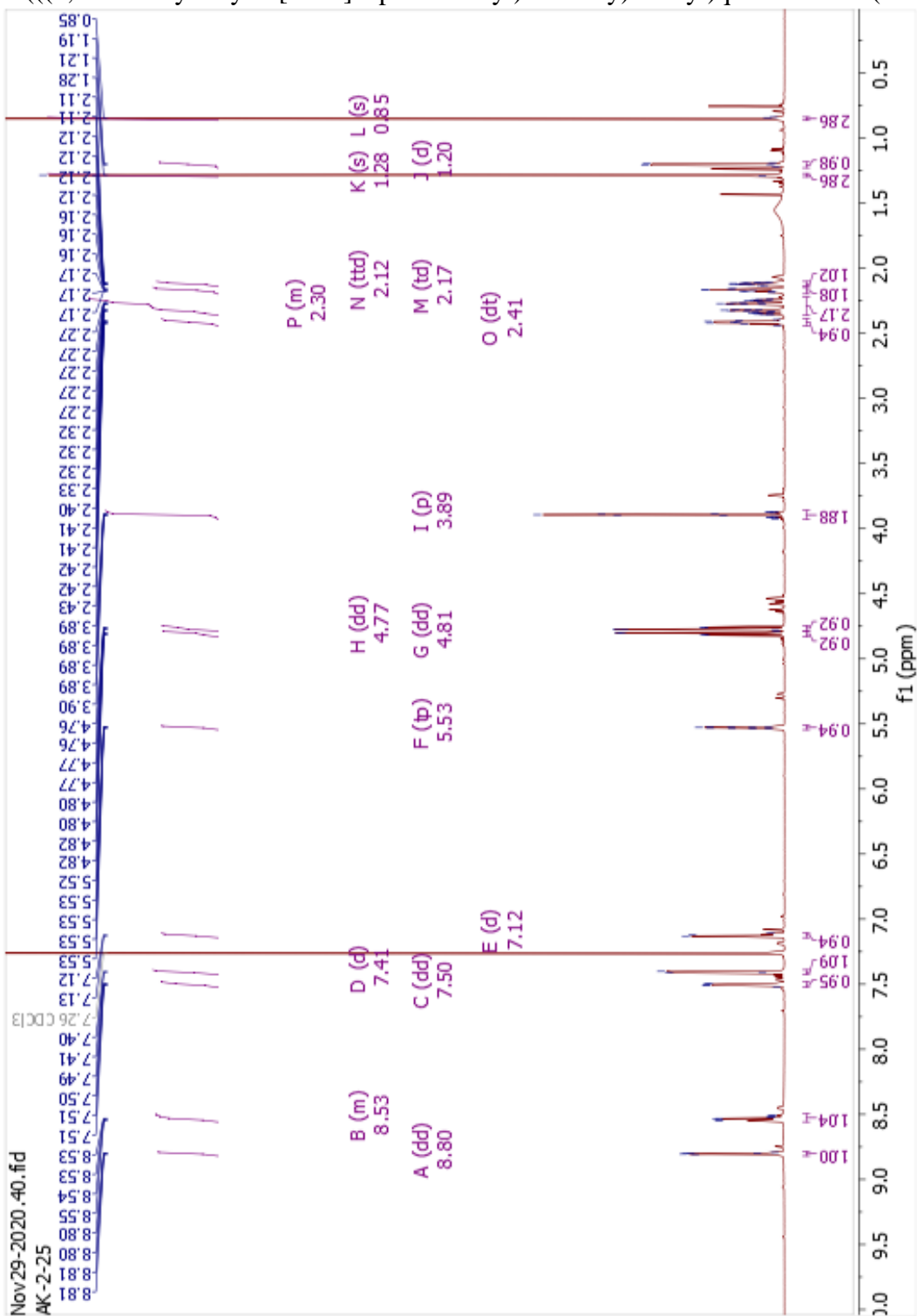5-(((3,5-dimethoxybenzyl)oxy)methyl)quinolin-8-ol (**1-42**):

5-(propoxymethyl)quinolin-8-ol (**1-43**):

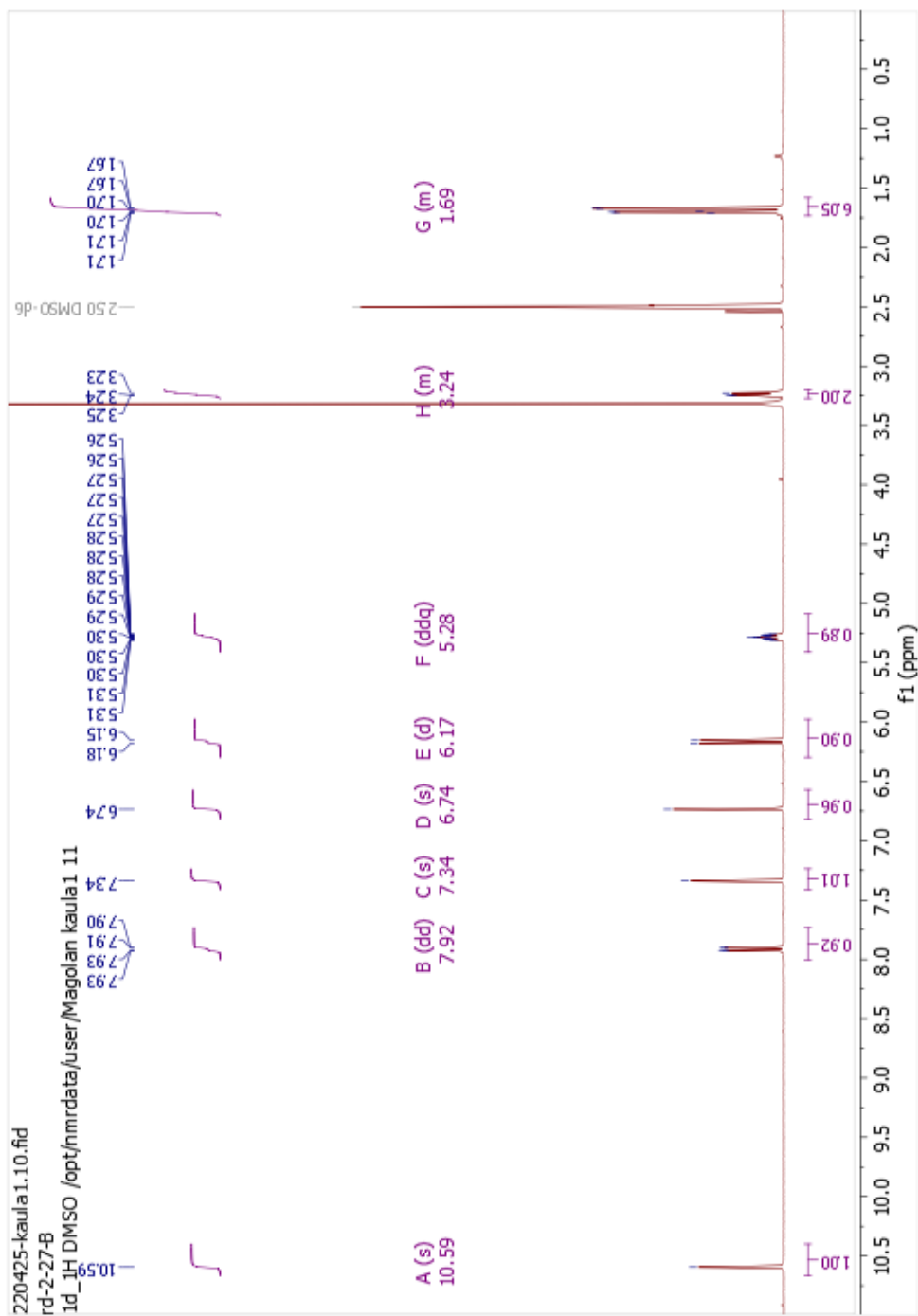5-((but-3-yn-1-yloxy)methyl)quinolin-8-ol (**1-44**):

5-((((6,6-dimethylbicyclo[3.1.1]hept-2-en-2-yl)methoxy)methyl)quinolin-8-ol (**1-45**):

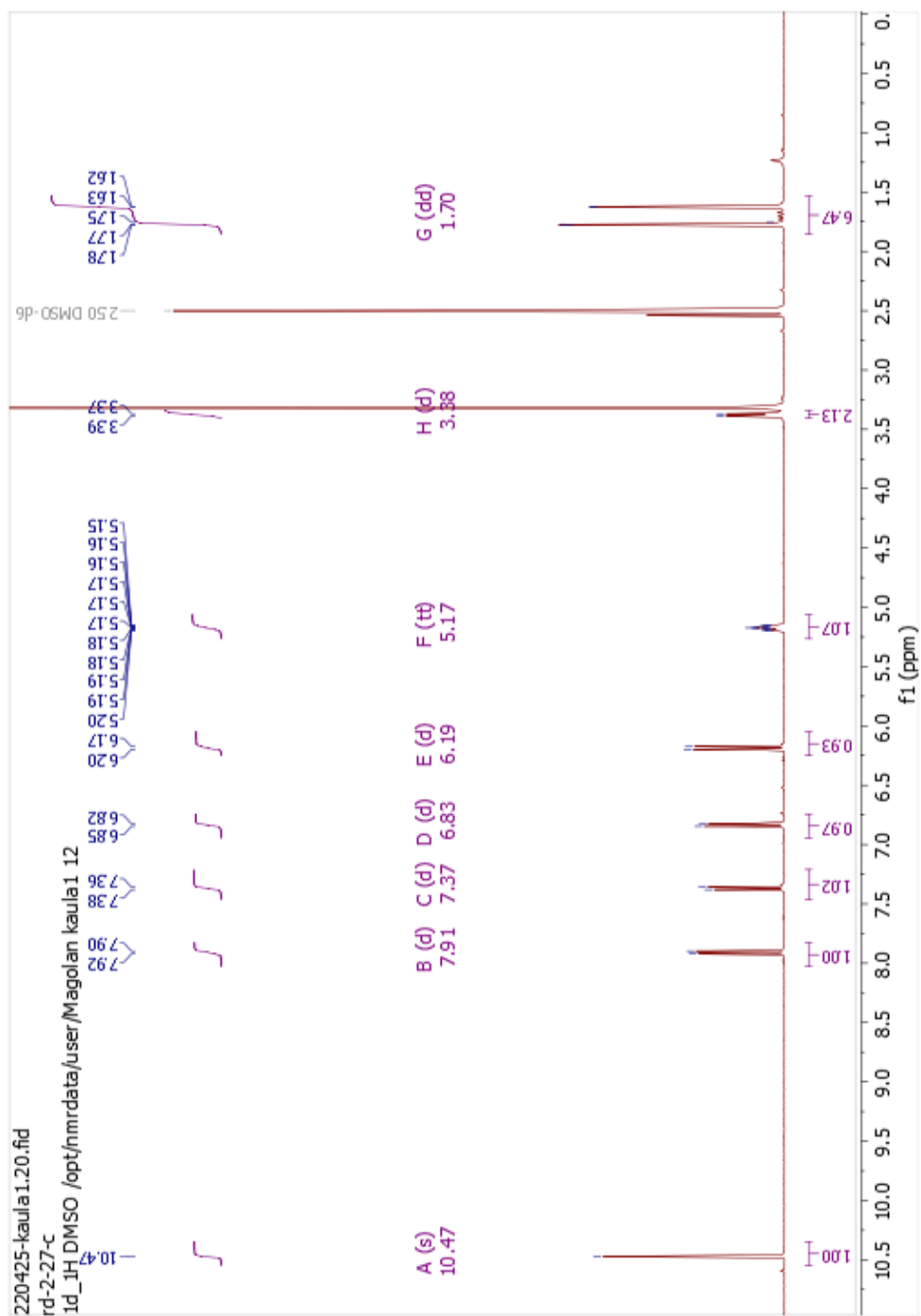5-(((2-bromobenzyl)oxy)methyl)quinolin-8-ol (**1-46**):
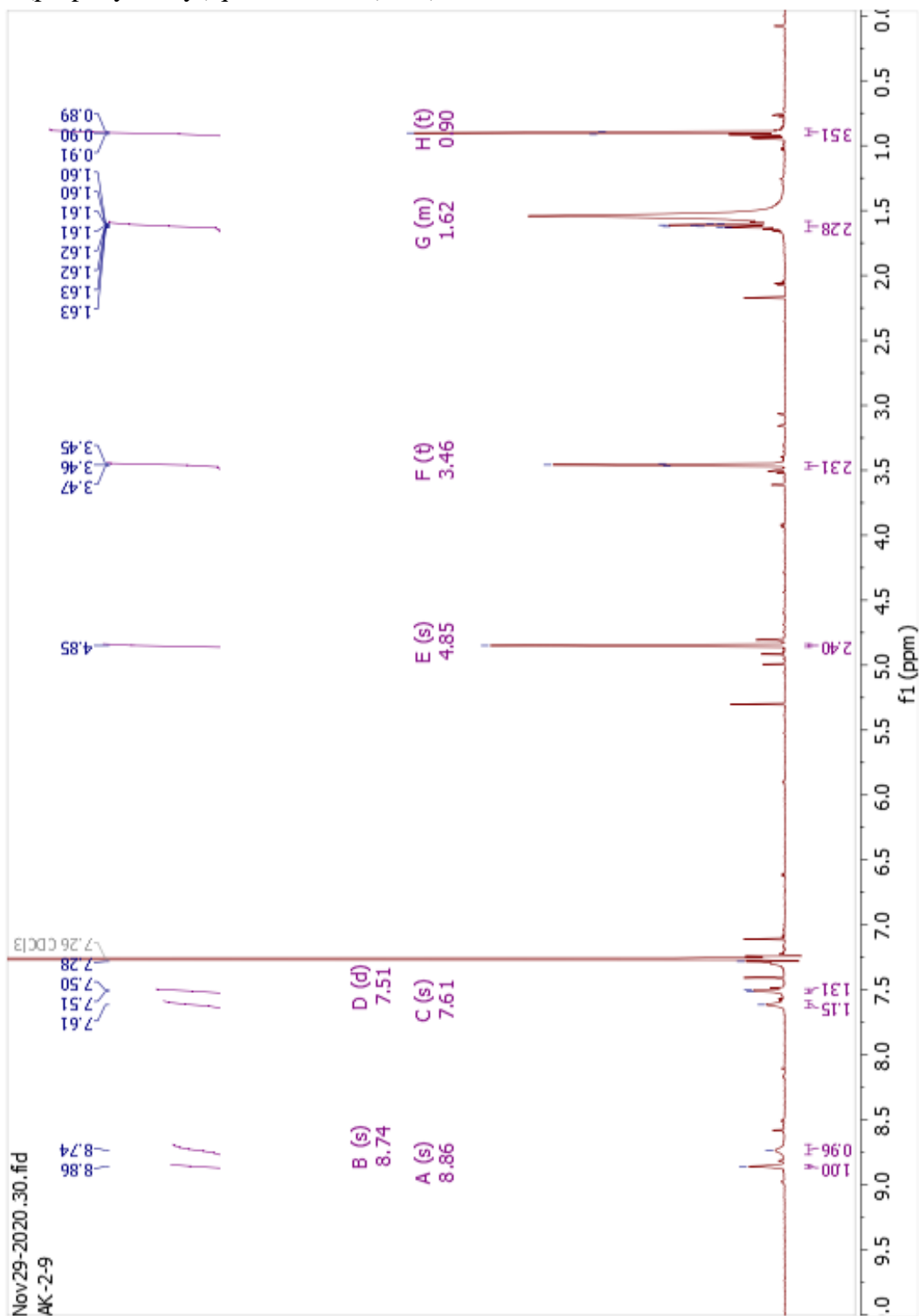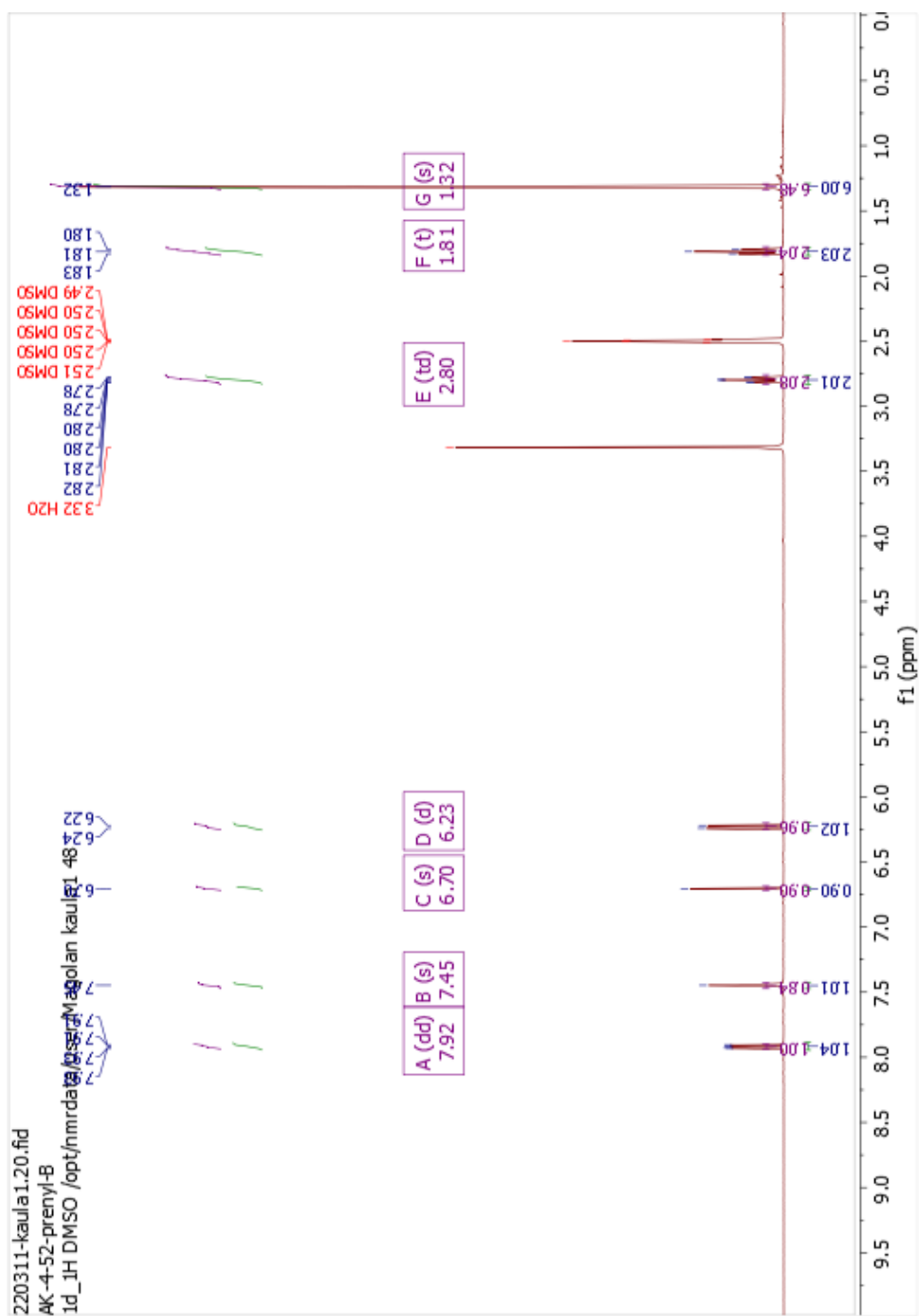
A.2.2: Spectra for Chapter 2
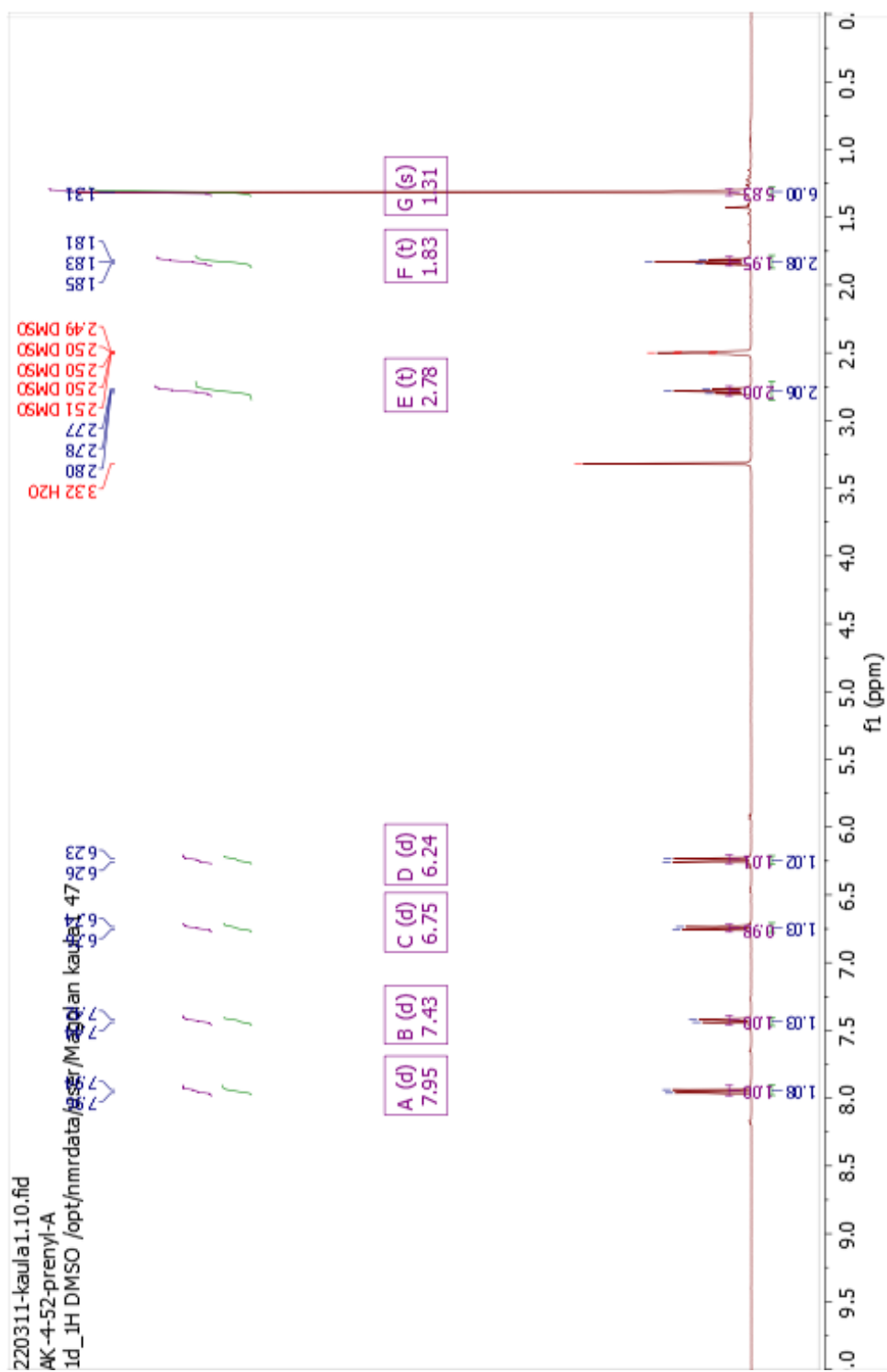
Demethylsuberosin (**2-2**):

Osthenol (**2-3**):

Dihydroxanthyletin (**2-34**):

Dihydroseselin (**2-35**):

Ostruthin (**2-4**):

8-geranylumbelliferone (**2-5**):